République Algérienne Démocratique et Populaire

Ministère de l'enseignement supérieur et la recherche scientifique

École Nationale Polytechnique
Département d'Électronique
Laboratoire des Dispositifs de
Communication et de Conversion Photovoltaïque

Doctoral Thesis

In : Electronics

A Study on Photovoltaic Power Plant Connected to the Distribution Network

Saida BOUACHA

Presented and publicly supported on (25/02/2021)

Dissertation Committee:

President :	**M. LARBES Chérif,**	Professor	ENP, Algeria
Supervisor :	**M. MALEK Ali,**	Res.Dir	CDER, Algeria
Co- Supervisor :	**M. HADDADI Mourad,**	Professor	ENP, Algeria
Examiner :	**M. MAHRANE Achour,**	Res.Dir	UDES, Algeria
Examiner :	**Mme. HASSAINE Linda,**	Res.Dir	CDER, Algeria
Examiner :	**Mme. AMROUCHE Badia,**	MCA	USDB, Algeria

ENP 2021

République Algérienne Démocratique et Populaire

Ministère de l'enseignement supérieur et la recherche scientifique

École Nationale Polytechnique
Département d'Électronique
Laboratoire des Dispositifs de
Communication et de Conversion Photovoltaïque

Doctoral Thesis

In : Electronics

A Study on Photovoltaic Power Plant Connected to the Distribution Network

Saida BOUACHA

Presented and publicly supported on (25/02/2021)

Dissertation Committee:

President :	**M. LARBES Chérif,**	Professor	ENP, Algeria
Supervisor :	**M. MALEK Ali,**	Res.Dir	CDER, Algeria
Co- Supervisor :	**M. HADDADI Mourad,**	Professor	ENP, Algeria
Examiner :	**M. MAHRANE Achour,**	Res.Dir	UDES, Algeria
Examiner :	**Mme. HASSAINE Linda,**	Res.Dir	CDER, Algeria
Examiner :	**Mme. AMROUCHE Badia,**	MCA	USDB, Algeria

ENP 2021

République Algérienne Démocratique et Populaire

Ministère de l'enseignement supérieur et la recherche scientifique

École Nationale Polytechnique
Département d'Électronique
Laboratoire des Dispositifs de
Communication et de Conversion Photovoltaïque

Thèse de Doctorat

En : Electronique

Étude d'une Centrale Photovoltaïque Connecte au Réseau de Distribution Électrique

Saida BOUACHA

Présentée et soutenue publiquement le (25/02/2021)

Composition du Jury :

Président :	**M. LARBES Chérif,**	Professeur	ENP, Algérie
Rapporteur :	**M. MALEK Ali,**	Dir. Rech	CDER, Algérie
Co-rapporteur :	**M. HADDADI Mourad,**	Professeur	ENP, Algérie
Examinateur :	**M. MAHRANE Achour,**	Dir. Rech	UDES, Algérie
Examinatrice :	**Mme. HASSAINE Linda,**	Dir. Rech	CDER, Algérie
Examinatrice :	**Mme. AMROUCHE Badia,**	MCA	USDB, Algérie

ENP 2021

ملخص- تحلل هذه الرسالة أداء محطة توليد الطاقة الكهروضوئية المصغرة المتصلة بشبكة الكهرباء وامتثالها لجميع القواعد الفنية الجزائرية الجديدة لربط النظام المتجدد بشبكة الكهرباء. تنشأ هذه المشكلة لأن الشبكة المتصلة بالشبكة تقدم كحل لتحقيق أهداف الطاقة المتجددة في الجزائر. ركز هذا العمل على محطة طاقة صغيرة بقدرة 9.5 كيلوواط متصلة بشبكة الجهد المنخفض (LV)بمركز تطوير الطاقة المتجددة (CDER) .اخذ هذه المحطة الكهروضوئية لدراستها، للكم المتنوع من المعلومات حيث لديها 14 عامًا من التشغيل ومجهزة بنظام مراقبة. تطلب العمل الحالي إعادة تشغيل الوحدة ونظام المراقبة الخاص بها في المقام الأول. سمحت قاعدة البيانات التجريبية بتقييم جودة الطاقة عند نقطة التوصيل المشتركة (PCC)وفقًا للمعيار الدولي،EN 50160 وتحليل أدائها وفقًا لتوجيهات المعيار الدولي IEC 61724 باستخدام برنامجPVsyst بين عامي2016 و2018. وبالتالي، يمكن مقارنة أداء محطة الكهروضوئية بتلك المحاكاة بواسطة هذا البرنامج. لقد سمح لنا هذا العمل بملاحظة أن أداء محطة لا يزال يُعتبر مرضيًا نظرًا لأنها تعمل منذ أكثر من 14 عامًا مع تحقيق نسبة أداء تعادل 70٪. نستنتج بعد ذلك أن الاستثمار الكهروضوئي المتصل بالشبكة واعد جدًا في هذا الموقع.
الكلمات الرئيسية: الكهروضوئية متصل بالشبكة ، جودة الطاقة ، تحليل الأداء .

Résumé- La présente thèse, analyse les performances d'une minicentrale photovoltaïque connectée au réseau électrique et sa conformité avec l'ensemble des nouvelles règles techniques algériennes de raccordement du système renouvelable au réseau électrique. Cette problématique s'impose du fait que le connecté au réseau se présente comme une solution pour atteindre les objectifs de l'Algérie en matière d'énergies renouvelables. Le travail s'est porté sur une minicentrale de 9,5 KW installée au Centre de Développement des Énergies Renouvelables (CDER) connectée au réseau basse tension (BT). Cette centrale constitue un cas d'étude riche en enseignements, c'est une centrale qui cumule 14 années de fonctionnement et qui est dotée d'un système de monitorage. Le présent travail a nécessité la remise en marche de la centrale et de son système de monitorage en premier lieu. La base de données expérimentale a permis l'évaluation de la qualité d'énergie au point de couplage commun (PCC) par la norme internationale EN50160, et l'analyse de ses performances selon les directives de la norme IEC 61724 moyennant le logiciel PVsyst entre 2016 et 2018. Ainsi, les performances de la centrale ont pu être comparées avec celles simulées par ce logiciel. Ce travail nous a permis de constater que les performances du système sont toujours jugées satisfaisantes étant donné qu'il fonctionne depuis plus de 14 ans tout en atteignant un ratio de performance équivalent à 70 %. Nous concluons alors que l'investissement PV connecté au réseau est très prometteur sur ce site.
Mots clés : photovoltaïque connecte au réseau, performances analyse, qualité d'énergie.

Abstract- This thesis analyzes the performance of a photovoltaic plant connected to the grid and its compliance with all the new Algerian technical connection rules for connecting the renewable system to the network, This problem arises because the grid connected system presented as a solution to achieve Algeria's renewable energy objectives. The work focused on a 9.5 KW photovoltaic grid connected plant installed at the Renewable Energy's Development Center (CDER) and connected to the low voltage network (LV). This plant constitutes a case study rich in information that has accumulated 14 years of operation and equipped with a monitoring system. The present work required restarting the plant and its monitoring system in the first place. The experimental database allowed the evaluation of the power quality at the common coupling point (PCC) by the international standard EN50160,and the experimental analysis of its performance according to the directives of the IEC 61724 standard and simulated using the PVsyst software between 2016 and 2018. Thus, the calculated performance could be compared with those simulated by this software. This work has allowed us to observe that the system performance is still considered satisfactory. Given that it has been operating for more than 14 years, it achieving a performance ratio equivalent to 70%, concluding that the PV investment connected to the grid is very promising on this site.
Keywords: photovoltaic-grid-connected, performance analysis, power quality.

Dedication and acknowledgements

I would like to thank the following people, without whom I would not have been able to complete this research, and without whom I would not have made it through my PHD thesis degree!

I would like to thank my previous supervisor Prof. Ali MALEK (May Allah bless his soul) for his guidance in this thesis and who passed away before witnessing the culmination of this work as a published paper;

Prof. Mourad HADDADI for his consistent support and guidance during the running of this thesis, his support, encouragement and especially his patience;

The grid connected team at University of California San Diego especially Prof. Jane keissel, who taught me the basics and essence of research work regardless of the topic under investigation and whose insight and knowledge into the subject matter steered me through this research. And special thanks to Ouafa Benkrouada at University of Illinois, who had supported me and had to put up with my stresses and moans throughout my PhD journey! Whose support as part of her PhD allowed my studies to go the extra mile (sorry for all the extra work Ouafa!).

The grid connected team in CDER, who took the time to install and fix the various issues in the plant of CDER and without whom I would have no data for my thesis.

This acknowledgment would not be completed without the mention of my thesis committee: Professors Cherif LARBES at ENP, Achour MAHRANE at UDES, Linda HASSAINE at CDER , Badia AMROUCHE at USDB in Algeria for their time and insightful comments. I am indebted and thankful to all of the Professors in the jury, who graciously guided me to the end of this thesis work.And my biggest thanks to my family for all the support you have shown me through this research, the culmination of three

years of distance learning. For my mother for her patience and encouragement, thank you for your delicious and war meals, For my kids, sorry for being even grumpier than normal whilst I wrote this thesis! And for my husband Fouad, thank you for all your support, without which I would have stopped these studies a long time ago. You have been amazing, and I will now clear all the papers off the kitchen table as I promised!

Table of Contents

List of Tables

List of Figures

Figure **Page**

List of Acronyms and Abbreviations

A_i Diode ideality constants.

a_i Diode ideality factor.

Am module area in m^2

a_{si} Amorphous Silicon

BIPV Building Integrated Photovoltaic .

BAPV Building Applied Photovoltaic .

PV Photovoltaic.

CDER Energies Development Center.

CF/CUF Capacity Factor/Capacity utilization factor.

COP Conference of Paris.

CPRTCE Comite Permanent de Regles Techniques et Conduite Electrique.

C_t Temperature coefficient (%/C).

FIT feed-in tariff.

FRT Fault Ride Through Capability.

G(STC) Solar irradiance in [W/m2].

G(STC) Irradiance at STC [W/m2].

GC Grid Code.

H_t solar radiation.

I_0 The reverse saturation current [A].

I_{0i} Reverse saturation current [A].

IAM Incidence Angle Modifier.

IEA International Energy Agency.

IEC International Electrotechnical Commission.

I_{mp} Current at the maximum power point [A].

Iph (STC) Photo current at STC [A].

k Boltzmann constant (1.3810-23J/K).

K_i Temperature short circuit coefficient.

Lcm Miscellaneous capture losses [KWh/d/Kwp].

Lct Thermal capture losses .

LTC LTCs load tap changers.

LV Low Voltage .

MPP Maximum power point [W].

MPPT Maximum power point tracking.

MV Medium Voltage .

N_{cell} Number of series cells.

NOCT Nominal Operating Cell Temperature.

$\eta_{(inv)}$ Inverter efficiency.

$\eta_{(PV)}$ Array efficiency.

$\eta_{(sys)}$ System efficiency.

Pc5 power obtained by five parameters model(Wp) .

PCC Common Coupling Point .

Pcw power obtained by PVwatt model(Wp).

Pm measured power (Wp) .

PR Performance ratio [%].

PV Photovoltaic.

PVPP Photovoltaic power plants .

q Electron charge(1.60210-19C).

RE Renewable Energy.

R_p Parallel resistance [Ω].

R_s Series resistance [Ω].

RTU Remote Terminal Unit.

SKTM Shariket Kahraba wa Taket Moutadjadida.

SM Simplified model.

STC Standard test conditions.

T(STC) PV Cell temperature at STC[K].

TCR Technical connection rules

TLST Transformer Low Single Tracker.

V_{mp} Voltage at the maximum power point [V].

WCPR Weather-Corrected Performance Ratio.

Y_T Corrected reference

General introduction

Energy usage has been significantly increasing in the past several decades and is anticipated to double by 2060 [1]. Along with the growing demand for energy and worldwide climate change, new policies are advocating for the propagation of renewable energy[2]. As a result, The Paris Agreement COP(Conference of the Parties, referring to the countries that have signed up to the 1992 United Nations Framework Convention on Climate Change) holds accountable the partaking countries and companies to sustainability targets each entity has set for itself by 2030 [3]. Just like most developing countries, the Algerian government has developed 'The National Program for Renewable Energy and Energy Efficiency's as a practical step towards a sustainable future. The national program in Algeria has set a target to cover 40% of its national electric needs from renewable energy resources by 2030 [4]. It has committed most of its renewable energy sourcing from solar photovoltaic (PVs) due to its vast solar exposure which covers 90% of the country with an area of 2,382 million km^2[5]. The estimated sunshine is valued at 3000 hours per year and daily energy reaching up to $5kWh/m^2$[6].

During the first phase of the national program, the total installed capacity of 343 MWp PV grid- connected was in Medium Voltage (MV). However, there is not any PV grid-connected installed in Low Voltage (LV), thus the potential contribution of a small-scale PV grid-connected electricity generation is not well understood in Algeria. In this research, the study aims to fill this gap of knowledge by focusing on a comprehensive understanding of the PV systems, the energy flows between system components, and the integration of grid assist and grid-tied PV systems into the LV utility grid. Algeria

has adopted a law of feed-in tariff support schema, which is the most common financial support system [7], utility companies are obliged to purchase electric power produced by any renewable source. This means that producers are guaranteed financial benefits even when they do not reach their rated capacity. In theory, PV plants are expected to generate a certain range of power based on standard test conditions. However, in practice, the average generated power rarely equates to anticipated outputs. Subpar production is mainly attributed to the penetration of shading, defects found in equipment and installation, failure of the inverter(s), and deviations from the manufacturer's specifications in the PV modules[8]. This inefficiency affects the profitability of utility companies and has been a problem in many countries like Spain, France, Italy and Germany[8–10]. Consequently, performance studies became a necessity for obtaining higher quality PV systems that assure efficiency and equity. Designers and researchers use a performance study to identify the malfunction and operational issues to make better investment decisions. Most conducted performance studies around the world analyzed the grid connected PV systems which were newly installed and have been operating for a maximum of one year. However, such systems rarely show any vulnerabilities within the one-year period and research has confirmed that the performance ratio was about [11].Therefore, those studies fall short in providing a realistic insight on how a PV system connected to the grid continues to perform with time. In fact, this is the most important factor for investors and utility providers as they need to assure the system‘s sufficient production in the future to guarantee continuous revenue and return on investment. This thesis presents a simulation and experimental results obtained from field performance monitoring a 9.5 kW roof mounted PV system in Algiers. Our study plays a vital role in understanding and assessing long-standing grid connected PV systems (working more than 14 years) and their performance. Our research tries to compute the PR of the system after operating for more than a decade and compares the three sub-systems that have the same type of modules and inverters and are located on the same site. We evaluate the system based on power quality quantities which are obtained from our on-site PV grid-connected system. This reveals the relation between power quality injected into the

network and solar irradiance, and we investigate the integration requirements for PV grid connected to LV. We aim that our study sheds light on long-time PV systems and the reliability of their performance. This research is divided into four main goals:

- Evaluate the performance of the system by using the performance standard guide developed by the International Electrotechni cal Commission (IEC);
- Compare the measured and predicted performance of a photovoltaic grid connected system.
- Evaluate the power quality quantities which are obtained from the PV grid-connected system.
- Investigate the recent integration requirements for new Technical Connection Rules (TCR) which have been created in Algeria to permit the integration of photovoltaic power plants into the low voltage.

Our work is arranged as follows: **Chapter I** discusses renewable energy strategies, production of energy in Algeria and an overview of the grid connected PV system where a description of the important parts are given.**Chapter II** provides a state of the art, which presents a literature review on PV grid connected system performance analysis and presents the performance analysis according to the International Energy Agency (IEA) guidelines of standard IEC 61724. Additionally Algeria's new Technical Connection Rules (TCR) for integration of PV to the LV network was described **Chapter III** provides the shadow mask of our PV grid connected plant of CDER and the case study is simulated with the PVsyst software. **ChapterIV** presents the results and discussion. Simulation results are analyzed for each of the case studies and comparative analysis with experimental results is presented. Finally, the voltage, the injected active power and reactive power are analyzed to inspect whether the PV power fulfills the grid code's requirements.

CHAPTER 1

PHOTOVOLTAIC GRID CONNECTED SYSTEM OVERVIEW

1.1 Introduction

This chapter is dedicated to present the renewable energy in the world and the Algerian energy strategy, policy and the issues related to the integration of renewable energies into the grid in Algeria. Next, the main concepts of photovoltaic grid connected system. Understanding photovoltaic grid connected system and being able to model each part of it, presents an essential step to start the photovoltaic grid connected system analysis. Many challenges are facing users of photovoltaic grid connected systems under different aspects mainly including cells, modules and arrays, and inverter modeling.

1.2 Renewable energy in the world

According to the International Renewable Energy Agency (IRENA)[12] (Figures 1.3 and 1.1), in 2020 the cumulative worldwide installed capacity of renewable generation was above 2500 GW, where 1153 GW corresponded to renewable hydropower plants,698 GW to onshore wind, 34.3 GW to offshore wind, 707 GW to PV plants, 6.47 GW to solar thermal, 87 GW to solid biomass, 20 GW to biogas, 15 GW to bioenergy (renewable municipal waste), and 14 GW to geothermal.

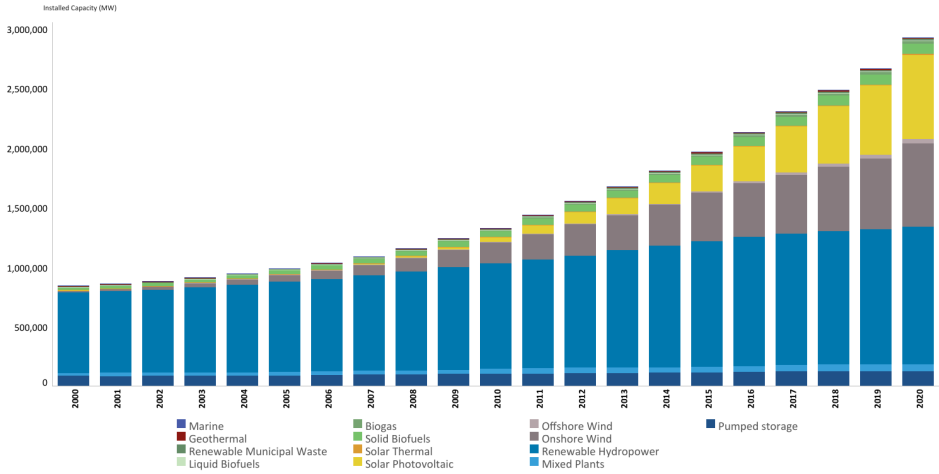

Figure 1.1: The installed renewable energy capacity worldwide between 2000 and 2020 [12]

According to the World Energy Council [1], future trends show an increasingly important role for solar power plants, also with a strong development of onshore and offshore wind.

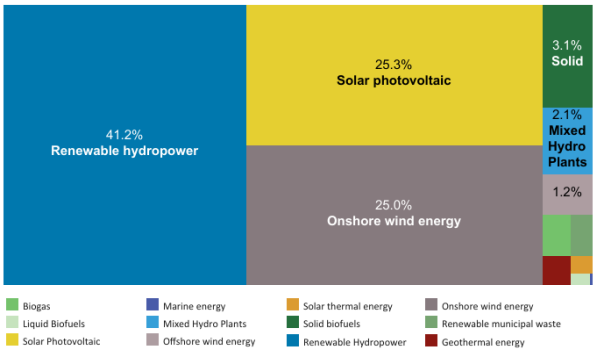

Figure 1.2: The installed renewable energy capacity worldwide between 2000 and 2020 [12]

Due to the cost of the energy produced by renewable energy sources has been decreasing in recent decades, the development of renewable is being experienced worldwide, not only in some specific countries as shown in (Figure1.3),that presents the installed capacity of renewable energy by region in 2020.The Asia region with 1286 GW that represent 49 % of global installed capacity followed by Europe region with 609.499 GW represent 23.26%, North America with 421.7GW represent 16 %,South America with 233 GW (8.89%), and Africa with 53.68 GW represent only 2%.

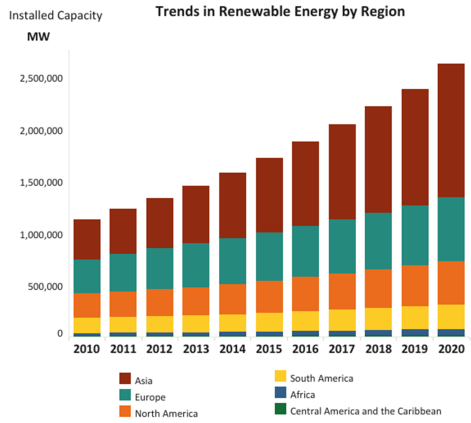

Figure 1.3: The installed renewable energy capacity worldwide by region [12]

In Figure 1.4 it is shown that China is leading worldwide in terms of installed capacity of PV plants, followed by the United States (US), Japan, and Germany.

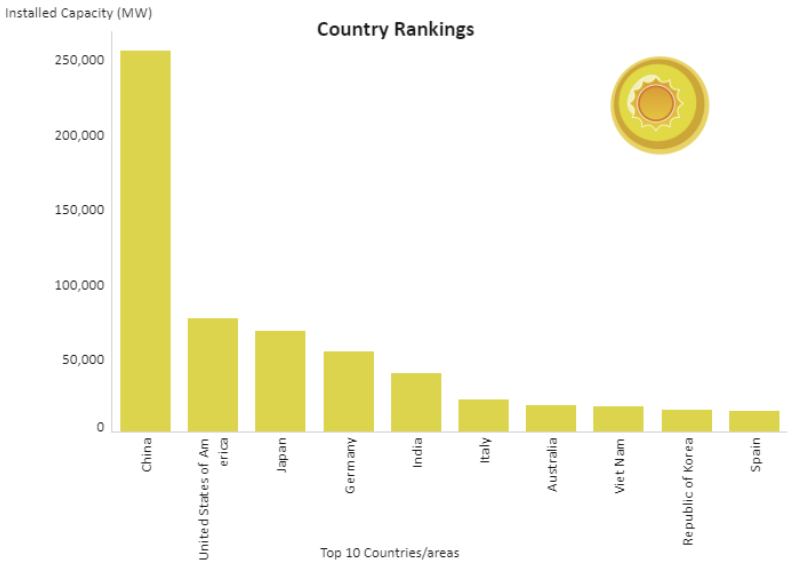

Figure 1.4: The installed renewable energy capacity worldwide by region [12]

Figure1.5 show the installed photovoltaic capacity worlwide for on and off grid plants between 2000 and 2020, we can see that the photovoltaic grid connected system is increasing fast from 0.7 GW in 2002 to 702 GW, mean while installed photovoltaic capacity off grid is 0.05 GW to 4.58 GW for the same periode.

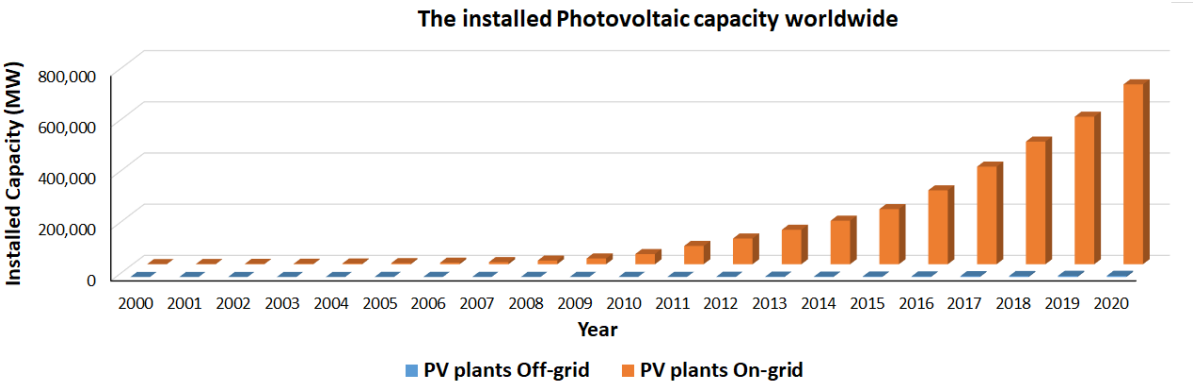

Figure 1.5: The photovoltaic installed capacity on and off Grid [12]

1.3 Algeria target concerning Renewable energy

Algeria is rich in natural resources. It has the world's tenth largest proven natural gas reserves, is the sixth largest exporter of gas and has the third largest shale gas reserves[6]. It also ranks sixteenth in proven oil reserves [13]. Algeria is keenly interested in taking an active part in the development of new technologies for exploiting and utilizing renewable sources of energy because of the following considerations:

(i) Algeria's domestic electric power consumption has grown steadily, with official estimates of demand growth 32 % between 2010 to 2014[14].

(ii) In the past the energy fossil fuels were generously consumed and dissipated. For that, the government plans to introduce renewable energy into the local power market to save volumes of natural gas for export to finance the national economy [15].

The Algerian government is committed to increasing the penetration of renewable resources. Therefore, it has developed two programs:

a) **The National Program for Renewable Energy and Energy Efficiency**:

This is a practical step in aims of moving towards a sustainable future. Algeria's national policy has set a goal for 40 per cent of its national electricity requirements to be met by renewable energy supplies by 2030 [3]. The government plans are increasing the power generating capacity by 22 GW, between the years 2011 and 2030. It Adopted a two-phase approach; Phase 1 was from 2015-2020, Phase 2 is from 2021 to 2030. The new capacity will be coming from different resources, with solar power accounting for 13.5 GW, followed by wind energy accounting for 5 GW, solar CSP for 2 GW, biomass for 1 GW, CHP for 400 MW and geothermal for 15 MW [16]. The renewable energy targets for each source and phase are depicted in Table 1.1[6].

As seen from the Figure1.6, Algeria will be committing most of its renewable energy sourcing from PV at 61% due to susceptibility of the country's geography in receiving

Table 1.1: installed capacity by phases [**?**]

	1st phase 2015-2020	2st phase 2021-2030	Total MW
Photovoltaic	3000	10575	13575
Wind	1010	4000	5010
CSP	-	2000	2000
CHP	150	250	400
Biomasse	360	640	1000
Geothermal	05	10	15
Total	4525	17475	22000

a large amount of solar radiation on its territory and has a large number of sunshine hours per day, especially in the summer.

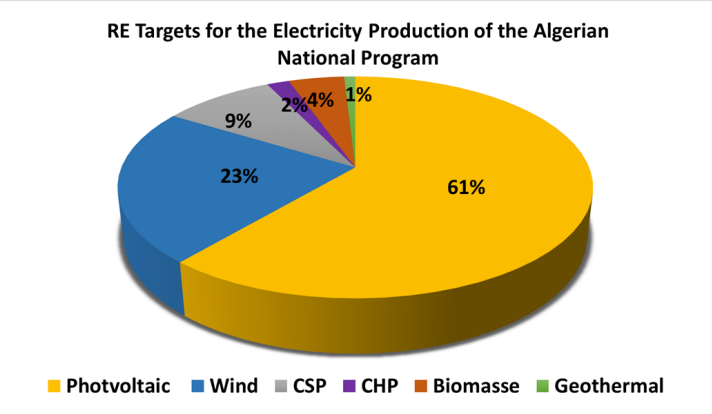

Figure 1.6: Breakdown by technology of renewable energies in Algeria [17]

b) **Feed-in tariff support:**

In order to diversify its national energy mix, and speed up the RE development to achieve established RE targets[18], the Algerian government introduced a feed-in tariff mechanism in 2014. In this system, the Algerian utility buys PV and wind electricity from customers for 20 years contract at a guaranteed rate[19], with a lot higher than conventional electrical costs. In that context, Algeria has set an acceptable purchasing price scale for electricity generated from the different sources. This scale is based on energy and the period of the exploitation of the investment (the first five years and

the remaining 15 years)[19]. Table1.2 summarizes the feed-in tariff aligned with the different exploitation periods and quantity of electricity output.

Table 1.2: feed in tariff of electricity generation for PV and Wind source [19]

	Power(MW)	Feed-In Tariff(DZD/KWh)	
		5 Initial Year	15 Remaining Years
Wind	1-5	13.10	9.55-16.66
	≥ 5	10.48	7.64-13.33
Solar PV	1-5	15.94	11.80-20.08
	≥ 5	12.75	9.44-16.06

1.4 Solar Radiation data and installed plants in Algeria

Solar photovoltaic is the most common application suitable in Algeria. This is due to its vast solar exposure which covers 90% of the country with an area of 2,382 million km^2[5]. Estimated sunshine is valued at 3000 hours per year and daily energy reaching up to 5 kWh received from any horizontal surface in most parts of the country. However, one of the barriers in solar power development is the inconsistency and variability of solar irradiation which can be geographically dissimilar from one site to another. Site selection has a direct impact on the potential RE projects in many different ways including technical, economic and environmental aspects [20]. As shown in the Figure1.7, a huge amount of solar radiation is in the southern part of the country with values of 7 kwh/m2/day. The pilot phase of the program (2011-2014) witnessed the establishment of three different stations, including 150 MW Solar-Gas Hybrid Plant in Hassi R'mel (Laghouat) and 10MW of the wind farm located in Kabertene (ADRAR), the last one is the Photvoltaic Pilot Plant of Oeud N'Chou with 1.1 MWp in (Ghardaia) as illustrated in the Table1.3. If we see the distribution of grid-connected photovoltaic plants in relation to solar radiation as shown in Figure1.7, the selection was appropriate for the sites as the first phase of the underlined program (2015-2020) by choosing site for different solar radiation from 5.80 kwh/m2/day for the site of SOUK AHRAS to the maximum

Table 1.3: Installed PV grid connected plant in Algeria [**?**]

Province	Site	Power(MW)	Commissioning
ILLIZI	Djanet	3	2/19/2015
ADRAR	Zaouiet.Kounta	6	1/11/2016
	Kabertene	3	10/13/2015
	Aoulef	5	3/7/2016
	Reggane	5	1/28/2016
	Timimoun	9	2/7/2016
	Adrar	20	10/28/2015
TAMANRASSET	Tamanrasset	13	11/3/2015
	In-Salah	5	2/11/2016
TINDOUF	Tindouf	9	12/14/2015
LAGHOUAT	El Kheneg (I)	20	4/8/2016
	El-Kheneg (II)	40	4/26/2017
DJELFA	Ain-El-Ibel (I)	20	4/8/2016
SOUK AHRAS	Oued El Keberit	15	4/24/2016
NAAMA	Sedrate Leghzal	20	5/3/2016
SAIDA	Ain-Skhouna	30	5/5/2016
SIDI-BEL-ABBES	Telagh	12	9/29/2016
EL BAYADH	Biodh Sidi Chikh	23	10/26/2016
M'SILA	Ain-El-Melh	20	1/26/2017
OUARGLA	El-Hdjira	30	2/16/2017
DJELFA	Ain-El-Ibel (II)	33	4/6/2017
LAGHOUAT	El-Kheneg (II)	40	4/26/2017
BATNA	Oued El-Ma	2	1/16/2018
Total	Algeria	343	20/03/2020

of 7 kwh/m2/day for the site of Tamanraset. The performance study of this plants will be very helpful in selecting sites for the second phase of the 2020-2030 program. Even though there has been a major increase in the amount of PV grid connected plants, the production is still only 2% of Algeria energy production from renewable energy in 2019 as shown in Figure1.8. Also, the integration of small system to the distribution network is still few and is only installed at research centers. On the one hand, this is due to the lack of investors in this field as all the plants were installed by state institutions such as SKTM, and the lack of technical connection rules (TCR) for the integration of PV systems into the grid in Algeria, where it was only introduced until February 2020 on the other hand.

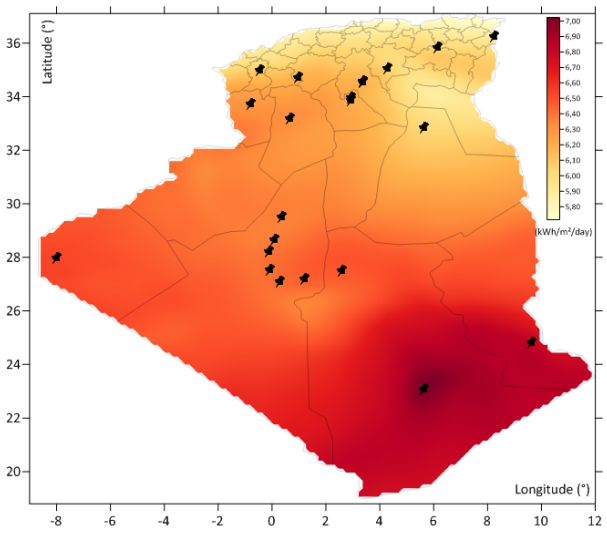

Figure 1.7: Radiation map and installed PV grid connected plant in Algeria.

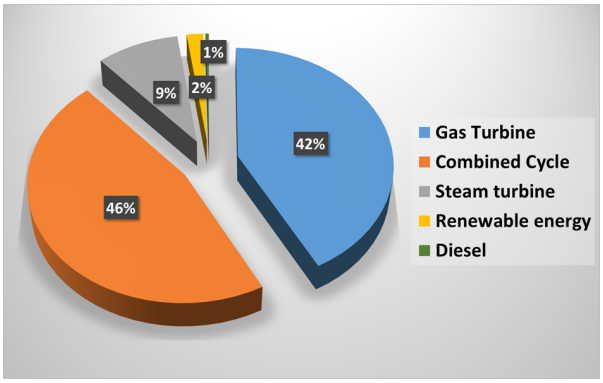

Figure 1.8: Production energy by different sources in Algeria in 2019

1.5 Photovoltaic grid connected system overview

1.5.1 Classification of the PV system

Photovoltaic power systems can be classified into three different groups as shown in Figure1.9

a) Stand-alone PV systems:

Stand-alone PV systems are used for small self-consumption, for remote areas where the AC main grid is not accessible. A charging battery or backup supply is needed to store

the excess energy during the high solar irradiation time and supply to the load when the PV energy is not available [21].

b) Hybrid:

The hybrid PV systems are used in rural areas as well. its includes more than one energy-producing source combined with PV (diesel generator,wind,.....etc) and may be designed to include a battery-bank to provide 24-hour electricity in a more affordable and effective manner or without battery bank [22].

c) Grid connected:

which are PV systems connected to the local distribution grid and supply it with electricity. The PV systems can be connected directly to the public grid or first to the house grid that covers the house's energy demand and only provides the public grid with any surplus[23]. These systems can be divided into small systems, which are located on some residential the roofs' areas, and large Grid-connected systems.

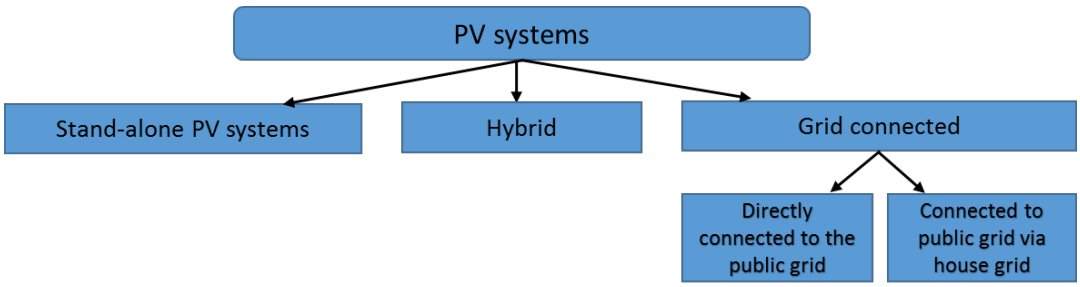

Figure 1.9: Classification of the PV system

1.5.2 Benefits of Grid-Connected PV Systems

A great advantage of the grid-connected systems is that they offer the opportunity of generating significant amounts of energy near the consumption point, minimizing that way the transmission and distribution losses [24]. Moreover, utilities and customers can benefit from installing these systems.

- Customers: The main benefit for customers is to take advantage of the incentives provided by the government to install the Feed-In tariff PV system[25].

- Utilities: the gains of installing PV systems are mainly operational benefits, where it aids to decrease the feeder losses, improve the voltage profile of the feeder[26], and reduce the lifetime operation and maintenance costs of transformers load tap changers (LTCs)[27].

1.5.3 Classification of the PV Grid connected system

The connected photovoltaic grid system can be divided into two main groups: Grid connected decentralized or distributed systems and centralized systems.

1. **Decentralized Grid-connected System:**

Decentralized photovoltaic grid systems have low power capacity range from $1kW$ to $100kW$ [28]. These small systems are used for the supply of residential loads where the PV module can be mounted on a roof (BAPV) or incorporated into a roof (BIPV) [22]. The building applied photovoltaic(BAPV),PV modules are simply attached to the top of the skin of the building and are thus usually known as technical devices added to the building without any particular technical or architectural purpose as shown in the Figure1.10a. However,the building integrated photovoltaic (BIPV) systems instead, the PV modules are integrated into the envelope constructive system, being an integral part of the building. PV modules, in this case, replace traditional building components and are able to fulfill other functions required by the building envelope (e.g. providing weather protection, heat insulation, sun protection, noise protection)[29]as shown in the Figure 1.10b. The main difficulty with these systems is that the roof identifies and sets the orientation of the PV array.

2. **Centralized Grid-connected Systems:**

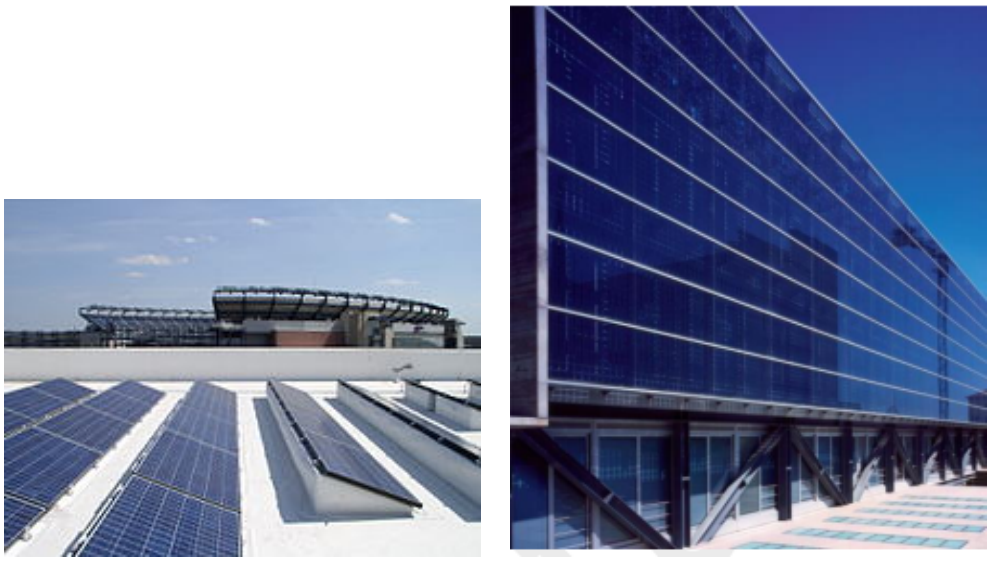

(a) (b)

Figure 1.10: (a)Applied Photovoltaic BAPV (b) integrated photovoltaic BIPV

Central grid connected systems such as solar farms directly feed the medium and high voltage grids[28]. In these systems, in case of islanding they disconnected. Most studies are focusing on preventing the disconnection of these systems when a fault occurs [22].

Figure 1.11: centralized plant

1.5.4 Photovoltaic grid connected system

Grid-connected PV systems have become increasingly popular for applications in the built environment. Grid-connected photovoltaic power systems consists of photovoltaic panels, solar inverters, power conditioning units and grid connection equipment as shown in Figure 1.12.

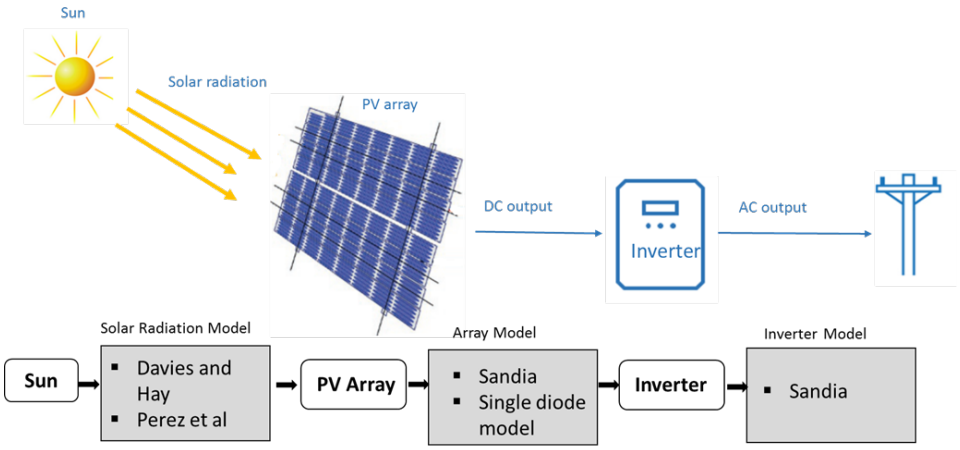

Figure 1.12: Diagram of mathematical model available in PVsyst

1.5.5 Modeling PV cell

The one-diode model is the most widespread model used for PV cells and PV modules due to its low complexity and good accuracy in the power-generating quadrants, The electronic properties of a solar cell are similar to a diode. The solar cell like any electronic device has a finite resistance which must be considered. The one diode model including Rs and Rsh can be drawn as a circuit diagram as shown in Figure 1.13.

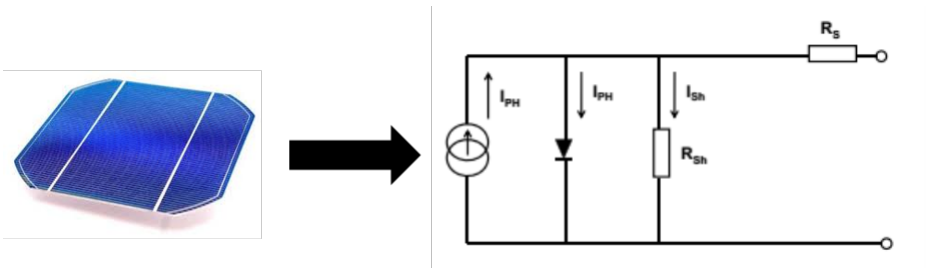

Figure 1.13: Equivalent two-diode circuit model of a PV cell.

1.5.6 Modeling of module and array

A PV module consists of many jointly connected PV cells. Multiple PV modules can be stacked in series forming strings of modules. As a result, the voltage increases. By connecting multiple strings in parallel, PV arrays are formed. The equivalent module

circuit equation for a (Ncell) PV cells in series, shown in the equation 1.1 below [30]:

$$I = I_{Ph} - I_0\left[\exp\left(\frac{V+R_sI}{V_ta}\right)-1\right] - \frac{V+R_sI}{R_p} \tag{1.1}$$

$$I_{Ph} = (I_{Ph(STC)} + K_i(T - T_{(STC)}))\frac{G}{G_{(STC)}} \tag{1.2}$$

$$V_t = (\frac{KT}{q})N_{cell} \tag{1.3}$$

with the variables and parameters represented, in the standard test conditions (STC) by:

STC : Standard test conditions.

$I_{Ph(STC)}$: Photo current at STC [A].

$T_{(STC)}$: PV Cell temperature at STC[K].

T: PV Cell temperature [K].

$G_{(STC)}$: Irradiance at STC [W/m^2].

G: Solar irradiance in [W/m^2].

K_i: Temperature short circuit coefficients.

I_0: Diode saturation current[A].

V_t: the thermal voltage.

q: Electron charge($1.60210^{-19}C$).

k: Boltzmann constant ($1.3810^{-23}J/K$).

a: Diode ideality constants.

R_s: Series resistance [Ω].

R_p: Parallel resistance [Ω].

N_{cell}: Number of series cells.

I_0: Reverse saturation current.

1.5.7 PV Characteristic Curves

From equation 1.1 the I-V and P-V curves of a practical PV unit,either cel,module or array can be produced, as show in Figure 1.14,mention the basic points such as short circuit current (I_{sc}), open circuit voltage(V_{oc}) and the maximum point (MPP). The I-V and P-V characteristics depend totally on the particular climatic conditions which are

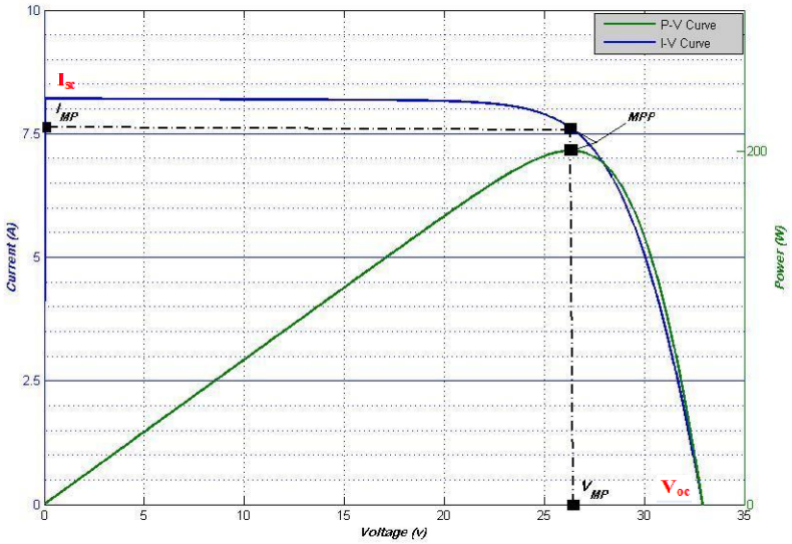

Figure 1.14: Typical PV characteristics (I-V, P-V).

irradiance and temperature as seen in the eqt1.2.Figure 1.15 highlights the effect of different levels of irradiance and temperateure on the characteristic curves of a PV panel. it shows the variations of the irradiance slightly changes the open-circuit voltage. Its most notorious effect is on short-circuit current which is directly proportional to the irradiance as seen in Figure 1.15a.Keeping the irradiance constant at 1000W/m2 and changing the temperature does not affect the short-circuit current but it reduces the open-circuit voltage as seen in 1.15b.

1.5.8 Inverter

PV array connected to the grid via inverters, which converts the DC to AC and also secures the synchronization with the grid in voltage and frequency [31]. They connected to public grid via house as a small system or large-scale system directly connected to the public grid as illustrated in Figure 1.12.

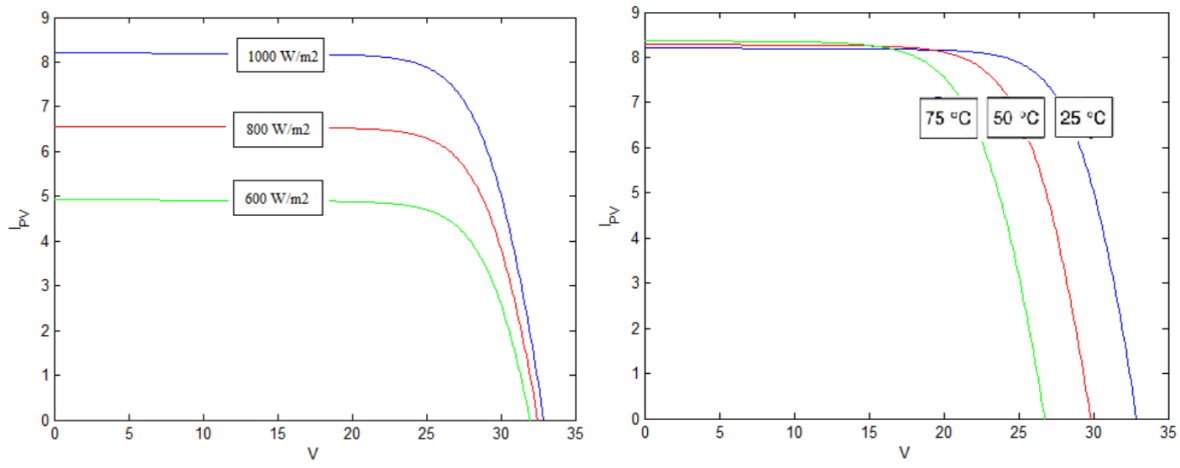

(a) (b)

Figure 1.15: PV characteristic under various climatic conditions: (a) I-V curve under various G levels. (b) I-V curve under various T levels.

1.5.8.1 Inverter Modeling

The empirical model developed by SANDIA laboratories (Sandia National Laboratories) is applicable to all commercial inverters used in PV systems. It is a simple model that allows you to accurately calculate the output power (Pac) based on the input power (Pdc) of the inverter. The equations below describe the inverter model[32]

$$P_{ac} = \left[\left(\frac{P_{ac0}}{A-B}\right) - C(A-B)\right](P_{dc}-B) + C(P_{dc}-B)^2 \tag{1.4}$$

Where:

$$A = P_{dc0} * [1 + C_1 * (V_{dc} - V_{dc0})] \tag{1.5}$$

$$B = P_{s0} * [1 + C_2 * (V_{dc} - V_{dc0})] \tag{1.6}$$

$$C = C_0 * [1 + C_3 * (V_{dc} - V_{dc0})] \tag{1.7}$$

Where: the direct voltage (Vdc) and the direct power (Pdc) are considered as independent variables to calculate the output power of the inverter (Pac).

P_{ac} = ac-power output from an inverter based on input power and voltage (W).

P_{dc} = dc-power input to an inverter, typically assumed to be equal to the PV array

maximum power (W).

V_{dc}= dc-voltage input, typically assumed to be equal to the PV array maximum power voltage (V) .

P_{ac0}= maximum ac-power “rating”for an inverter in reference or nominal operating condition,assumed to be an upper limit value (W) .

P_{dc0}= dc-power level at which the ac-power rating is achieved at the reference operating condition (W) .

V_{dc0}= dc-voltage levels at which the ac-power rating is achieved at the reference operating condition (V) .

P_{so}= dc-power required to start the inversion process, or self-consumption by an inverter, strongly influences inverter efficiency at low power levels (W) .

Pnt= ac-power consumed by an inverter at night (night tare) to maintain circuitry required to sense PV array voltage (W) .

$C0$= parameter defining the curvature (parabolic) of the relationship between ac-power and dc-power at the reference operating condition, default value of zero gives a linear relationship (1/W) .

$C1$= empirical coefficient allowing Pdco to vary linearly with dc-voltage input, default value is zero (1/V) .

$C2$ = empirical coefficient allowing Pso to vary linearly with dc-voltage input, default value is zero (1/V) .

$C3$= empirical coefficient allowing Co to vary linearly with dc-voltage input, default value is zero (1/V) .

These parameters can be obtained from the manufacturer’s technical sheets by considering the default values of the coefficients or of the test databases carried out in recognized international laboratories.

1.6 Conclusion

In this chapter, an overview of the principles of photovoltaic grid connected system, equivalent circuit for the cell, mathematical model for the module, and inverters are presented. Additionally, their advantages for the customer and utility also were discussed. In this chapter we introduced Algeria's plan and targets with regards to renewable energy, especially the PV grid connected plants. We also thoroughly explain the different sites that were selected to be installed during the first phase. As such, our next chapter (Chapter 2) we showcase the importance of performance studies in choosing the future sites to be installed in the second phase.

CHAPTER 2

TOOLS FOR PERFORMANCE ASSESSMENT AND CONTROL OF PV PLANTS

2.1 Introduction

The manufacturer specifications for the PV system grid connected components alone are not sufficient to accurately assess PV operation under various climatic conditions. Hence, PV grid connected field performance monitoring and data analysis are necessary for the better understanding and development of PV system field behavior [33]. In this chapter we describe the methodology selected for assessing the performance of a grid-connected system by using the International Energy Agency (IEA) guidelines of standard IEC 61724 and the International Energy Agency PV Power System (IEA-PVPS) Program TASK 2 [34].

2.2 Modeling of solar photovoltaic modules of CDER plant

In order to determine the maximum power output (Pmax) delivered by the PV module as function of the solar irradiance intensity and the PV-module temperature, a comparison of two mathematical models PVwatts, and the analytical five-parameter model have been used with team of our lab in[35].

the PVPM2540C device connected with sensors box (reference cell and temperature sensors)is used to measure the I-V curve of PV module of PV module of CDER plant,they took two measurements for each PV module (see Fig 2.1) .

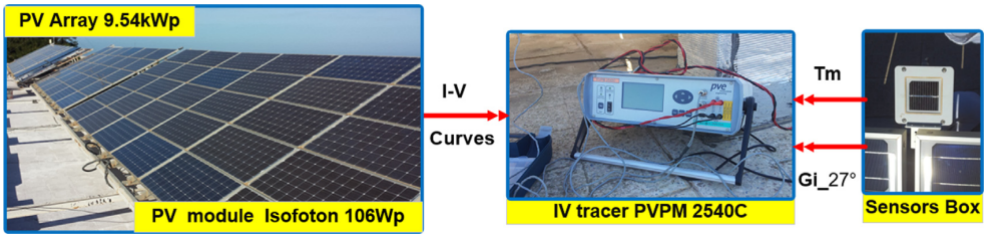

Figure 2.1: IV Tracer using PVPM2540C [35]

PVWatts model is it developed by the National Renewable Energy Laboratory (NREL)

where the effective irradiance and PV cell temperature are used as input. Meanwhile the single diode model as is descriptive in subsection 1.5.6, the well-known five parameter model.it needs the determination of the five parameters extraction.The details of how the measured standardized values are compared to the reference ones given by the manufacturer's data of PV module is in [35].

After comparison between the PVWatts model and Five parameters to measured values model in Fig2.2, which represents maximum power obtained by PVWatts model (Pcw), analytical five parameters model (Pc5) and the measured values (Pm) for the subarray G1, G2 and G3. We can see that the values given by the models fit well with measured ones. Nevertheless, the model based on five parameters fits the best.

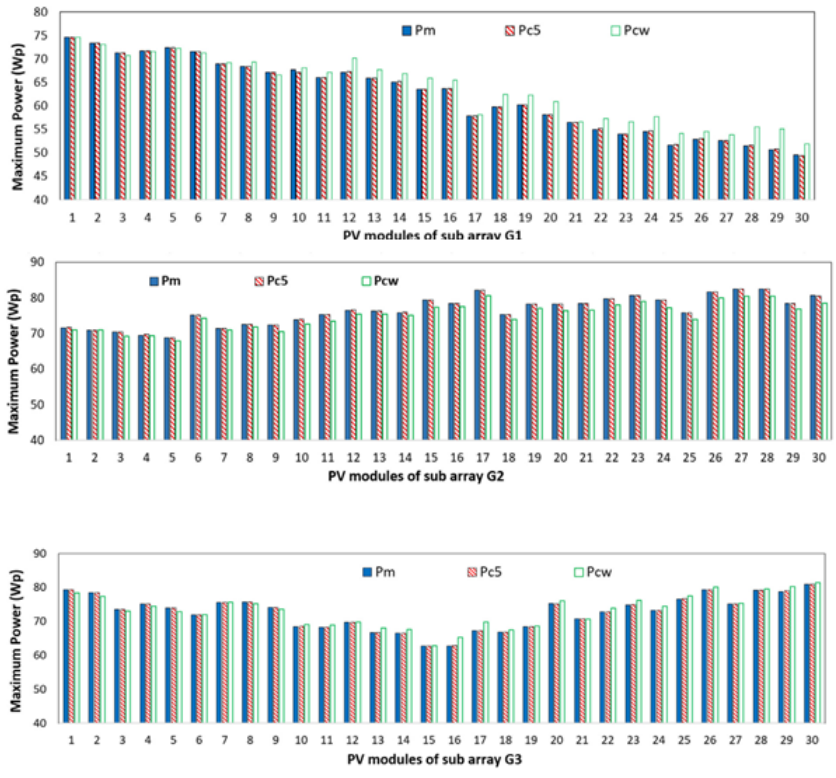

Figure 2.2: Maximum power comparison of PV modules of three sub-array[35].

2.3 Modeling inverter of CDER plant

Converting DC power into AC power allows this power to be injected into the AC network with high efficiencies, but there are energy losses that must be estimated. In the literature, several algorithm models are used to estimate this DC / AC conversion efficiency[] we proposed a simplified model of performance for PV inverters connected to the internal electricity grid of the Renewable Energy Development Center (CDER).This model is based on measured experimental data and compared with the Sandia mathematical model which descriptive in section 1.5.8.1.

We selected measurement data obtained for 10 clear day and 7 cloudy days of the PV system under normal operating conditions to estimate the conversion efficiency of PV inverters. The power measured on both the DC side and the AC side of the three inverters is plotted in Excel as a dispersion, in order to show the relationship between DC power and AC power, this relationship represents our model simplified inverter (MS).

Table 2.1 show the scatterplot (scatterplot) results for the three inverters, showing the relationship between AC power and DC power over a 10 day clear sky period.

Table 2.1: 10-day clear sky scatter plot results for three inverter

N	Date	Inverter1			Inverter2			Inverter3		
		a	b	R^2	a	b	R^2	a	b	R^2
1	11/06/2018	0,9581	12,707	1	0,9557	11,998	1	0,9563	14,200	1
2	24/06/2018	0,9582	15,443	1	0,9533	14,131	1	0,9550	10,108	1
3	27/06/2018	0,9572	12,532	1	0,9525	12,436	1	0,9578	13,583	1
4	02/07/2018	0,9547	17,252	1	0,9514	15,514	1	0,9566	16,187	1
5	12/07/2018	0,9604	8,2376	1	0,9547	8,5067	1	0,9565	10,543	1
6	18/07/2018	0,9589	12,618	1	0,9518	13,223	1	0,9581	13,443	1
7	24/07/2018	0,9592	7,8036	>0,99	0,9557	7,9007	>0,99	0,9594	10,376	>0,99
8	29/07/2018	0,9568	14,966	1	0,9513	5,3707	1	0,9562	15,685	1
9	30/07/2018	0,9596	5,1413	>0,99	0,9546	5,3707	>0,99	0,9597	6,5977	1
10	31/07/2018	0,9598	5,3146	>0,99	0,9570	5,3707	>0,99	0,9576	5,8731	>0,99
10 days for clear day		0,9589	10,007	>0,99	0,9546	9,6126	>0,99	0,9574	11,571	>0,99

Figures 2.3a, 2.3b and 2.4 are the data scatter plots for three SMA SB-3000 inverters

recorded during system operation at CDER, showing the relationship between AC power and DC power over a 10 day clear sky period.

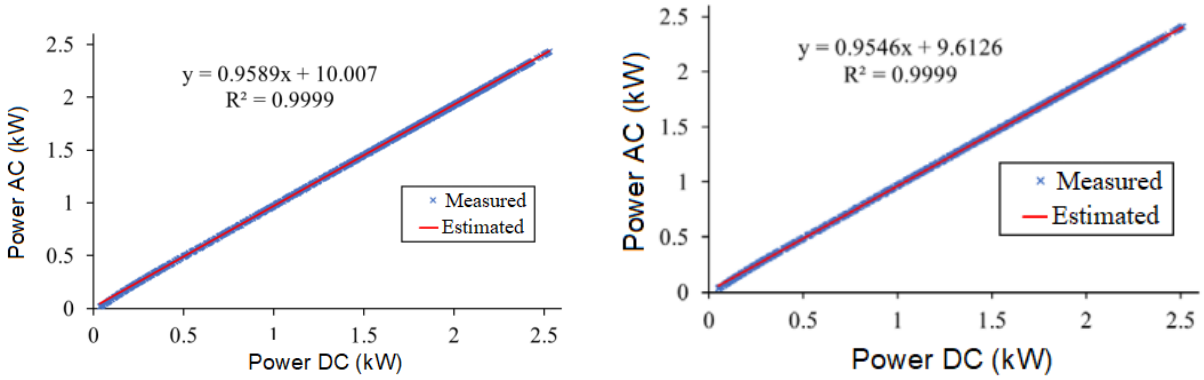

(a) (b)

Figure 2.3: Data scatter plot, showing the relationship between AC power and DC power over an extended 10-day clear sky test period (a) Inverter N1 (b) Inverter N2 [36]

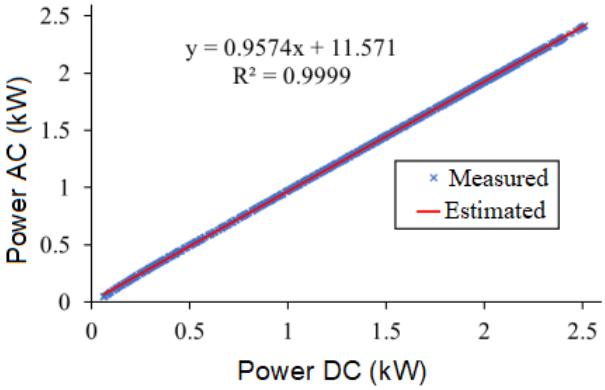

Figure 2.4: Inverter N 3 data scatter plot, showing the relationship between AC power and DC power over an extended 10-day clear sky test period [36]

Table 2.2 show the scatter plot results for the three sub-inverters, showing the relationship between AC power and DC power over a 7 day cloudy sky period.

Figures 2.5a , 2.5b and 2.6 are the data scatter plots of the three SMA SB-3000 inverters recorded during operation of our system at CDER, showing the relationship between AC power and DC power over a 7 day cloudy sky period.

Table 2.2: 7-day cloudy sky scatter plot results for three inverter

N	Date	Inverter1			Inverter2			Inverter3		
		a	b	R^2	a	b	R^2	a	b	R^2
1	26/06/2018	0.9585	11.398	>0,99	0.9528	12,263	>0,99	0,9599	7,0086	>0,99
2	03/07/2018	0.9604	9,5246	1	0.9542	8,7694	1	0,9591	11,014	1
3	09/07/2018	0.9565	16,883	1	0.9513	18,911	1	0,956	17,016	1
4	16/07/2018	0.9512	8,227	>0,99	0.9555	8,433	>0,99	0,9578	9,3457	>0,99
5	17/07/2018	0.9616	6,821	1	0.9562	7,6684	1	0,9603	9,0051	1
6	25/07/2018	0.9570	10,148	>0,99	0.9510	15,036	>0,99	0,9545	16,032	>0,99
7	26/07/2018	0.9576	7,3038	1	0.950	9,251	1	0,9544	10,86	1
7 days for clear day		0.9593	9,3592	>0,99	0.9536	10,443	>0,99	0,9573	11,578	>0,99

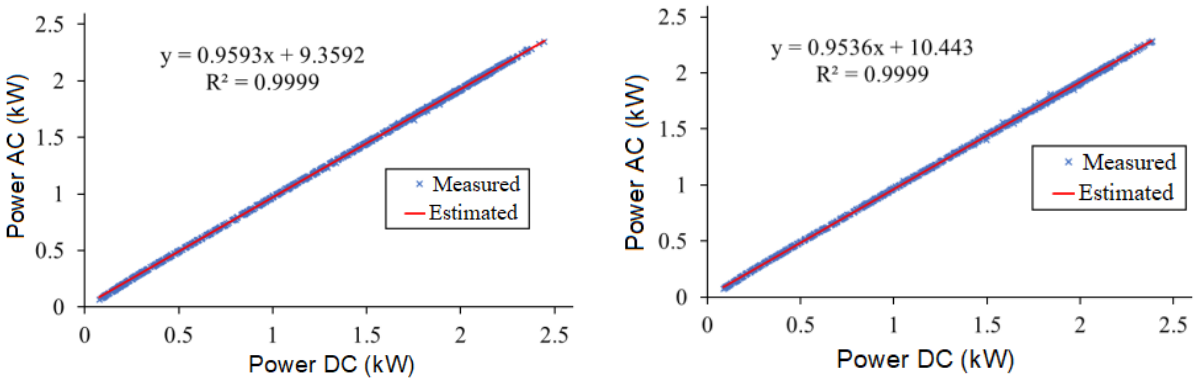

(a) (b)

Figure 2.5: Data scatter plot, showing the relationship between AC power and DC power over an extended 7 day cloudy sky test period (a) Inverter N1 (b) Inverter N2 [36]

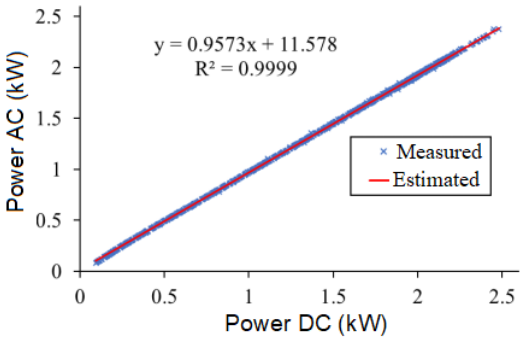

Figure 2.6: Inverter N 3 data scatter plot, showing the relationship between AC power and DC power over an extended 7 day cloudy sky test period [36]

Table 2.3 shows the results of the scatter plot of the data grouped of the three inverters by 1) Clear sky, 2) Cloudy sky, and 3) Clear and cloudy skies.

Table 2.3: Scatter plot results for the three inverters

Days	a	b	R
Clear day	0.9570	10.362	>0,99
Cloudy day	0.9568	10,395	>0,99
Clear and Cloudy	0.9569	10,361	>0,99

Figures 2.7a,2.7b and 2.8 are the grouped data scatter plots of the three SMA SB-3000 inverters recorded during system operation at CDER, showing the relationship between AC power and DC power over a period of 17 days including clear and cloudy days.

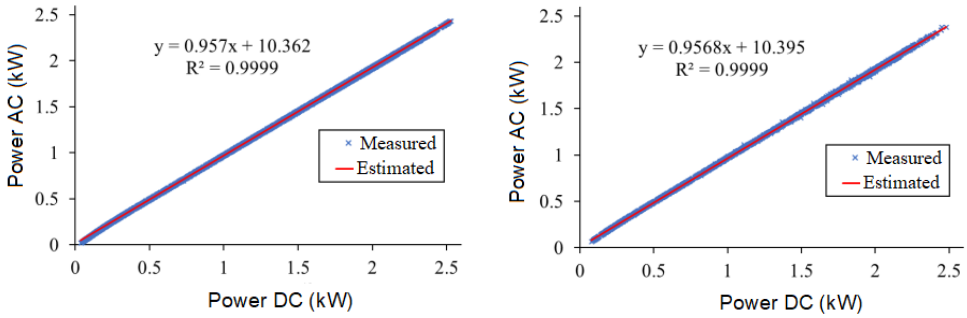

(a) (b)

Figure 2.7: Scatter plot of the grouped data of the three inverters, showing the relationship between AC power and DC power (a) clear days (b) cloudy days [36]

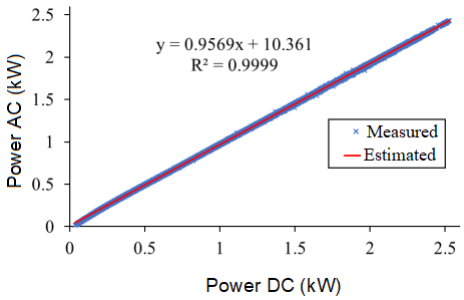

Figure 2.8: Scatter plot of the grouped data of the three inverters, showing the relationship between AC power and DC power for clear and cloudy days [36]

After analyzing the data measurement of DC (Pdc) and AC (Pac) power for the three SMA SB-3000 inverters for 10 days in clear skies and 7 days in cloudy skies using an Excel point cloud with a trend line , the relation drawn between AC and DC power is presented by the following equation:

$$P_{ac} = a.P_{dc} + b \tag{2.1}$$

a= Varies between 0,95 et 0,9616

b= Varies between 5,14 et 18,911

The regression coefficient R obtained is between 0.9998 and 1; which is more than enough to represent our simplified model. In order to compare our model to the Sandial model(SNL), the coefficients of the SNL inverter model were identified using the curve fitting toolbox in MATLAB software, where the fit is based on the nonlinear least squares method and the algorithm. region of trust see 2.9

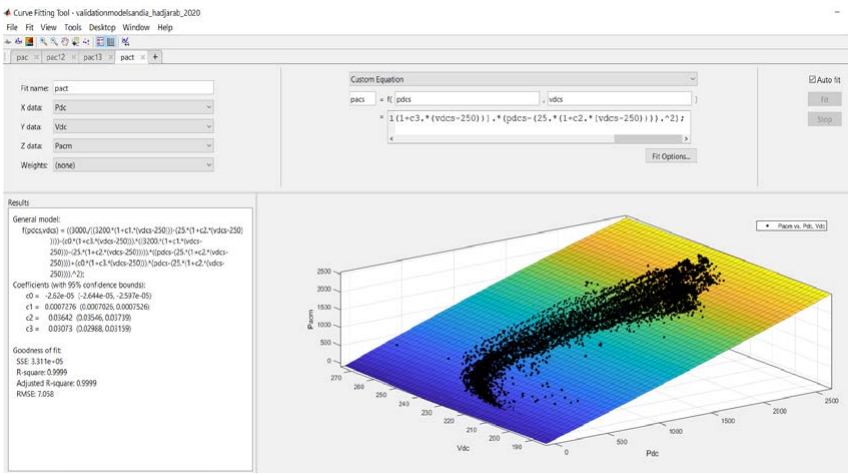

Figure 2.9: Identification coefficients in Matlab using the curve fitting tool. [36]

To have a similar electrical behavior of the inverter (SMA SB-3000TL) with good precision, four model parameters have been defined in the following values based on the specifications of the datasheet: P_{ac0} = 3000 W, P_{dc0} = 3200 W, V_{dc0} = 250 V and P_{S0}= 25 W

Tables 10 and 11 show the identified parameters of the SNL and SM models respectively for the three inverters.

Table 2.4: Identified parameters of the SNL model for the SMA SB3000TL inverter.

Days	C0	C1	C2	C3	R	RMSE(W)
Inverter1	-2,614e-05	0,001057	0,0627	0,04221	1	4,39
Inverter2	-5,179e-05	0,002884	0,03986	0,04761	>0,99	8,64
Inverter3	-2,645e-05	0,000742	0,03955	0,0301	>0,99	6,09
Three inverters	-2,62e-05	0,000728	0,03642	0,03073	>0,99	7,06

Table 2.5: Identified parameters of the SM model for the SMA SB3000TL inverter.

Days	a	b	R	RMSE(W)
Inverter1	0,959	9,746	>0,99	5,25
Inverter2	0,9542	9,912	>0,99	5,54
Inverter3	0,9574	11,56	>0,99	5,14
Three inverters	0,9569	10,36	>0,99	6,25

The results of the simulation of the AC power of the two models SM and SNL are presented during 5 days under different conditions: Clear sky, Cloudy sky,Shading on the PV generator,Very cloudy sky,Low illumination on the three inverters Figure 2.10 show AC power measured and estimated for Low illumination on the three inverters ,the results for different case is in detail in [36]

The comparison between the measured data of the AC power for five days with the data calculated by the two models (SNL and SM),show that The empirical model developed faithfully reproduces the characteristics of the AC power delivered.It has been shown that using this simple model is sufficient to obtain all parameters; this is very useful for quick energy sizing with only one parameter to identify especially if we do not have the performance parameters of the inverter.

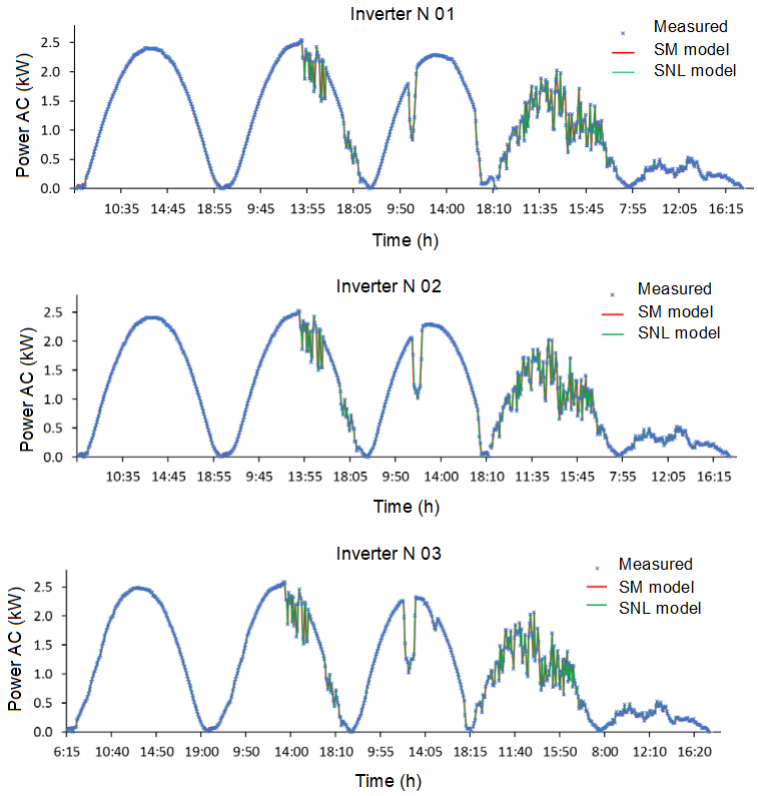

Figure 2.10: AC power measured and estimated for the three inverter. [36]

2.4 Norm IEC 61724

The IEC 61724 norms is a series of international standards for specifications for the measuring and monitoring of PV systems and provides recommendations for the analysis and monitoring of the performance of PV systems. Although IEC 61724-1, -2, and -3 have replaced this standard [37], guidance on data processing and measurement approaches for short-term capacity and long-term system performance is provided.

2.4.1 The Standard IEC61724-1

PVS performance monitoring was revised and released on February 2017, in which "accuracy classes" are defined [38]. The accuracy classe is not dertemined by the devices that used ,but also by quality checks and measurement procedures.

a) Accuracy classes

The standard contains detailed specifications at monitoring system component level. Other means, such as satellite observation, can be used to derive small-scale PV systems, Class C, radiance and environmental measurements and it is acceptable to estimate some measurements from other nearby and reliable data sources for Class B[39]. However, for Class A all parameters must be monitored at the site, the most important criteria in different class is shown in Table2.6 [40]

Table 2.6: IEC 61724-1 PV plant performance monitoring classifcations[40]

Typical applications	Class C Basic Accuracy	Claa B Medium Accuracy	Class A High Accuracy
Basic system performance assessment	X	X	X
Documentation of a performance guarantee		X	X
System losses analysis		X	X
Electricity network interaction assessment			X
Fault location			X
PV technology assessment			X
Precise PV system degradation measurement			X

b) Communication and Connection

A 2-wire Rs-485 with Modbus RTU protocol, using separately addressable inverters and monitoring equipment on a minimal number of data bus loops, is now required for data communication within PV plants[38].

c) Number of Plant Monitoring Systems

On the basis that all PV modules are installed in the same orientation, the recommended minimum number of monitoring systems, IEC 61724-1 refers to the plant's installed AC power capacity are shown in Table 2.7[40]

d) Equipment and measurements

Table 2.7: IEC 61724-1 minimum number of monitoring systems by plant capacity[40]

Plant capacity (AC)	Number of monitoring systems
< 5MW	1
≥ 5 MW to < 40MW	2
≥ 40 MW to < 100MW	3
≥ 100 MW to < 2000MW	4
≥ 200 MW to < 300MW	5
≥ 300 MW to < 500MW	6
≥ 500MW to < 750MW	7
≥ 750 MW	8

Measurement instruments and procedures are recommended to comply with IEC 61 724-1 class A specifications on all calculated parameters. However, a class B or class C evaluation may also be completed by using the default test boundary [38].

2.4.2 The Standard IEC61724-2

In IEC TS 61724-2 the performance quantified with a shorter test, Even if there might be significant uncertainty associated with that test.This is as a supplement to the IEC TS 61724-3. This method adjusted the measured parameters by the correction factor,then compared with the target plant performance to identify whether the plant operates above or below expectations at the target reference conditions [41].

2.4.3 The Standard IEC61724-3

Performance of the photovoltaic system- Part 3: Energy evaluation process describes a one-year test that analyzes performance over the full range of operating conditions and is the preferred method for assessing system performance[42]

2.5 Literature Review

Several existing parameters are typically used to study and assess the performance of a PV plant. The most common methods are 1) specific yield, 2) capacity factor (CF), and 3)

performance ratio (PR). The specific yield is a non-normalized criterion, which is most effective in comparing the performance of PV plants sharing the same location, regardless of their mounting structure [11]. The CF/CUF parameter is a good method for identifying the PV's total power capacity and is frequently reported as part of plant performances. This parameter is most effective for comparing various sources of energy [43]. The second parameter, namely 'specific yield' is a non-normalized criterion which is most effective in comparing the performance of PV plants sharing the same location, regardless of their mounting structure [11]. The third parameter Performance Ratio (PR) is considered the most reliable method as it gives a deep and complete study of performance by taking into consideration different losses that occur in the PV plant such as losses from environmental parameters, PV array losses, and inverter losses [44]. The PR is also independent of the size which makes it easy to compare it to any other PV plant in the world [45–47]. There are different methods to calculate the PR of a grid-connected PV plant. The most used methods are the ones indicated by The International Energy Agency (IEA) guidelines of standard IEC 61724 and the International Energy Agency PV Power System (IEA-PVPS) Program TASK 2[48–51]. Past research has shown the different aims and purposes for conducting performance studies. Some existing research studied the individual components of the PV system connected to the grid (i.e: PV array or inverter and grid). For example, the work conducted by [52–57, 57, 58] used the performance study to compare the different technologies of PV modules (Amorphous Silicon (a-Si), Poly Crystalline Silicon (p-Si), and mono Crystalline Silicon, cadmium-telluride (Cd-Te)). Research by [31, 46] reviewed the degradation of PV modules under outdoor conditions in aims of improving the PV qualification standards. On the other hand, papers [49, 59] assessed the different problems in the inverter and the connection to the grid to identify any malfunction and/or operational issues in the PV plant. Mathematical models for the system are developed based on the collected monitored data to provide accurate performance models in the study [60] . Rather than focusing on subparts of the PV system, [60–66] conducted a complete study on the entire PV system and used the PR to analyze the performance in different sites to see the influence of meteorology (geography)

or different climatic conditions on PV plants. In [67–72], the performance study was used to compare the different architectures of PV plants(BIPV, BAPV, fixed, tracking panel or different tilt and orientation). Another set of studies focused on analyzing simulation results [73–78] mostly produced by softwares such as PVsyst and Matlab. Other studies compared simulated performance parameters of grid-connected PV plants to those from a measured one [48, 50, 79–84]. Furthermore, a set of studies looked into assessing the effect of time on the deterioration of performance. Works [47, 61, 66, 85–92] conducted an experimental analysis of performance by using data monitored and collected from BIPV, BAPV, or a fixed plant and compared it to another plant in different places around the world and assessed its performance through time (between 6 months and 3 years). However, such investigations fall short in providing a realistic insight on how a PV system actually performs with time, especially that the assessment period is less than three years where newly installed PV systems rarely show any vulnerabilities. This is for the wild world research, for Algeria research about PV grid connected system it still few, the most research was done on the PV grid connected system installed at the lab of renewable energy institute(CDER), because it is the first system in Algeria and the only one connected to the distribution network .the research took different aspect, the search deal with evaluation of global solar irradiation on inclined surface according to different models for the Bouzareah site in[93], the PV module modelling of the plant in [35, 94]and Evaluate their energy production after 12-Years of Operating in [95],the inverter modelling in [36].simulation of component of the plant of CDER with different software, with Simulink in [96, 97], with PSpice in [98] and with mathematical model in [99]. The monitoring of the system by using the LabVIEW in [84, 100, 100–103] and detect faults diagnose in system with different approach was studied in [104–107],The deferent losses were studied for the system ,the dust impact in [108, 109], the aging for the pv module by studying the Degradation rate in [110**?**], and Mismatch Power Losses in [111, 112].the studies Power Quality in term of voltage ,current and THD at the injection point PCC of the CDER plant , in [113–116, 116],An Experimental Analysis According to DIN VDE 0126-1-1 in [117], and reactive power issues in the system in

[118],the Performance Analysis per season was done in [119] with the presence an inverter with transformer. our study plays a vital role in understanding and assessing long-standing PV systems (working for more than 14 years) and their performance. Our research tries to compute the PR of the system for three last year from 2016 to 2018 after operating for more than a decade and compares the three sub-systems that have the same type of modules and inverters and located on the same site. We aim that our study sheds light on long-time PV systems and the reliability of their performance

2.6 Root cause exploration of decreasing performance

The system has more then 14 year of operation, even inverter replacement of CDER plant.The performances parameters will decrease theoretically, we need to know the main causes for this reducing, our methodology consist of the steps below:

a) Analyze the performance of the systems of our plant with the norm IEC 61724 Fig2.11;

b) Analyze the performance of each sub-systems of our plant; Check whether the 3 subsystems have the same performance since they are identical and operate under the same metrological conditions.

c) Draw the curve of the hourly energy injected into the electrical networks as a function of radiation to find all the days during which the performance of the power plant decreases.

d) Deepen our knowledge of the causes of sub-system disconnection, which reduces the amount of energy injected into the network..

e) In order to deal with deferent losses of the system,PVsyst software was chosen to simulated our system. which it will descripted in the next chapter.

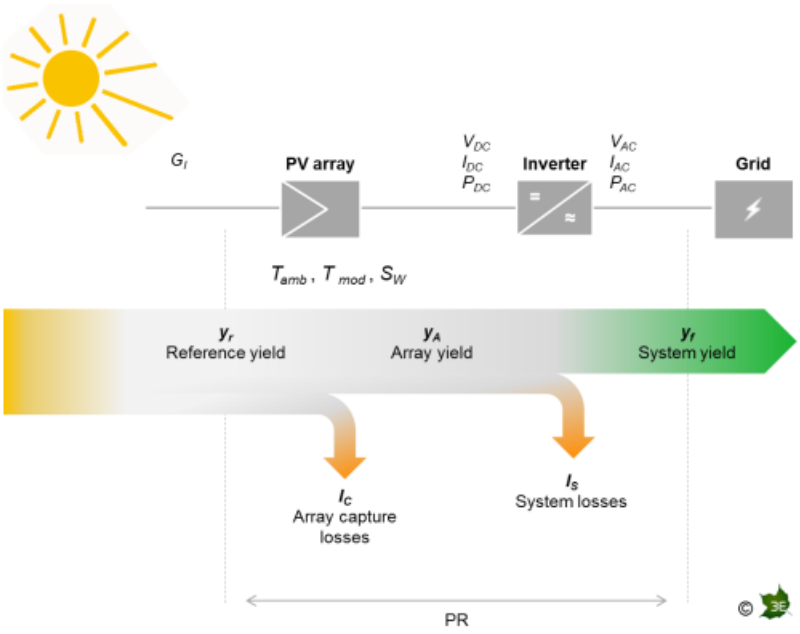

Figure 2.11: Performance Diagram [34]

2.7 Performance parameters

2.7.1 Energy output DC

The total daily $E_{(AC,d)}$ and monthly $E_{(AC,m)}$ energy generated by the PV system [46, 47]

$$E_{(AC,D)} = \sum_{t=1}^{24} E_{AC,t} \tag{2.2a}$$

$$E_{(AC,m)} = \sum_{d=1}^{N} E_{AC,d} \tag{2.2b}$$

Where N is the number of days in the month and $E_{(AC)}$ is the instantaneous measured value. The instantaneous energy output is obtained by measuring the energy generated by the PV system after passing the DC/AC inverter at a 5 min time step.

2.7.2 System yields

The system yields, also known as 'normalized indicators' act as key variables for comparing the performance of the existing grid-connected PV systems under various

operating conditions. They are classified into three types as shown in Figure 2.11: a) Array yield, b) Final yield and c) Reference yield.

a) Reference Yield (Y_R)

The Reference Yield is the theoretical obtainable solar energy for a certain period of time at a certain location where the PV power system is installed [56]. In technical terms, reference yield is the ratio of total energy in plane solar insolation $Ht(kWh/m^2)$ to the reference irradiance $G(1kW/m^2)$ [46].

$$Y_{(R)} = \frac{H_t(kWh/m^2)}{G(kW/m^2)} \tag{2.3}$$

b) Array yield (Y_A)

The array yield (Y_A) is defined as the energy output from a PV array over a defined period (day, month or year) E_{DC} divided by its rated power ($P_{PV,rated}$) and is given as [47]:

$$Y_{(A,d)} = \frac{E_{DC,d}}{P_{pv,rated}} \tag{2.4a}$$

$$Y_{(A,m)} = \frac{1}{N}\sum_{d=1}^{N} Y_{A,d} \tag{2.4b}$$

a) Final yield (Y_F) The Final yield (Y_F) is the total energy generated by the PV system for a defined period (day, month or year) E_{AC} divided by the rated output power ($P_{PV,rated}$) of the installed PV system at standard test conditions (STC) and is given by the following equation [11, 120]

$$Y_{(F,d)} = \frac{E_{AC,d}}{P_{pv,rated}} \tag{2.5a}$$

$$Y_{(F,m)} = \frac{1}{N}\sum_{d=1}^{N} Y_{F,d} \tag{2.5b}$$

2.7.3 System Efficiency

Efficiency is the metric used to calculate how much of the available solar energy is in fact converted to actual utilized electrical energy, by which the performance of the installed PV system is assessed. Depending on the type of collected data and desired level of resolution, efficiency can be classified into three types: a) PV module efficiency, b) System efficiency and c) Inverter efficiency. The period granularity of efficiency can be calculated instantaneously, hourly, daily, monthly or annually.

a) Array efficiency

Module efficiency or also known as PV efficiency is the ratio of PV output power to the power of the sun (solar radiation) on the PV surface at a specific time interval [60]. The monthly module efficiency is calculated using the following equation 2.6 where P_{DC} is the DC power in kW and Ht is the solar radiation and A_m is the PV module area in m^2.

$$\eta_{(PV)} = \frac{P_{DC}}{H_t * A_m} \tag{2.6}$$

b) Inverter efficiency

The inverter efficiency, frequently called conversion efficiency is the ratio of AC power produced by the inverter to the DC power generated by the PV array system [48, 120]. The monthly inverter efficiency is calculated using the following equation:

$$\eta_{(inv)} = \frac{P_{AC}}{P_{DC}} \tag{2.7}$$

c) System efficiency

The energy efficiency of PV systems is the ratio of DC power output generated by the PV (or the electrical power generated to the energy input), which is the product of the solar array area and the insolation incident on the PV surface [48] The monthly system efficiency is calculated using the following equation:

$$\eta_{(sys)} = \frac{P_{AC}}{H_t * A_m} \tag{2.8}$$

2.7.4 Losses in PV grid connected systems

Loss is a metric used to calculate the amount of lost energy from solar energy collection by the PV modules to electrical energy production. This metric help in investigating the sources of losses and precisely allocating inefficiency. There are various sources by which energy losses occur in the PV plant where some are merely dependent on external factors such as climatic conditions (i.e: fog) while other are related to the system itself such as the PV arrays, inverters, etc. Therefore, losses are categorized into two types: a) Array Losses and b) System Losses as shown in Figure2.12 .

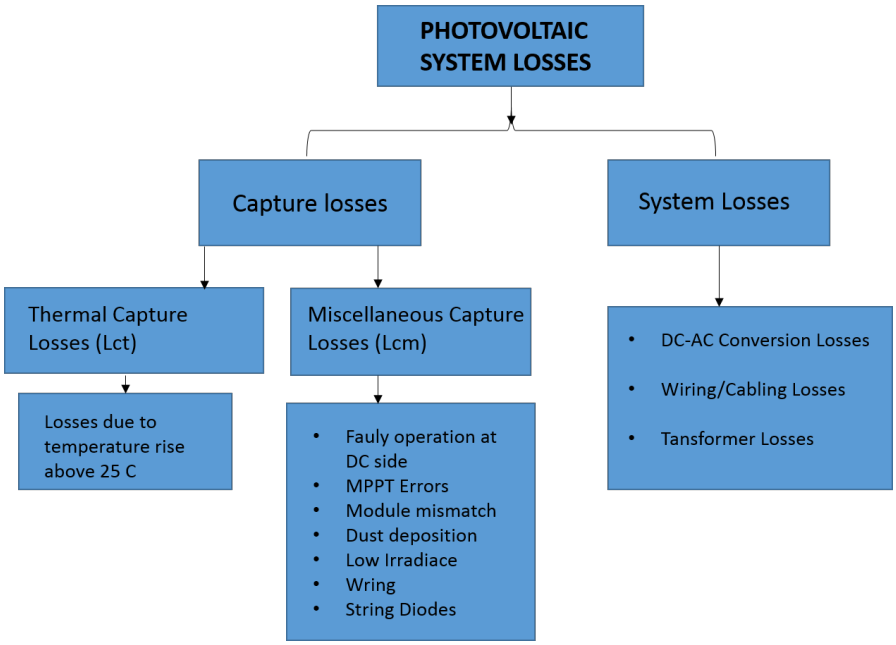

Figure 2.12: Categorization of losses in PV Grid connected system

a) Array losses

Array losses also called "Capture Losses (Lc)" are due to the PV array losses. They are defined as all the events penalizing the available array output energy with respect to the PV-module nominal power STC conditions [48]. These events include (but not limited to) the following: shading losses and thermal behavior of the PV array, Mismatch losses, MPP loss to the efficiency of the Maximum Power Point Tracker (MPPT) technique

employed [121]. Furthermore, there are other small events that might also slightly add to losses such as the soiling effect, ohmic wiring losses, and degradation losses. Array capture losses (Lc) can be defined as [47, 91]:

$$L_c = Y_R - Y_A \tag{2.9}$$

- Thermal capture losses (LCt) Thermal capture losse results from an array operating temperature other than 25°C as recorded under standard test conditions (STC) The thermal capture loss is the difference between the reference yield and the corrected reference yield,given by the equation[122]

$$L_{ct} = Y_R - Y_T \tag{2.10}$$

  Where the corrected reference yield is given by the equation:

$$Y_T = Y_R(1 - Ct(T_m - 25)) \tag{2.11}$$

  where C_t is the temperature coefficient (%/C) and T_m is module temperature.

- Miscellaneous capture losses (Lcm) Miscellaneous capture losses may occur for one or several reasons, such as wiring losses in the cables between PV panels and inverter, losses due to soiling, diodes, shading and/or component failure. Miscellaneous capture loss is the difference between array capture losses and thermal capture losses, given by the equation [90]:

$$L_{cm} = L_c - L_{ct} \tag{2.12}$$

  The “mismatch losses, modules and strings”is related to the normal small differences between the modules, even if they are fabricated in the same way.

- Lcr and Lsr, we can also define Lcr and Lsr are relative values, normalized to the incident energy:

$$L_{cr} = \frac{L_c}{Y_r} \tag{2.13}$$

$$L_{sr} = \frac{L_s}{Y_r} \tag{2.14}$$

b) System losses

System losses (Ls) result from the inverter losses during an operation related to the efficiency curve, loss due to power threshold and inverter losses due to low or upper voltage MPP window [121] and are given as [64]

$$L_S = Y_A - Y_F \tag{2.15}$$

2.7.5 Capacity factor(CF)

The capacity factor (CF) is defined as the ratio of the actual annual energy output (EAC,a) of the PV system to the amount of energy the PV system would generate if it operates at full rated power (PPV, rated) for 24 h per day for year and is given as [21]:

$$CF_m = \frac{E_{AC,m}}{(P_{pv,rated} * 24 * N)} \tag{2.16}$$

$$CF_y = \frac{E_{AC,y}}{(P_{pv,rated} * 8760)} \tag{2.17}$$

Where CF_m and CF_y represents monthly and yearly capacity factor respectively and N the number of day in the month,

2.7.6 Performance ratio

Performance ration is used to evaluate the long-term changes in the performance and the overall effect of losses in the plant [46]. The performance ratio corresponds to the ratio of useful energy to the energy which would be generated by a lossless ideal PV plant (theoretical energy) on a predetermined periodic basis. This ratio is very important as it is independent of the size and location of the system, hence acts as an unbiased metric for studying and comparing the different PV systems. It is defined as the ratio of the final yield (YF) to the reference yield (YR) and it represents the total losses in the PV system when converting from DC to AC. It is a dimensionless quantity. The performance

ratio is also expressed as[47]:

$$PR = \frac{Y_F}{Y_R} \tag{2.18}$$

According to the to the European PV Guidelines the system is below expected rates refere to the According to the European PV Guidelines, Any PR rate ranging between 0.8-0.85 is considered acceptable as per European PV Guidelines, whereas values falling short of 0.75 indicate an issue with the performance[72].

2.7.7 Weather-Corrected Performance Ratio (WCPR)

The performance characteristics of the PR formula are based on STC, which corresponds to a 25°C module temperature. Since the modules work under normal conditions at higher temperatures, a temperature adjustment of the STC power can be performed. This calculation of the temperature corrected performance ratio (PR) is based on the measured back panel temperature [123].

$$WCPR = \frac{PR}{1 + \gamma_{mmp}(T_m - 25°C)} \tag{2.19}$$

Where

γ_{mmp} is the temperature coefficient of the solar cell.

T_m the temperature of the module.

2.8 Grid connection

2.8.1 Grid requirements for PV systems

The connection PV system to the grid requires to ensure smoother penetration , without compromising the power quality and stability of the grid [23]. Photovoltaic power systems affect mostly low and medium-voltage network and only approximately 1% of the high-voltage network is fed by PV power [124], meaning that the demand for grid stability reflects the low and the medium voltage networks. The GCs represent these requirements

and address to network operators, project designers as well as component manufacturers (mostly PV inverter manufacturers) in order to design their products according to some uniform guidance [125]. However, due to the different grid characteristics there are many different GCs that has been introduced around the world. Countries like USA, China and Australia have different requirements among them. Even inside Europe there are many differences.

2.8.2 Laws and regulations

In order to integrate the renewable energy in Algeria, the Ministry of Energy create the Standing Committee for monitoring and updating Technical Rules for Connection to the medium and low voltage Network of Electricity (CPRTCE)[126]. The committee coordinate with Sonalgaz which is a government-owned company that controls and regulate Algeria National Grid to make sure that the grid is stable it has to be a balance between the produced and consumed electricity. In February 2020 have introduced a new code referring to the connection and operation of distributed power generation plants to the medium and low-voltage power grid. This code was published as a consequence of the Code of 2008.
Since February 1^{st}, 2020, all the new PV plants should comply with this code. The main requirement for the integration plant to the low voltage network as follows :

1. Telecommunications and remote information system The Solar Plant must have technical equipment at the Grid Connection Point to process and or transfer the following information for the power system management systems furnished with a real-timestamp. The Measured values from the Solar Plant:
    - Active Power(total KW)
    - Reactive Power (total kVAr)
    - frequency (H)
2. Energy metering equipment.

3. Non-synchronous production installations must be equipped with a system consisting of protection and a decoupling device.

4. The decoupling device must comply with the adopted standards and must include the following functions:

   - Overvoltage and Undervoltage;
   - Over-frequency and under-frequency
   - Anti-islanding;

2.9 The new Technical Connection Rules (TCR) requirement

The production plant to be connected to the distribution network of less than or equal to 10MW, The normal operation requirements can be divided to the frequency deviation, voltage deviation, and reactive power control.

2.9.1 Frequency deviation

According to the Technical Connection Rules (TCR) [126], a small PV system connected to the LV grid side has to operate properly within a frequency range of 49.8 Hz - 50.2 Hz based on nominal frequency of 50 Hz. This means that the PV plant has to trip when the frequency drops to 49.8 Hz or increased to 50.2 Hz.

2.9.2 Voltage Deviation and Reactive Power

In the case of reactive power, the new TCR require that the photovoltaic power plants PVPP injects or absorbs reactive power according to a predefined relationship between the active and the reactive power (power factor (pf)) or a specific value of reactive power. The TCR presented by the committee requires that the PVPP work under a specific capability curve (Figure 2.13)[126].

1. Under normal operating conditions, non-synchronous production facilities must be designed for a cos (phi) of 0.95 at the injection point at nominal active power.

2. Active power, the non-synchronous electricity production installation must be able to absorb a maximum of reactive $Q = -0.30xP_{nom}$ at nominal voltage.

3. At an active power greater than $P = 0.1xP_{nom}$, non-synchronous production installations must operate in the operating range defined by the diagram (P, U, Q) without limitation of duration at any point within this normal operating range. The diagram (P, U, Q) is that specified by Figure 2.13 below. The voltage variation ranges are between the minimum and maximum values (Uminn and Umaxn defined as follows:

   a) For overhead networks, ±12% around the nominal value of the voltage.

   b) For underground networks, ±6% around the nominal value of the voltage.

4. At an active power lower than $= 0.1xPnom$ (including powers less than 0), non-synchronous installations must be able to operate at reactive power in the range $Q_{min0} < Q < Q_{max0}$ with $Q_{min0} = -0.05xPnom$ and $Q_{max0} = 0.05xP_{nom}$.

5. Non-synchronous production facilities must be equipped with regulators to control the reactive power or the power factor at the injection point.

2.9.3 Reactive power control

The Solar Plant must be able to control reactive power at the Grid Connection Point with $cos(\phi)$ equal to 0.95. In addition, it be able to control reactive power with two option:

- Active power as a function of voltage.

- Reactive power as a function of voltage Q(U).

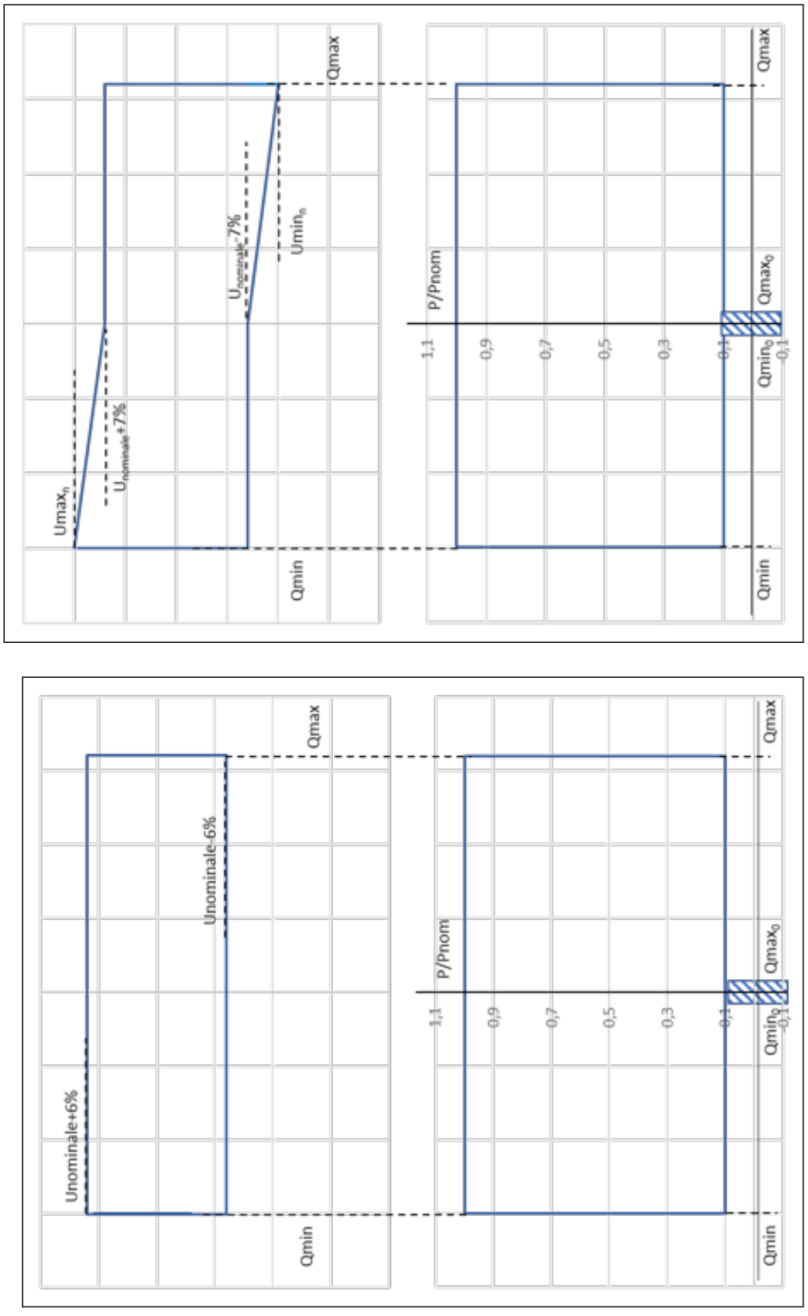

Figure 7 : Capacité réactive exigée des installations à production non-synchrones raccordées au réseau de distribution aérien (a) et souterrain (b)

Figure 2.13: Voltage Deviation and Reactive Power [126]

2.9.4 Voltage during a fault

The non-synchronous production installation must remain coupled and synchronized to the electrical network during faults with a nominal voltage for a duration of 0.3

seconds and during faults with a retained voltage of 10% of the nominal voltage for a duration of 0.6 seconds. The voltages and time delays for which the Non-synchronous production units must remain in service are specified in Table 2.8and Figure 2.14 as show below. During the temporary voltage drop Solar Plant must must inject reactive

Table 2.8: voltage and time during a fault[126]

Voltage	Time
U > Umin	unlimited
0.1 p.u< V < Umin	t_{rec1}=0.6 sec and t_{rec3}=3 sec
0< U < 0.1 p.u	t_{clear}=0.3 sec

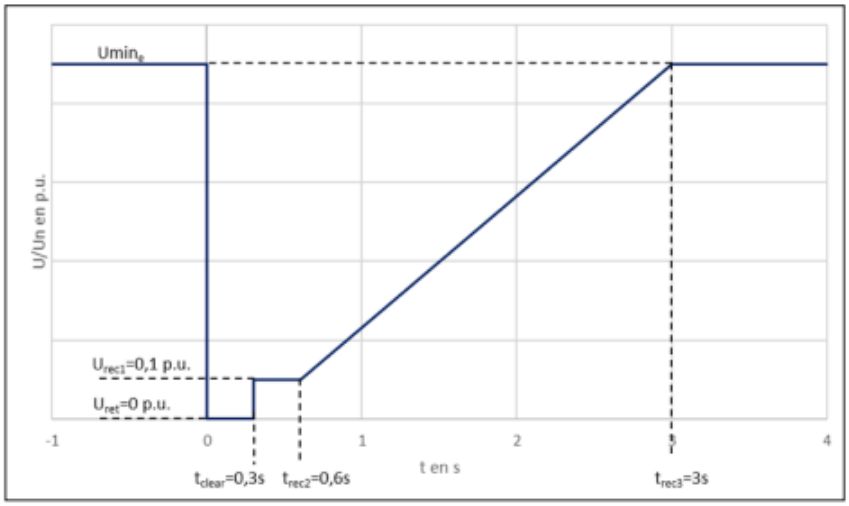

Figure 2.14: Voltages and time for which non-synchronous production plant connected to the distribution network must remain in service[126].

current according to Figure 2.15 during time 60 ms. The above line represents the required minimum reactive current, expressed by the ratio of the reactive current and the nominal reactive current in per unit, against the voltage drop, expressed by the ratio of the actual voltage value and its nominal value in per unit at the grid connection point. The Δi_q is the required reactive current change during fault,Δu_t relevant voltage change during the fault,and the factor Kshall be adjustable in the range from 0 to 10.

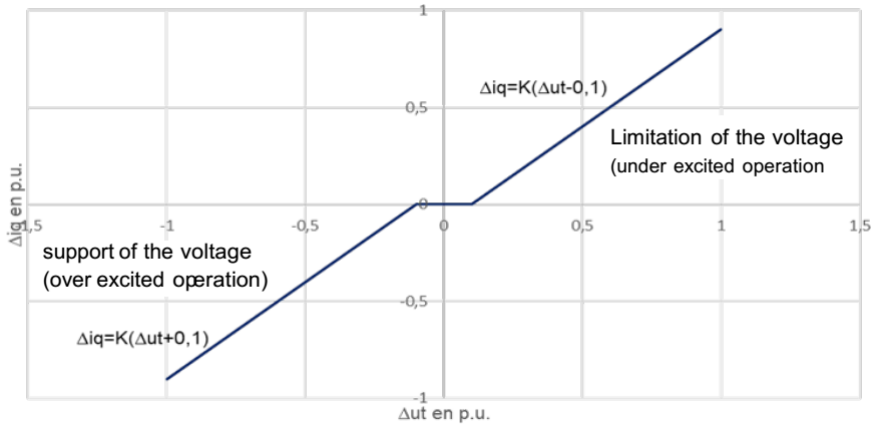

Figure 2.15: Current injection during the fault. [126]

2.10 Conclusion

The performance parameters are presented according to the three parts of the new Standard IEC61724, each monitoring system classification provides a guideline of what measurements can be done. The monitoring classes are divided in three parts with A being the one with highest accuracy and class C being the most basic one and a medium accuracy level of class B. Our plant fits class A accuracy, which we will see it in the ChapterIII . The new parameters of performance take into consideration the effect of temperature to the losses in the array and to the PR in the IEC61724-3 compared to the PR of old norm. This newly added parameter has been named as 'weather-corrected PR'. Different uses of Performance analysis studies that have been reported in the literature was presented. The The new Technical Connection Rules (TCR) of 2020 is described to determine the requirements for new or modified Solar Energy Plants for connection to the low voltage, so that it ensures security and quality parameters of the grid.

CHAPTER 3

SIMULATED PERFORMANCE PARAMETERS

3.1 Introduction

This section describes the details of the grid-tied PV system used in this study as well as the methods utilized for simulation analysis and performance calculation. The first subsection delves into reporting the PV plant and its characteristics while also explaining how data is acquired and its flow in the PV system. The second subsection investigates methods of computing predictive Performance parameters.

3.2 Plant Description

The PV system of this work commemorates the first practical application of a grid-connected system in Algeria. The project entitled "Photovoltaic Experimentation Center for Algeria" was funded by the Spanish Agency for International Cooperation (AECI) [127], and fully implemented by an internal CDER team, the photovoltaic grid connected schema of CDER is shown in Figure 3.1. The plant has been continuously generating

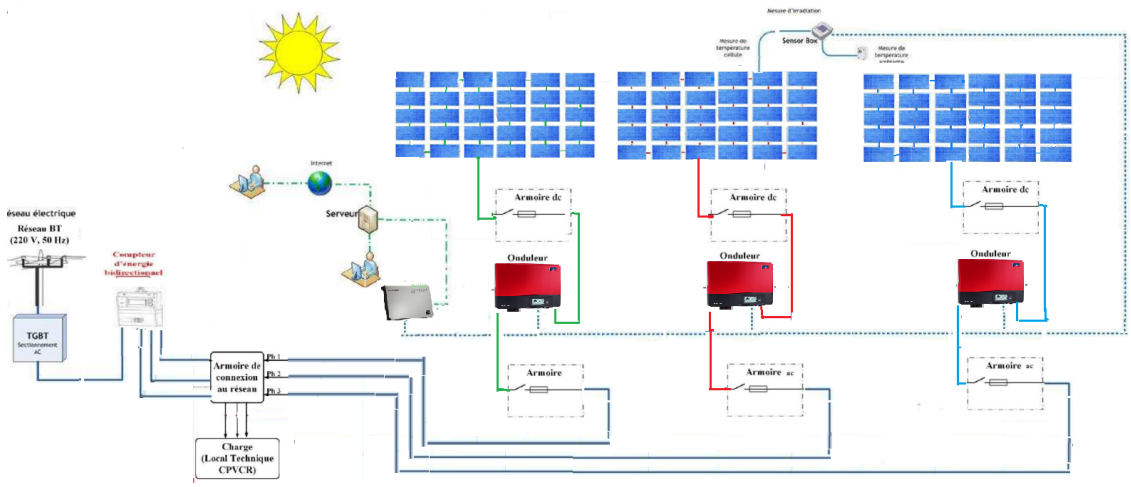

Figure 3.1: schema of Photovoltaic grid connected plant of CDER

power since 15 October 2004 with the exception of two short periods when inverters were replaced twice in February 2010 and February 2016 respectively. Unlike the inverters the photovoltaic panel themselves have not been altered since their initial installation. An inside view of the control room is illustrated in Figure 3.2.

Figure 3.2: An overview of the control room and sub-array.

3.2.1 Array

The plant is comprised of 90 polycrystalline modules (Model: ND-235E1H) covering a total area of 77 meter-squared.The plant is divided into three sub-systems of 3 kWp arranged in two parallel strings, 15 per string(see Figure3.3). Each module is capable of producing a peak power of 106 Wp at the efficiency of 12.1% As mention in Table 3.1.

Table 3.1: PV module specifications

PV module	Specification
Type of material	mono-crystalline
maximum power(Pmax)	106 Wc
Open circuited voltage (Voc)	21.8 V
Short circuited current (Isc)	6.54 A
Efficiency	12.5 %

Hence, the system can generate a total of 9,5kWp of installed capacity. For best results, modules should be tilted at an 'ideal 'angle. The optimum tilt angle for maximum annual collection is the latitude itself provided the azimuth angle is less than 160° [85, 128, 129]. In our case, however,the panels were fixed at a tilting angle of 29° as opposed to 36 °, which favors summer sunlight direction as electricity consumption increases dramatically due to the usage of air conditioners. Additionally, since the building has a rectangular shape with its longest side facing southwest and due to the

roof's restricted configuration, the panels were oriented southwest instead of south in order to maximize PV utilization.

Figure 3.3: overview of the plant in the roof of the lab

3.2.2 Inverter

Each subsystem is connected to a single phase inverter (SMA Sunny Boy 3000TLST-21, Germany) which is the most successful PV inverter for residential systems with a rated power of 3.0 kW in order to convert the DC to AC . These are transformerless inverters (transformer low TL) with a single input with MPPT tracker (Single Tracker ST) and integrates several functions ensuring both the optimization of production and the safety of the installation, the technical characteristic is shown in Table 3.2.

Table 3.2: Inverter characteristics

Inverter	Specification
Rated power	3000VA
AC voltage	220-240V
Efficiency	96.0%

The generated energy is mainly consumed by the office users and overhead at the research center. In cases of energy overflow, the excess is injected into a phase of the public low voltage distribution network provided by the National Company (Sonelgaz) 220 V50Hz [84, 130]. When the plant is incapable of producing sufficient supply either due to high demand or lack of energy sources (at night), the deficit is supplied by the main grid. The built-in LCD screen as shown in Figure 3.4 the user to view up to the

minute, the current inverter operating data (Current power, daily energy, total energy since inverter installations, input voltage) as well as faults and malfunctions.

Figure 3.4: Sunny boy, 3000TLST-21 inverter

3.2.3 Protection System

Our plant is equipped with a protection system at two locations. The first is DC protection located between the PV array and the inverter, and the second is AC protection found between the inverter and grid injection as shown in Figure 3.2.

3.2.4 Grid Connection Block

The installation is equipped with two of the three-phase energy meter (IEM 3110) (electric meter manufactured by Schneider one for solar production and the second for the load. And two circuit breaker (DPE 4P) manufactured by Schneider, one for solar production and the second for the utility (Sonalgaz).

3.2.5 Data Measuring and Monitoring System

In order to precisely calculate the different performance parameters, data monitoring should be consistent and reliable throughout the complete assessment period. Data monitoring is one of the requirements for utility-scale PV systems where it is mainly used to assess PV performance and assure its compliance with regulatory reporting status as shown is Figure 3.5 more recently, data is being utilized in commercial applications [87]

Figure 3.5: Overview of the data monitoring equipment

3.2.5.1 Sunny SensorBox

Sunny SensorBox as shown in Figure 3.6,it installed on the PV module integrated an irradiation sensor as well as housing various instruments to measure climatic data (wind speed, ambient and panel temperature). The collected data in the PV plant is recorded

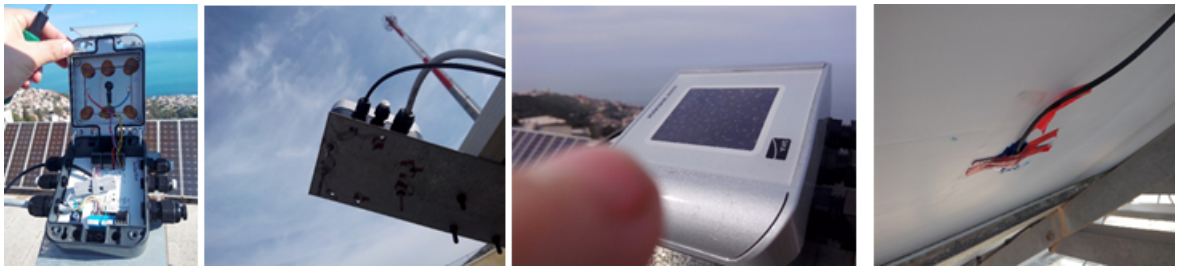

Figure 3.6: Sunny sensor box

at five minutes time steps and saved on a daily basis in SMA Sunny WebBox a data logger. These are then communicated with the WeBox through RS485 cables and a Power Injector (see Figure 3.7), which is an electronic analog-to-digital processing device that resides in the physical layer [87].

3.2.5.2 Sunny Webbox

Sunny WebBox is the central communication interface, it acts as a link between the PV plant and its operator. The Sunny WebBox collects and archives all data from the

Figure 3.7: RS485-Power Injector

connected devices, thus enabling comprehensive monitoring of the plant PV, All recorded data is made available to the operator by Sunny WebBox via an Internet connection or a GSM modem [3].

3.2.5.3 Data management

The Sunny WebBox provides various modern data processing options for professional data management. The recorded data values, which provide you with detailed information of your system, are saved in conventional CSV or XML file formats on the Sunny WebBox [131]. The ability to exchange data by FTP allows you to easily transfer these values to the PC(see Figure 3.8. In this way, valuable system data can not only be saved on your computer for the long-term, but can also be displayed according to your preferences using MS Excel, for example, and create straightforward evaluations over the course of the day, month and year. Additionally, it is possible to send plant data simultaneously to the Sunny Portal.

3.2.5.4 Sunny Portal

Sunny portal is another way to visualizing the data and have access to key data at any time, SMA inverter will connect to the Sunny Portal via WIFI or Bluetooth connection and all of your systems data will appear on our Sunny Portal PV system profile that was created and set the parameters to be shown,example CO2 savings,Power and Feed-in tariff [132]. Plant profile on Sunny Portal will also include the name of the plant

Figure 3.8: SMA data interface

(structure the panels are placed on), location, and a date of commissioning, plant power, annual production and the names of the operators see Figure3.9

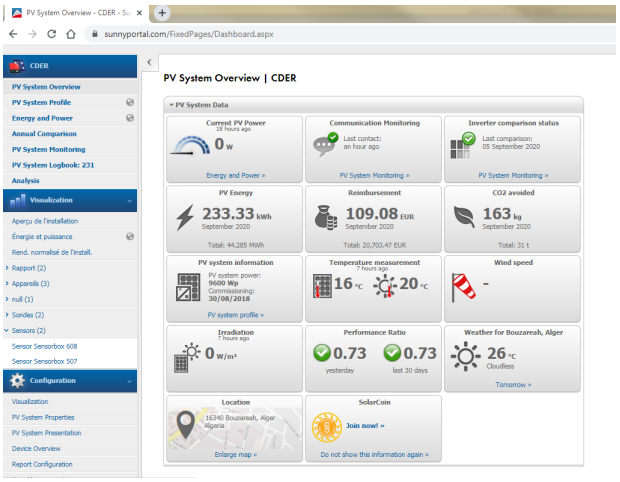

Figure 3.9: sunny portal interface

3.2.6 Different measure equipment of the grid

In order to perform a complete energy survey of CDER plant , the network measurement and monitoring bench at the PCC two equipment is used:

1. Arnoux chauvin network analyzer: The network analyzer (energy), type QUALISTAR plus C.A 8335 from the manufacturer CHAUVIN ARNOUX. 3.10a it makes it possible to [133]:

a) Measure the effective values of quantities and electrical disturbances in the distribution networks.

b) Obtain an instantaneous image of the main characteristics of a three-phase network.

c) Follow the variations of the various parameters over time.

(a) (b)

Figure 3.10: (a)Arnoux chauvin network analyzer (b) Network Tester

2. Electrical installation tester The C.A 6116N is a multi-function instrument for testing electrical installations for compliance with international standards (IEC 60364-6, NF C 15-100, VDE 100, FD C 16-600, and others)[134]. It measures continuity, resistance, insulation, earth and selective earth, loop impedances, as well as the voltage, frequency, current (via a clamp), active power, harmonics, and phase rotation. The instrument can store up to 1,000 tests, which can be downloaded and processed with the included DataView data analysis software.

3.3 Simulation of PV plant of CDER

Figure 3.11 shows a selection of the most important variables that are used in the simulation. The variables highlighted in red are the ones which have a corresponding measurement in this study.

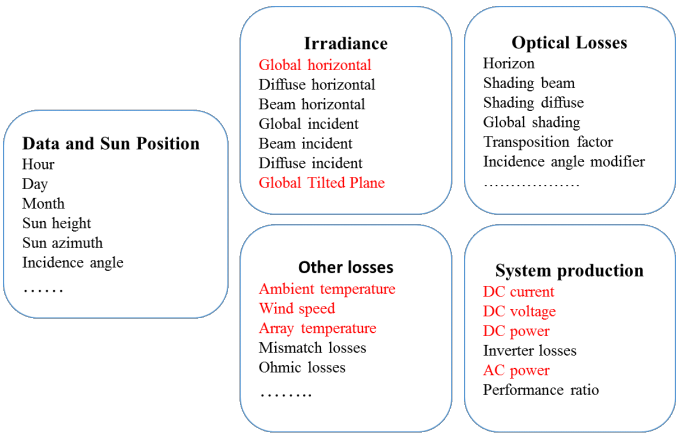

Figure 3.11: measured and simulated parameters

3.3.1 Simulation software

In this work, two software packages have been used:

1. Matlab was used to develop three codeds:

   a) Data check quality

   is the process of checking the measured data for consistency and other anomalies in the data (e.g. gaps), which is conducted in this study, based on the known parameter characteristics of the PV power station and meteorological conditions. According to the behavior of the PV power station and the environmental variables, a program in MATLAB software was coded using the different step in [135] to check the values of measured parameters to eliminate out-of-range measured data according to the IEC61724-1. The maximum and minimum allowable values for some parameters have been defined from [38]as below:

   - Solar irradiance: between 0 and 1400 W/m^2
   - temperature: between 20°C and 55°C
   - Module temperature: between 25°C and 80°C

   b) Shadow mask

In order to draw the shadow mask, a sun path for the CDER's site should be created to show the sun's height at a specific hour of the day and month with respect to the azimuth angle by using a developed code in Matlab, using the equation from [136].

c) PVsyst data format

To be able to compare the performance parameters based on the measured data in our CDER plant and the simulated values using PVsyst, we had to convert the data output format from our sunny webbox to fit the PVsyst software. Therefore, a program in MATLAB software was coded.

d) PVSYST (version 6.70):

PVsyst is a software used to study and simulate solar PV power plants and is regularly updated with new features in new versions of the software [131] . The software was coded to enable the development of PV technology in an optimal and reliable way. In short, it is used as a tool for architectures, engineers, researchers and as an educational tool. It offers an option to use any meteorological data. Furthermore, it has a large PV-components database which gives the ability to model most of the commercially available solar panels type connected to suitable inverters. The main purpose of using this software in this study is to predictive performance parameters and different losses of our PV grid connected plant and compared with measured study.

3.4 Simulation Using PVsyst

The overarching methodology used by PVsyst to model PV system performance is depicted as a data flow diagram in Figure3.12 During the simulation process the PV system assembled, meteorological data and geographical location for any case study using different meteo source available (NASA,PVGIS-v5,NREL's National Solar Radiation Database,Meteonorm,SolarGis ....).However most them is paid service or free limited year between (1990-2010).According to different work comparing the simulated to measured

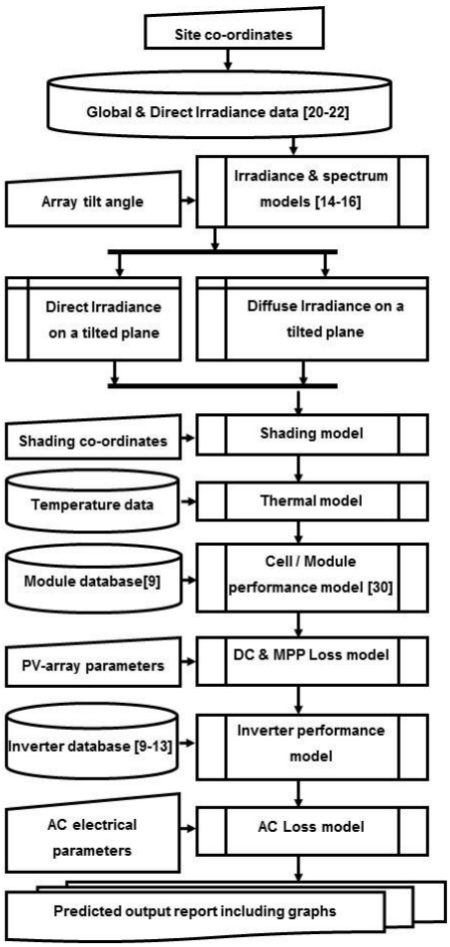

Figure 3.12: Flow chart of PVsyst simulation process.

Meteo data in [50, 137] in term of performance study using local meteo data give best result.To run the simulation it should choose the type of system PV grid connected as surplus injected to grid as shown in Figure 3.13.

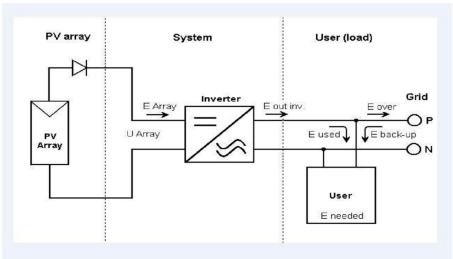

Figure 3.13: Overview of PV grid connected system in PVsyst.

3.4.1 Shading

Within the horizon in PVsyst, the user is able to incorporate shading effect of objects. Horizon measurements, that list heights and azimuth of some significant points, can be obtained onsite with a compass and a sun-path diagram, a detailed map, panoramic, fish-eye photography or other suitable instruments [132].

a) Shadow mask:

the shadow mask survey is based on the search for the main points defining all the architectural or natural objects likely to cast a shadow on the photovoltaic modules [138] as illustrated in Figure 3.14. For each point P detected, we denote

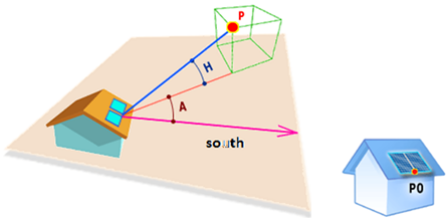

Figure 3.14: A shadow mask statement.

- Its angle A: the azimuth [-120 ° to + 120 °],the azimuth 0 being the south.
- Its angular altitude H [0 to 90 °], the altitude 0 being the lowest point P_0 of the field.

These azimuth / altitude pairs are then reported on a document called "Sun path diagram". At the scale of the planet, each geographical point potentially has its own file, the graphics of which depend on the longitude, latitude and altitude of the place. A very important notion in the study of masks is the Curve of variation of the course of the sun which is defined according to the months of the year [01 to 12] and the hours of the day [139] shown in Figure 3.14.

b) Material used

to raise the shadow mask of the CDER plant: For this study, the Google Earth application allowed us to represent the obstacles that generate shading on the photovoltaic plant as represented by Figure 3.15. After the designation of the various obstacles, we move on to measuring horizontal and vertical angles using the theodolite measuring device and we used an additional compass see the Figure 3.16,

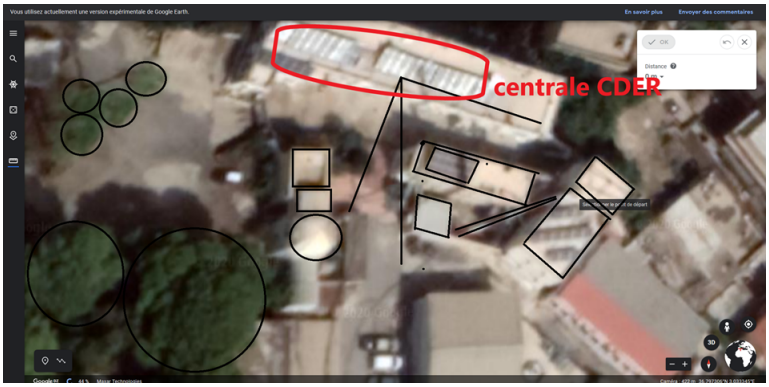

Figure 3.15: all main points of all architectural objects to cast a shadow on central CDER.

A theodolite is a precision instrument used for measuring angles both horizontally and vertically. The Theodolites can rotate along their horizontal axis as well as their vertical axis[140]. After pointing all horizontal and vertical angles with the theodolite

Figure 3.16: measurement by theodolite in CDER.

equipment we uploaded this data to MATLAB along with the sun path generated in MATLAB. Next, we used this aggregated dataset in PVsyst software as shown in the Figure 3.17

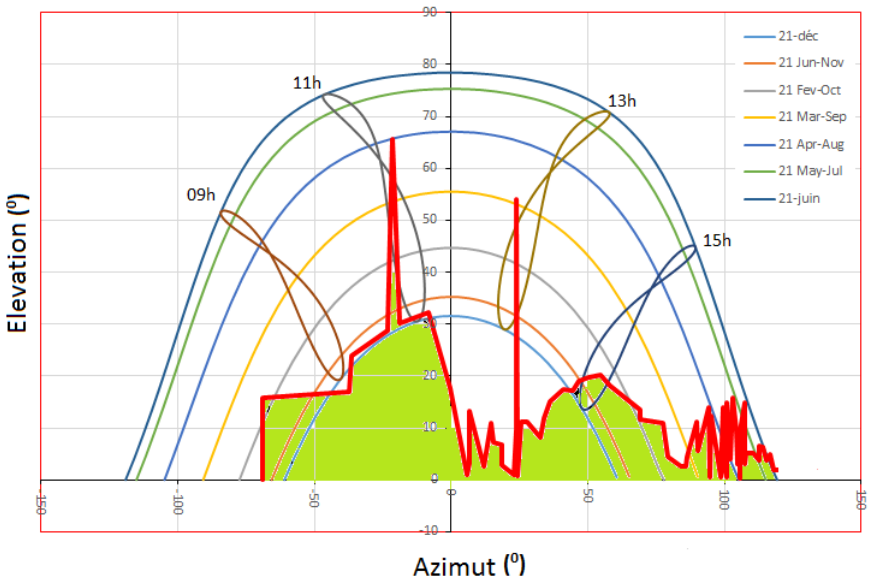

Figure 3.17: Sun path for the site of CDER.

3.4.2 The PV orientation

Numerous technologies can be explored in this part of the software. Alternatives are from fixed tilted plane, season tilt adjustment, tracking axis of different sorts, double orientation to unlimited sheds. In PVsyst, by using the plane optimization tool, one can easily find the optimal plane tilt and azimuth. According to this optimization feature, the optimal orientation for the CDER plant is a tilt angle of 36° and an azimuth of 0 °. These values were determined so that the loss is 0%.Figure 3.18 with respect to the plane optimization for yearly irradiation.

In our case, We set the modules without optimizer, to make them comparable with orientation modules used in real conditions (azimuth:20, tilt: 29).

1. The azimuth: PVsyst recommends adjusting the PV module of the CDER plant facing direct south 0°. Due to the restriction of the building as explained in the description part (3.2.1 description of the system) the orientation selected was 20°. From the curve of transposition Factor as function of the plane tilt and azimuth we can see that FT is 1.15 and the percentage loss with respect to the optimal orientation is -1.2%.

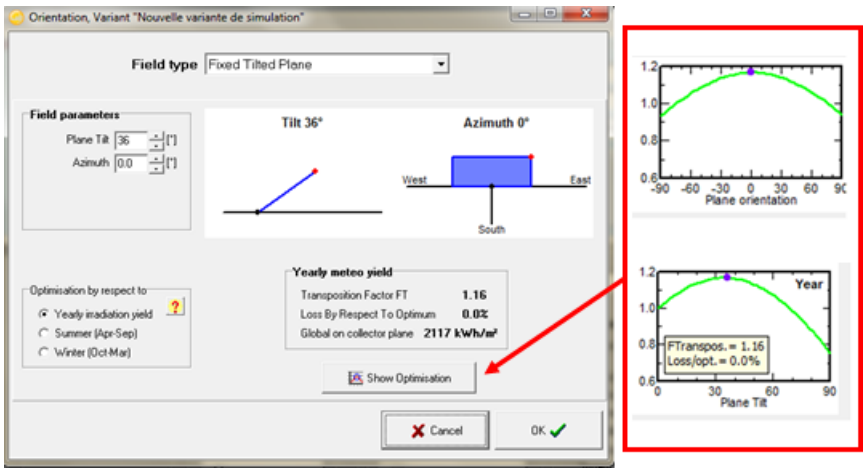

Figure 3.18: plane optimization for yearly irradiation.

2. Tilt :PVsyst recommends an inclination of 36° for the optimal case at the annual setting for the CDER Plant. However, our plant is tilted to 29°, which favors summer sunlight direction as electricity consumption increases dramatically due to usage of air conditioners, however, by using the plane optimization tool user for the summer season we find the best tilt is 21° However in yearly optimization the

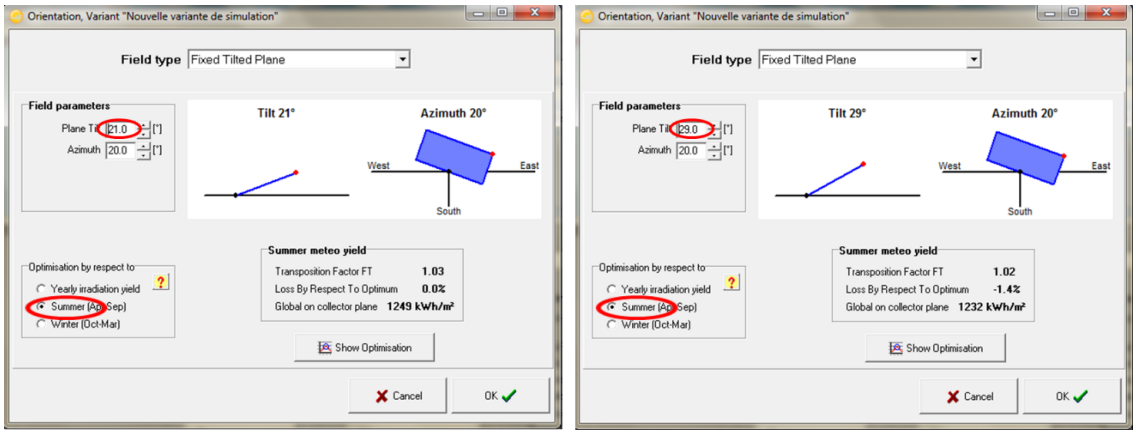

Figure 3.19: Plan tilted comparison between 21° and 29° summer optimization.

loss with respect to the optimum is -2.9% with tilt 21° and -1.2% with tilt 29° as shown in the Figure (3.19 ,3.20),for that we can conclude that our plant is well tilted with 29°

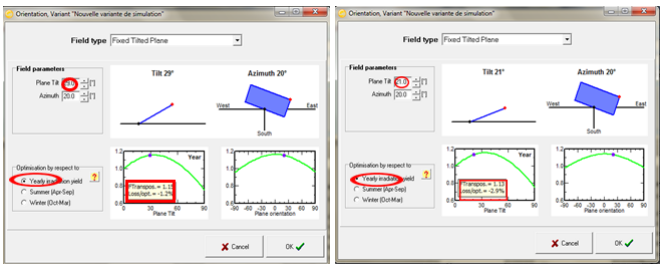

Figure 3.20: Plan tilted comparison between 21° and 29° yearly optimization.

3.4.3 Near shading

Near shadings is where the site's buildings and potential shade from nearby objects are taken into consideration[]. It is possible to construct the site in 3D, implement shading obstacles, and arrange the layout of the modules themselves. It is not possible to import drawings from other software, the only way is to construct the building. I had to use different types of blocks and connect them. Measurements have been taken from Google earth and from the AutoCAD drawings, and all lengths and sizes see Figure 3.21 3D scene of PV plant CDER

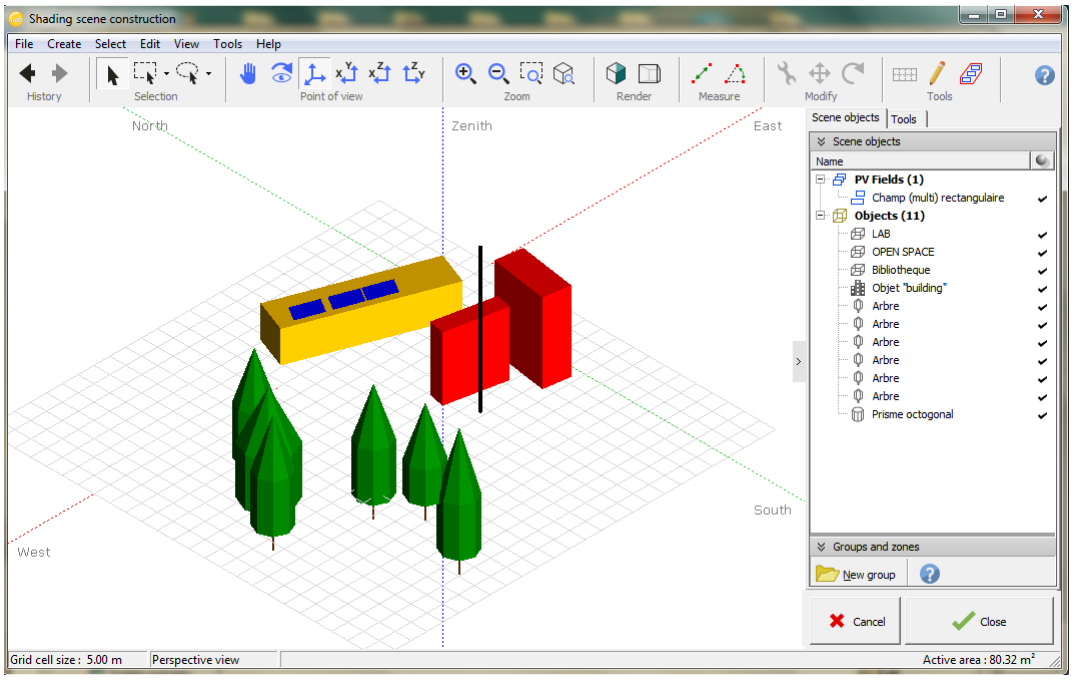

Figure 3.21: 3D scene of PV plant CDER.

3.4.4 Module Layout on 3D Shading

In the option called “module layout ”the connection between the modules is chosen as well is possible to simulate the position of the shadow in the PV array for all the days of the year and all the hours where each string takes number and color as shown is Figure3.22 the sub-array3 (S1,S2),sub-array2(S3,S4) and sub-array1(S3,S4) . Moreover, for each shadow conditions the I-V and P-V curve can also be extracted. In the discussion and results chapter, some I-V and P-V curves will be shown as well as the respective shadow condition in the PV array.

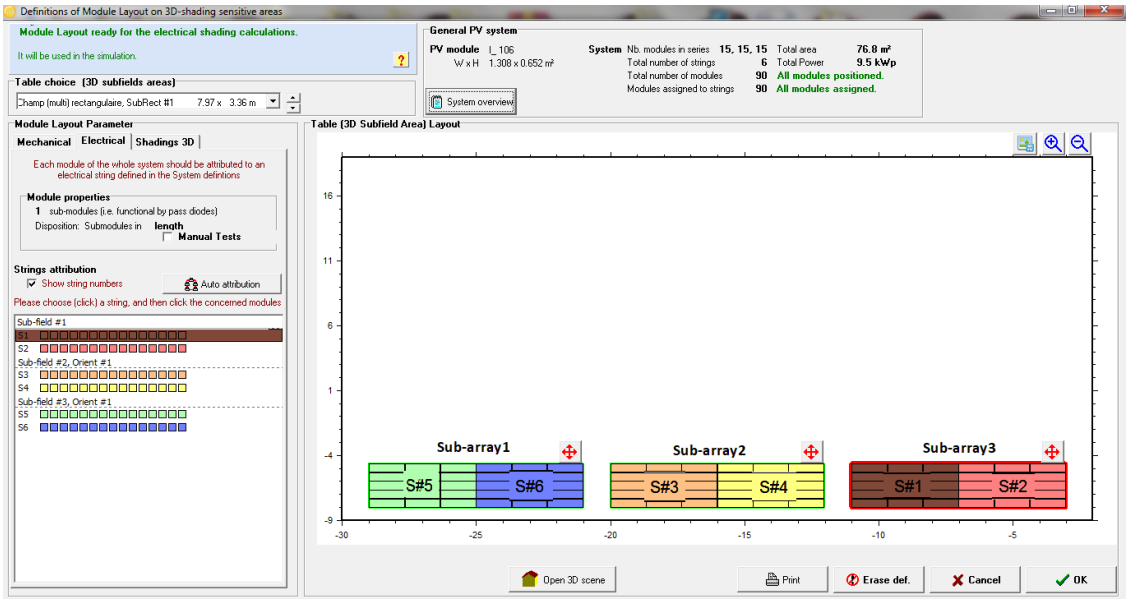

Figure 3.22: Module layout of our plat of CDER.

3.4.5 Array losses in PVsyst

Diagnosis and analyses of losses is considered as one of the mandatory parameters, which must be identified PVsyst takes several types of loss into simulation consideration including thermal losses, ohmic losses, module quality losses, mismatch losses, soiling losses and IAM losses. PVsyst gives each of these losses default values.However they can still be changed in particular that deal with real data case study. Like our system.

1. Array ohmic wiring losses: The ohmic losses were calculated from the wiring layout(see Figure3.23). The lengths of the $16mm^2$ and $5.5mm^2$ cables for the three sub-system were measured to be approximately for each sub-system as follows:

    - 10 m/circuit and 48*2 m/circuit for the sub-system1
    - 10 m/circuit and 39*2 m/circuit for the sub-system2
    - 10 m/circuit and 25*2 m/circuit for the sub-system3

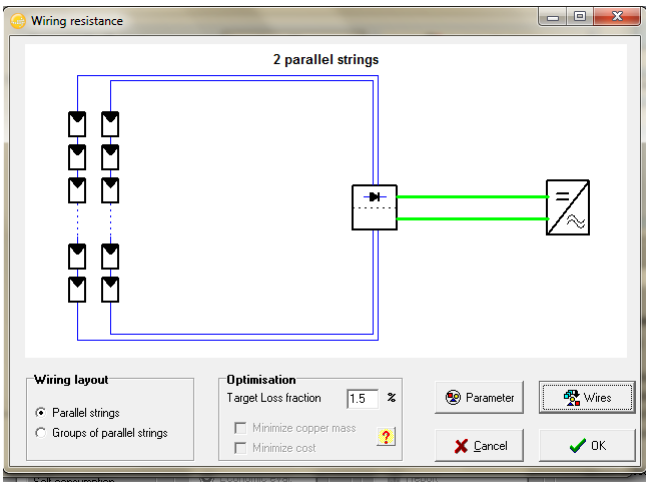

Figure 3.23: wiring loss setting.

2. Module quality and aging loss: The module efficiency loss was taken as 0.1% per year, which was the default value recommended by PVsyst [141]. Considering a power reduction due to aging of 12% over 20 years (0.4% each year for crystalline PV modules), 6.2% losses remain and can be attributed to series losses and mismatch losses3.24.

3. Soiling loss: Soiling loss is another main factor that affects the power output of PV modules. The influence of soiling loss depends on the location of the modules, the array mounted near industry or urban areas are more likely to become soiled. In PVsyst the soiling loss can be derived using a percentage over a year. Usually the soiling loss is 5% [142].

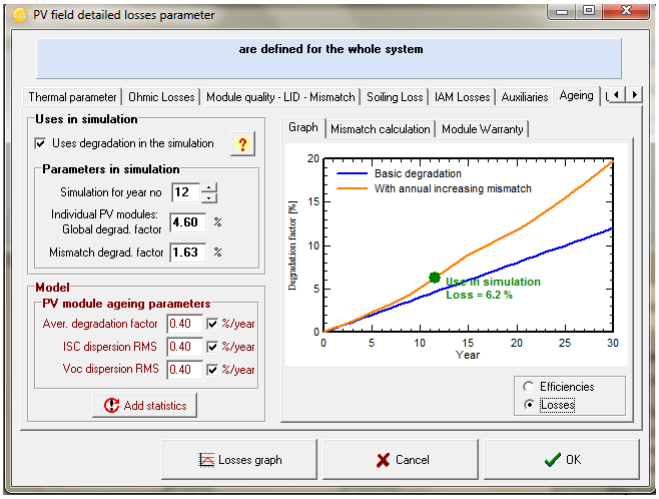

Figure 3.24: Aging loss.

4. IAM loss PVsyst defines the loss as the actual incident light when it reaches the surface of the array due to small particles in the air compared with the ideal case. It is represented the default value of b0 is 0.05 [79].

3.5 Conclusion

In this chapter we describe the PV grid connected system case study and find that monitoring system fits the norm requirement for IEC61724-1 of class A. The chapter also presented the collected data during the years of 2016 through 2018 to be used for the analysis of the performance parameters of our PV plant. The methodology of predictive performance using PVsyst software and setting parameters for simulating a PV system at CDER site we set in and presented. We also discuss the chosen inclination and orientation of the plant with respect to the optimal transposition factor. Finally, we mapped the mask shadow and constructed the 3D buildings of the CDER site to see the shading impact for different sub-array on the performance.

CHAPTER 4

RESULTS AND DISCUSSION

4.1 Introduction

The experimental results section discusses both the collected meteorological parameters and simultaneously lays them out with the PV performance parameters including the system yield, different losses, and the various efficiency. The comparison analysis studies the performance and meteorological status of three consecutive years (2016, 2017, 2018) while also inspecting and contrasting each of the three subsystems of the PV installation.

4.2 Irradiance and DC Energy Output Power

The total values for the annual solar radiation in 2016, 2017 and 2018 are 1491 kWh/m^2, 1667.3kWh/m^2 and 1466.5kWh/m^2, respectively. The corresponding average annual solar radiation for three years is 1542.16 kWh/m2. As shown in Figure4.1, the effective energy follows a similar trend to the solar radiation by which production is highest during the summer season and the least during winter. Throughout all three years, January is the month with least effective energy produced by the array with values of 446 kWh/month, 525 kWh/month and 540 kWh/month for 2016, 2017 and 2018 respectively. On the other hand, June is the month with the maximum energy production with values of 1393 kWh/month, 1291 kWh/month and 1217 kWh/month for 2016, 2017 and 2018 respectively.

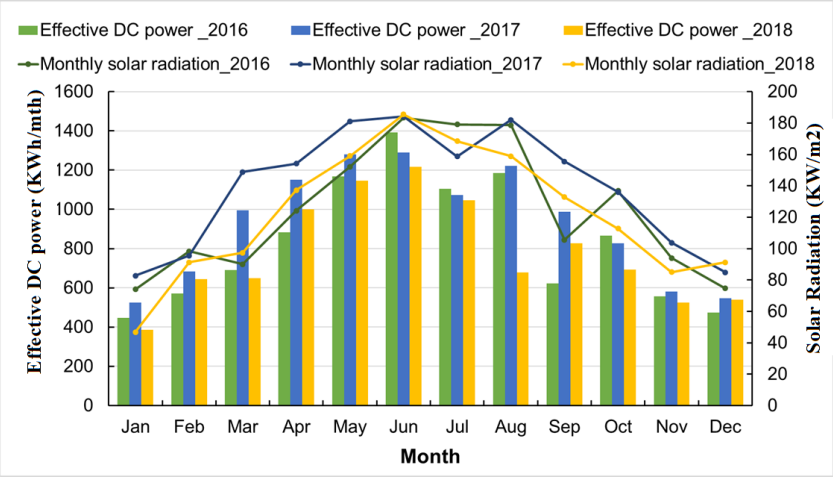

Figure 4.1: measured monthly solar radiation and the effective energy at the out of array

It's important to note that the effective energy of the system output during August 2018 is the least when compared to its instances of previous years, as well as its neighboring months, is relatively small. This inconsistency of data corresponds to a physical activity that took place during that August in which the system was deactivated to install new data acquisition equipment for the plant. a performance comparison between the three years is in the The table4.1

Table 4.1: Performance parameters for 2016,2017 and 2018

	2016	**2017**	**2018**	**Comments**
Irradiation (kWh/m2)	1492.7	1667.3	1466.5	The annual global irradiation of 2017 is the highest and characterized by a higher clear-sky daytime frequency then in 2016 and 2018.
Energy injected into the Grid (kWh)	9788	10741	9014	The energy injected into the network is maximum for 2017.
Normalized indicators (System yields)(h/day)	Yr=4.27 Ya=3.35 Yf=3.10	Yr=4.95 Ya=3.48 Yf=3.35	Yr=4.55 Ya=3.12 Yf=3.01	The difference between the reference and final yield is relatively high throughout the three years; it means that our system has losses and problems.
Efficiency (%)	η_a=8.10 η_{inv}=96	η_a= 8.10 η_{inv}= 96	η_a=8.9 η_{inv}=96	We note that the efficiency of the PV the module is 4% lower than the technical characteristic of our module, which is 12.5%.
Losses (%)	Lc=27.7 Ls=2.8	Lc=25.9 Ls=2.9	Lc=30 Ls=2.9	The losses in the inverter are 3% since their recent installation in 2016. For the three years, the losses in the subarrays are high (26%).

The performance study of the year 2017 as shown in Table4.1 is the most consistent as it is associated with no missing data and characterized with the highest radiation and the production values. Hence, in aims of accurate and comprehensive representation, this research has chosen to discuss in detail the performance and results of 2017, while

resuming to years 2016 and 2018 every while and then for further analysis. The meteorological equipment for measuring global solar radiation, ambient temperature, and module temperature is attached to the back of sub-system2 during the whole year. It's important to note however that wind speed and humidity data for the study period are not available and are considered one of the limitations in this study. Both information are indeed crucial as our building is located in great proximity to the sea and is surrounded by dense trees. As can be seen from Figure 4.2, the monthly average ambient temperature during 2017 varied between a range of 8.8°C in January and 25.8°C in July, while the PV module temperature varied between 10.33°C and 31.51°C in January and July respectively. The range of module temperature is generally higher than the ambient temperature; reaching a difference of 5.7°C in hot seasons.

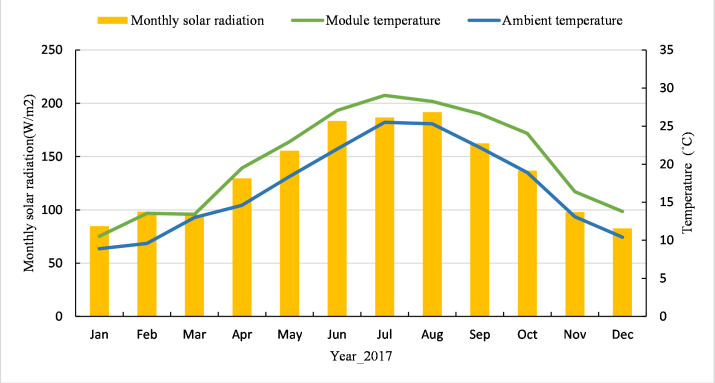

Figure 4.2: Monthly average radiation, ambient and module temperature during 2017

As temperature increases with solar radiation, it's noted that the solar radiation can result in increasing the module temperature which evidently affects the output production of the PV array; especially in high temperatures.which it is in our case can up to 63.5°C as shown in Figure4.3.The NOCT which is the operating temperature of our module is from -20°C to 46°C),that the production rate starts decreasing.

To confirm the aforementioned speculation, we plot the measured module temperature every 5 minutes against the DC power output of subsystem 2 and irradiation for the three years(2016-2018), (see Figure4.4). we can clearly observe that the production rate starts decreasing as temperature of the module throughout the three years.

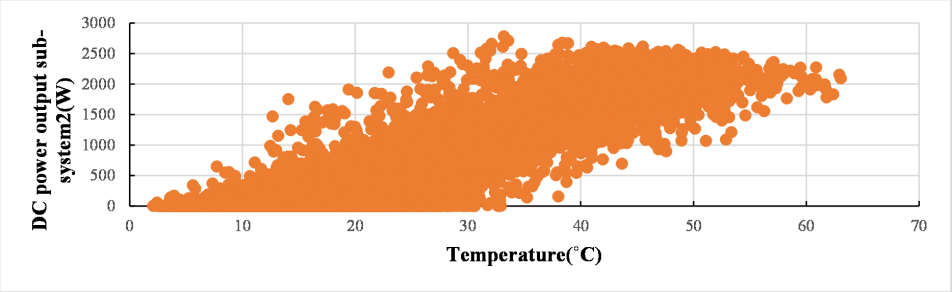

Figure 4.3: Describe the change of DC power output sub-system2 against monthly module temperature

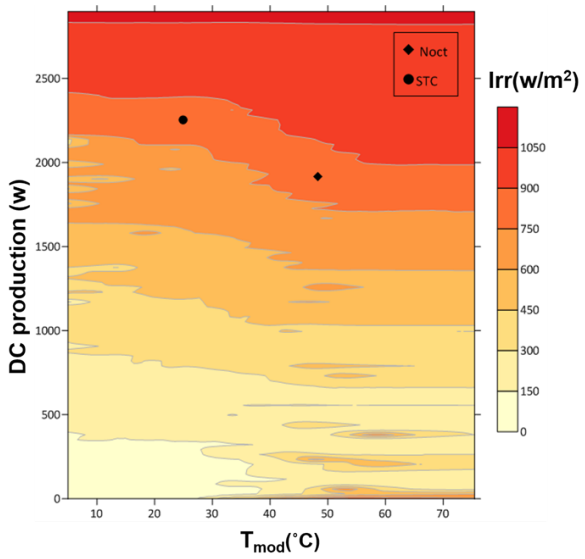

Figure 4.4: Contour Graph of Irradiation (Irr) as a function of Tmod and DC power output for sub-system2 throught three years (2016–2018). In the figure, STC (25°) and Noct (47°) are indicated with a circle and diamond symbols respectively.

The Table4.2 present the monthly average temperature of the module of CDER plant through the three years

Table 4.2: The monthly average monitored the temperature of the module through the three years

	Jan	Feb	Mar	Apr	May	Jun	Jul	Aug	Sep	Oct	Nov	Dec
2016	10.33	15.90	17.77	19.67	22.85	26.68	28.67	28.16	27.39	24.05	16.44	13.8
2017	10.33	14.01	17.77	20.84	24.02	28.66	31.51	28.27	26.11	22.70	16.17	13.80
2018	12.27	10.99	15.99	18.60	20.08	25.86	29.51	29.40	26.35	20.24	16.66	14.21

4.3 AC energy output (energy injected into the grid) and different problems occurring in the plant

Surveying Figure4.5 briefly, where the AC power input into the grid is plotted against solar radiation, we can confidently state that there is a positive linear relationship. It can also be observed from the graph that there is a simultaneous behavior taking place (inset circle A) which requires further investigation. The highlighted records show that

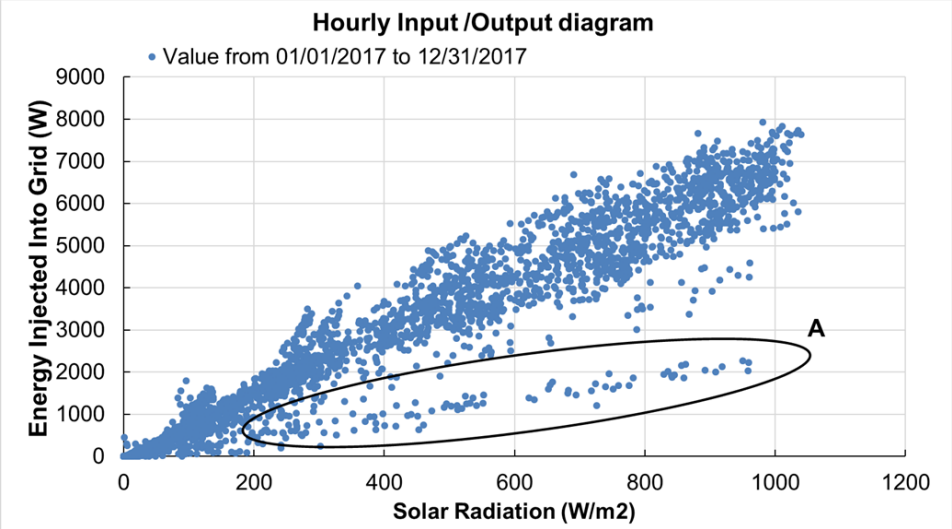

Figure 4.5: Energy injected into the grid against solar radiation

even with the presence of high radiation, the plant still has low production rates. This discrepancy is owing to a temporary crash down found in the sub-system as illustrated in Figure 4.6, that specifically happened on 20/05/2017. We can see that the DC output from sub-system1 follows a similar trend to the solar radiation, the DC energy output from sub-system2 and 3 do not start yielding until its past 12:45. From this we conclude that there must have been a disconnection in the inverter(s), causing in a much lower total amount of the AC energy to be injected into the grid, and hence the anomalous behavior of records highlighted in circle A. In the next sections, we will delve into a detailed investigation to analyze some issues found in our plant in correlation with weather conditions. The aim behind this step is to detect certain uncommon or unexpected trends that occur at the energy collection point or its effective energy output. Ultimately, with

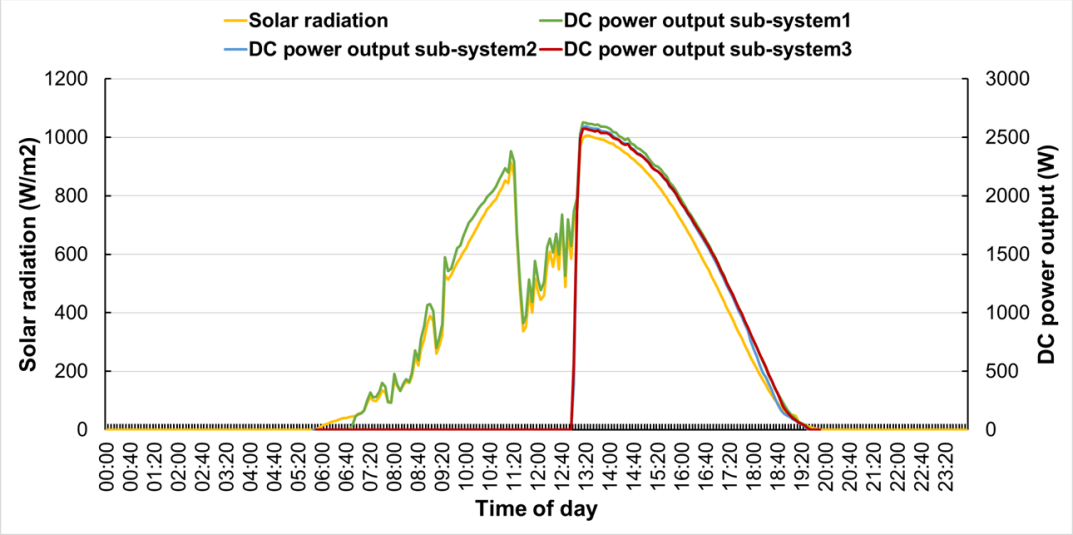

Figure 4.6: The instant solar radiation versus DC power output at subsystem 2 on 24/09/2017.

this local analysis, we should be able to detect the overall efficiency of our system, and if there are ways to reduce errors and malfunctions in the future. We have specifically

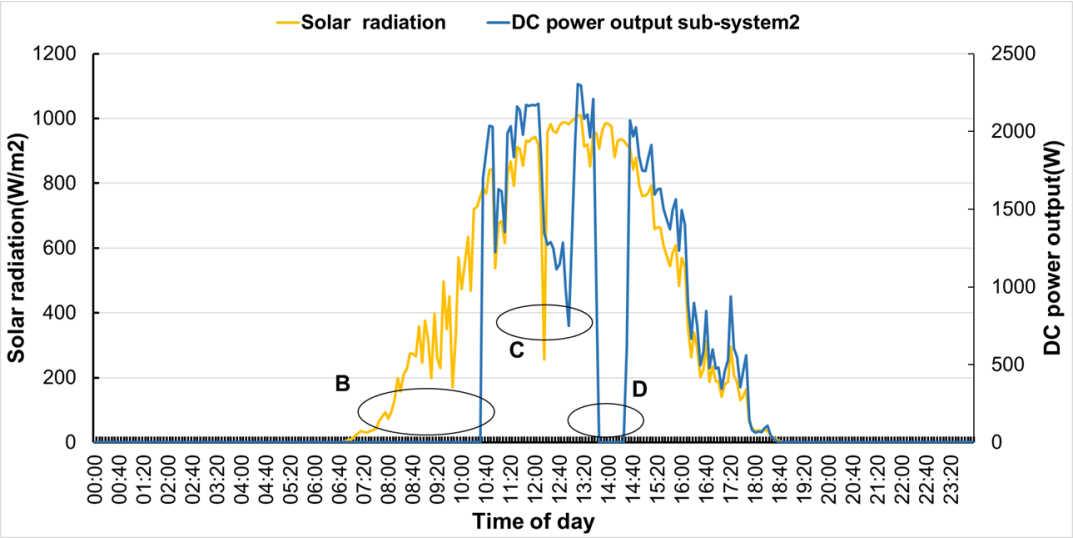

Figure 4.7: The instant solar radiation versus DC power output at subsystem2 recorded on 24/09/2017

selected day 24/09/2017 to summarize and represent the most prominent problems recurring with respect to DC power output throughout the year. Looking at Figure4.7, the drop detected in the behavior of DC power output at sub-system2 are due to either

one of the following problems: 1) leakage current, 2) shading effect, 3) ground fault , 4) insulation resistor. As can be seen in Figure 4.7, in contrast to what is expected, the DC output does not start generating energy until late in the morning; a couple of hours after solar radiation has been increasing. Denoted by circle B, this sudden overshoot is due to the incrementing of leakage current towards the ground. This type of leakage is very common in transformer-less inverters[143], which is the model used in our plant (Sunny Boy), where the inverter is connected to a very sensitive residual current device to protect against any indirect contacts. This 'high sensitivity' causes a high probability of tripping when the weather is overcast, rainy, humid or when the moisture is high as is the case in our site which is located very near to the sea. Looking at the second overshoot taking place at the afternoon (circle C),decrease of we have realized that this is not a technical problem in the system, but rather a physical consequence of overshading coming from the adjacent building. This problem was not accounted for during the installation of the plant as it didn't exist back in 2004. In 2013, a new structure was erected next to the building as well as a tall telecommunications tower was posted, in which both had a significant effect on energy production. Both, the amount of solar irradiation and power output suffer from this overshading which in some cases resulted in a 50% reduction in energy production.

This percentage varies depending on the number of panels affected by the shading, and the number of strings for each sub-array. In accordance, we will study two cases for the shading effect. Starting with the autumn when the sun's altitude starts to decrease and its shading effect becomes visible on our PV panels. The second case is during winter when the sun is very low and its shading effect is at its highest.

For Autumn, we look at the day 09/04/2020 as can be seen in Figure 4.8. Looking at the different shading moments, we can see that the shading effect is not the same between the subsystems. Due to the relatively high sun and the long distance between the structure and sub-system1, we can see that there in no shading effect on sub-array1. While on panel from sub-array2 was effected and a whole string of sub-system3 was impacted. This can be confirmed by analyzing the DC power for each sub-array in

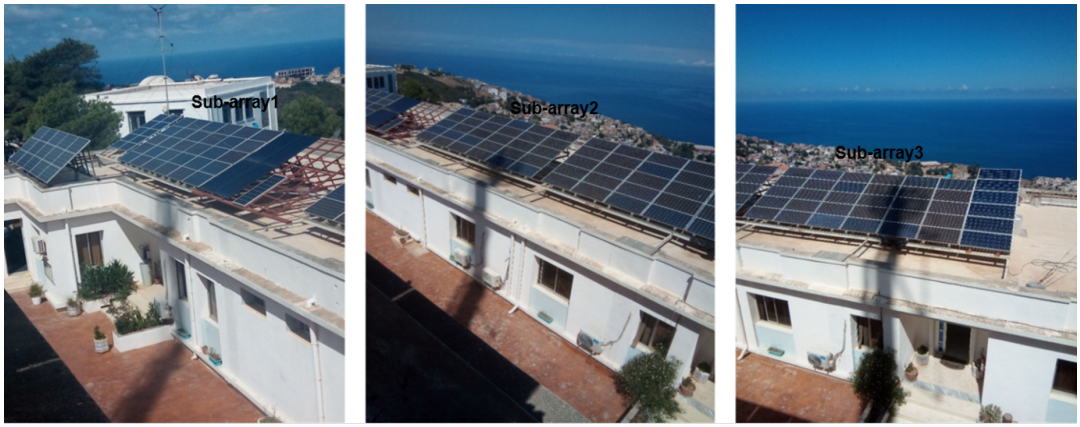

Figure 4.8: Position of the shadow on the three sub-array 1.2.3 on the day of 04/09/2020

Figure 4.9. In this figure we observe a small decrease in production for sub-array2, while production decreases from 2.4 kW to 1.5 kW in sub-array3. By calculating the ratio between the production of sub-array 1 and 3, we find that we have lost 10%.

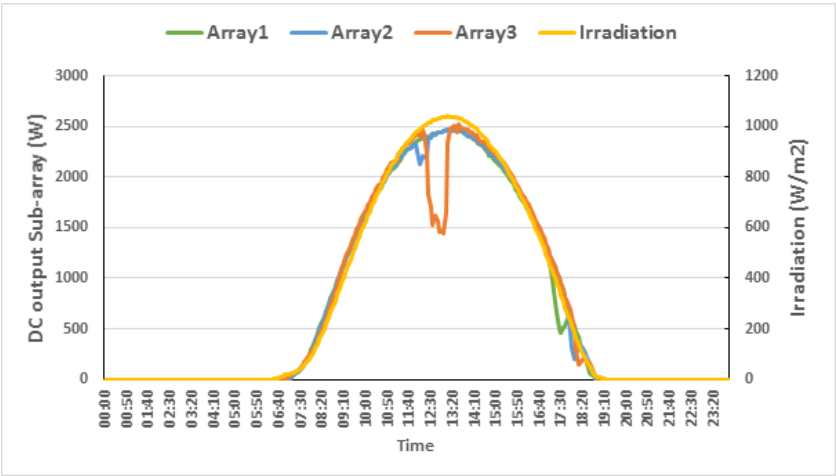

Figure 4.9: Dc power for three sub-array 1.2.3 on the day of 04/09/2020

For Winter, when the sun is lower, we can see that the shading effects all the sub-array. Looking at 05/12/2017 for example (see Figure 4.10), due to the shadow overlay occurring at 12:00 a.m. and 2:15 p.m. which is detected by the sensor-box, we can observe that the energy produced is reduced to more than half of the daily ultimate production. This can be further explained by comparing the energy production between sub-system1 and sub-system3 since the latter is not effected by shading when the former is. In Figure

4.10 we can see that during the first shadowing effect sub-system1 produces only 424W, whereas sub-system3 produces a total of 1726.6 W. Conversely, at the second event when sub-system3 is shaded while sub-system1 is not, sub-system3 only produces 720.52W and sub-system1 produces 1917 W. This percentage varies as it is dependant on the panel connection type and number of panels affected by the shading surface area, where in winter the percentages are expected to be higher since the sun is lower.Both, the amount of solar irradiation and power output suffer from this overshading which in some cases resulted in a 50% reduction in energy production.

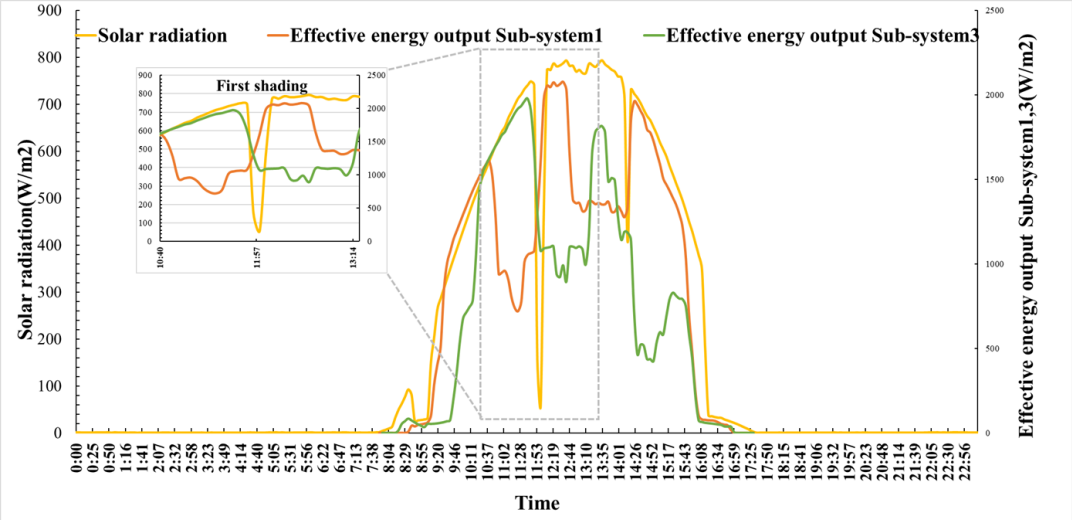

Figure 4.10: Effect of shadow overlay on solar radiation and effective energy output for sub-systems 1 and 3 on 05/12/2017

The third negative overshoot denoted by circle D stems from ground fault. Ground voltage should never exceed 15V at all times (this is unique to our case and is based on the technical characteristics of our inverter), otherwise the subsystem disconnects which is exactly the case at circle D. Subsystem2 disconnects from 13:51 pm until 14.40 pm due to earth leakage at which voltage of the ground at 13:51 pm has reached as high as 24.4V and should have been less than 15V (see Figure4.11).

A fourth problem that affects the overall PV plant production is the delay in the DC energy output occurring at the initiation of the inverter in the morning. The inverter displays an error message regarding the insulation resistor and therefore prompts further

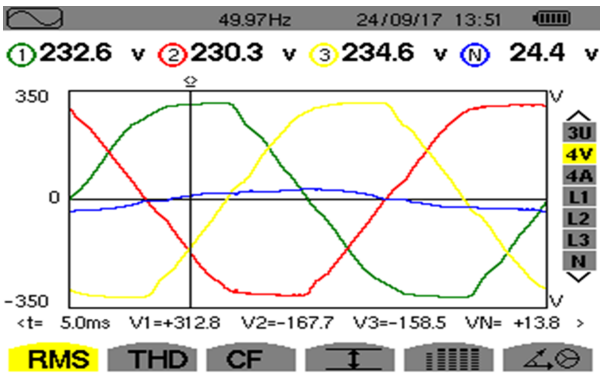

Figure 4.11: The different voltage measurements between the three phases on the PCC exactly at 13:51 PM on 20/08/2017 from the electrical network power analyzer of Chauvin Arnoux

investigation. and displaying the error message of the insulation resistor. Looking at Figure 4.12, we can see that the production of sub-system1,2 and 3 on 20/08/2017 is impeded in the morning times despite the presence of solar radiation since 8:20 am. The sub-system1 inverter doesn't trigger only at 8:55 am while sub-system2 at 8:15 am and sub-system3 at 9:15 am, which presents the problem of insulation resistance.It can be confirmed by Figure4.13 that the insulation resistance of all three inverters on the same day have values less than 500 Ohm after the presence of solar radiation until 8:55 am for sub-system1 meanwhile sub-system2 at about 08:15 am and sub-system3 at 9:15 am and the three subsystems are reactivated as shown in Figure4.12.

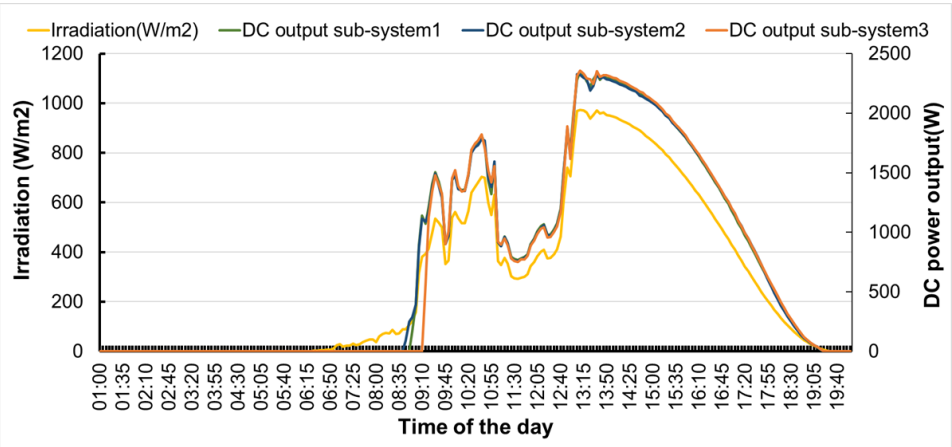

Figure 4.12: The morning lag of production in sub-system1,2,3 versus solar radiation on 20/08/2017

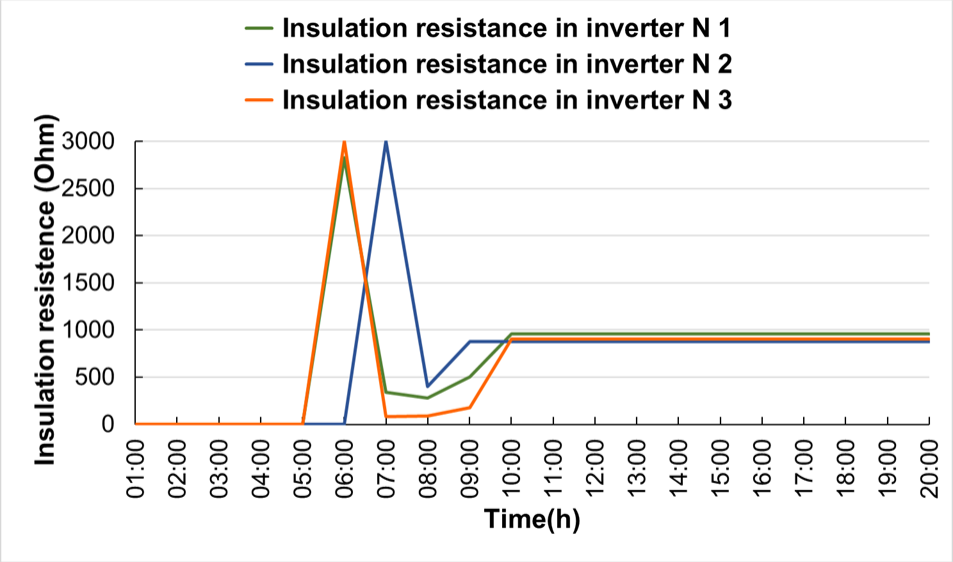

Figure 4.13: insulation resistance for the three inverters of sub-system1,2 and 3

4.4 Performance results

4.4.1 System yields

The system's performance can be assessed by comparing and contrasting the PV's reference yield, array yield, and final yield. Figure4.14 shows the monthly average of the PV system's three types of yields over the monitored period of 2017. It is observed that the highest values for average monthly reference yield, array yield, and final yield were obtained in April, with values of 6.04 h/day, 4.79 h/day and 4.61 h/day respectively. On the other hand, the lowest values for these yields were obtained in January, with values of 2.74 h/day, 1.85 h/day and 1.78 h/day respectively. Looking at the reference yields which indicate the available solar energy, we can see that the summer reaches its highest, and winter reaches its lowest. However, the difference between the reference and final yields is relatively high throughout the year. As previously noted, this is due to the excessive (high) temperature and humidity of the PV module which causes a reduction in the voltage of the PV to maximum power generation in summer, and shading from the construction of a new building in winter.

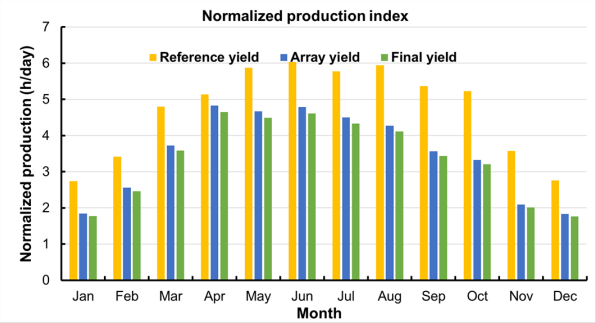

Figure 4.14: Variation of measured monthly reference, array and final yield for the year 2017.

4.4.2 System efficiency

Figure4.15 shows the monthly average daily PV module efficiency and system efficiency during 2017 period. we can conclude that the efficiency rates of both the PV array and the whole system follow similar trends. A noteworthy observation is that the maximum efficiency does not necessarily yield maximum output and vice versa. For example, the efficiency of the PV array and the system hit their minimum during November with 7.26% and 6.98%, while the lowest yields occurred in January. The maximum array and system efficiencies happened in April with 9.70% and 9.33% respectively. Note that the efficiency of the array is 3.8% less than the standard, which is 12%. This is due to the aging of the PV array as it was installed in 2004 in addition to the previously mentioned issues.

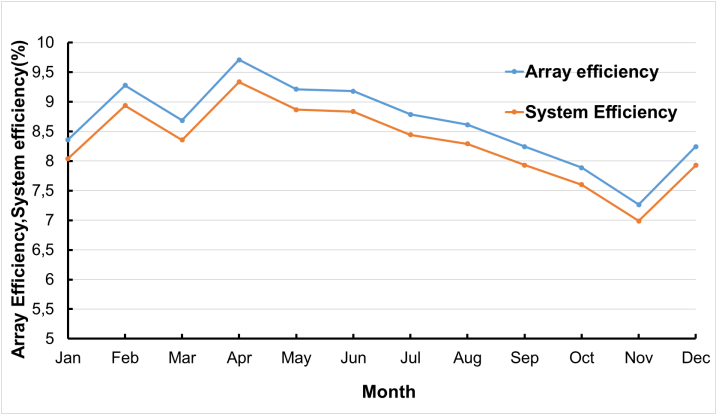

Figure 4.15: Array efficiency and system efficiency

4.4.3 Inverter efficiency

Figure4.16 shows the variation of inverter efficiency versus the power outputted from the array. The inverter efficiency is seen to increase as the level of array power increases from 0 to 2000 W and then remains fairly constant between 95% and 96%. The maximum inverter efficiency was 97.9% when the array power value was 556.6 W.

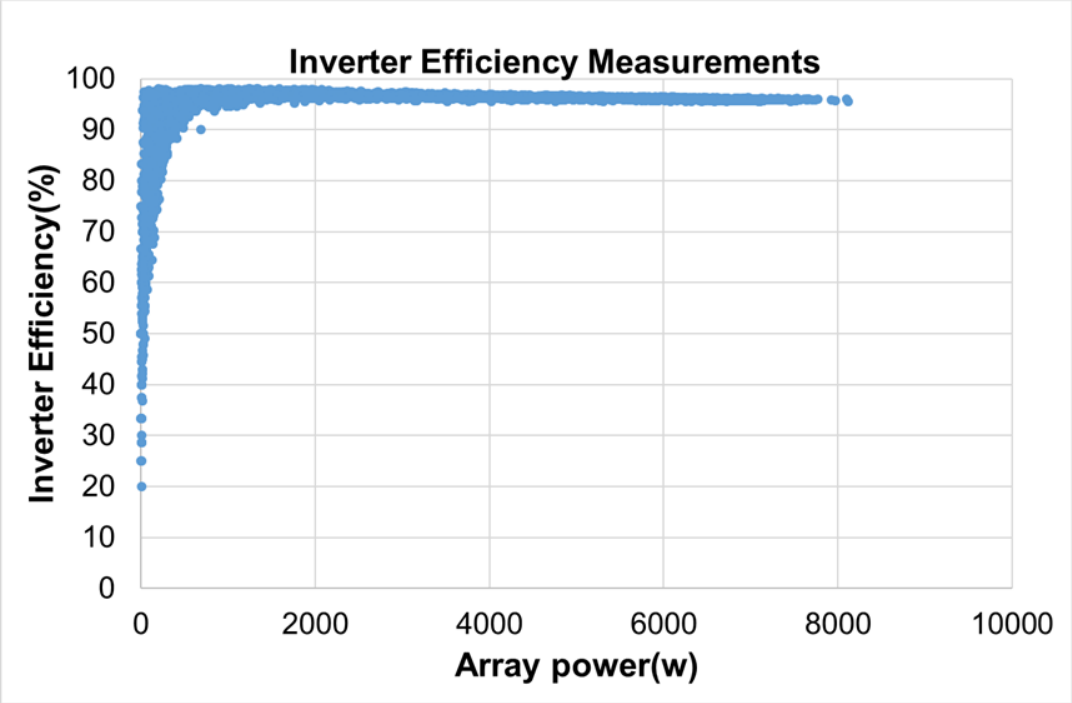

Figure 4.16: The relationship between inverter efficiency and array power

Table4.3 presents the PV module efficiency, system efficiency during the 2016, 2017 and 2018 period.

Table 4.3: different efficiency parameters for the system

	Efficiency (%) 2016			Efficiency (%) 2017			Efficiency (%) 2018		
	η_a	η_s	η_{inv}	η_a	η_s	η_{inv}	η_a	η_s	η_{inv}
Min	8.01	7.3	95.94	7.2	6.9	96.08	7.6	7.3	94.31
Max	9.95	9.58	96.77	9.7	9.3	96.36	10.72	10.12	97.05
Average	8.75	8.41	96.24	8.82	8.29	96.30	8.43	8.12	96.30

4.4.3.1 Losses

Figure4.17 illustrates the normalized losses, both for capture and system losses. System losses generally remain constant as they depend on the inverter efficiency. Since our inverter has been recently substituted by a new one, the low value in system loss means that the PV array matches well with the inverter. Capture losses, on the other hand, depend on the solar radiation as well as other different losses occurring in the array. In Figure4.17a we can see that the capture loss varies between 0.31 kWh/kWp/day in April and 1.90 kWh/kWp/day in October and the average loss is 1.16 kWh/kWp/day. While the system loss varies from 0.07 kWh/kWp/day in January to 0.37 kWh/kWp/day in June and the average loss is about 0.13 kWh/kWp/day. Figure4.17b reveals the percentage of the final yield, capture loss, and system loss, which are 71%, 26% and 3%, respectively. Table 4.4 presents the different losses for the 2016,2017 and 2018.

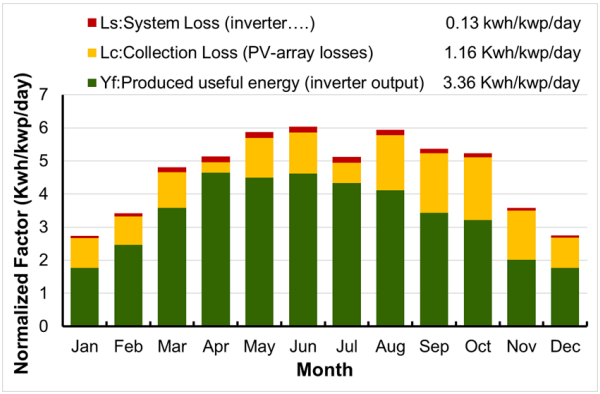

(a)

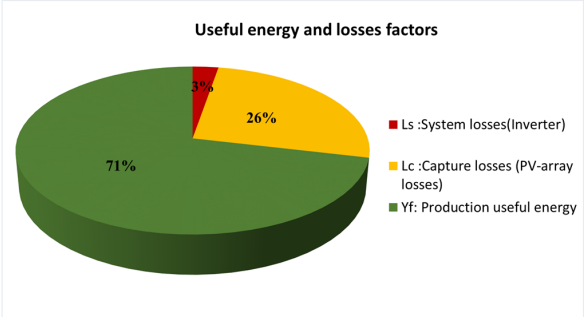

(b)

Figure 4.17: (a)Normalized production and loss factors. (b) Normalized production and loss factors in percentage

Table 4.4: different loss for 2016,2017 and 2018

	Detailed Losses(kWh/kWp/day)					
	2016		2017		2018	
	Lc	Ls	Lc	Ls	Lc	Ls
Min	0.40	0.07	0.31	0.07	0.02	0.06
Max	1.78	0.18	1.90	0.18	1.93	0.16
Average	1.17	0.13	1.16	0.13	1.12	0.10

a) Thermal capture losses (Lct)

In order to show the shape of normalized losses data distribution, its central value, and its variability in our system. The descriptive statistics were applied by using the boxplot for (Lct,Lcm,lcr,lsr).

The Figure4.18 shows the monthly thermal capture losses Lct of CDER plant. The centerlines, box height, and extended lines represent the median, the interquartile range and the full extent of the data,respectively. The analysis shows a slight dispersion of

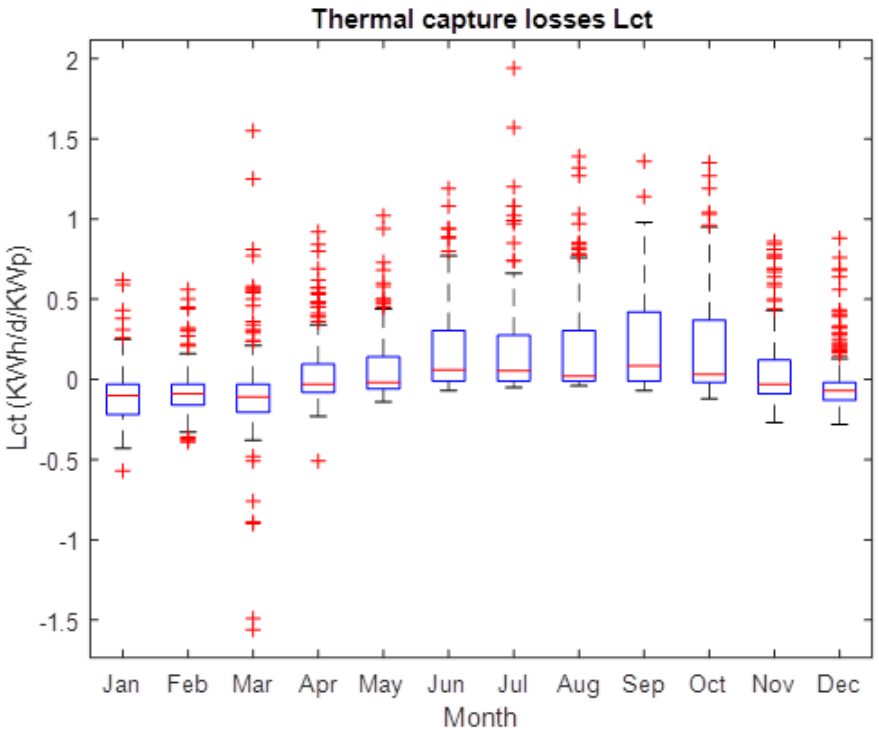

Figure 4.18: Monthly thermal capture losses Lct of field data (boxplot) for CDER plant over the year of 2017.

thermal losses around the median value during the months of summer and September due to the effect of temperature, while in winter months, the losses are close to the median value. We can see that the third quartile is negative for the winter months until March explained by the low temperatures of the photovoltaic array, while for the summer season until October the third quartile attains positive values around 0.5.

b) Miscellaneous capture losses (Lcm)

The Figure4.19 shows the monthly miscellaneous capture losses Lcm of CDER plant. Analysis of this figure while eliminating the temperature effect, we see a grouping of the Lcm values around the median value in summer and a slight dispersion around the median value for the remaining months. This is explained by the fact that during summer, there is less humidity on the sub-arrays than in the other months, and there is more shade in winter than in summer.

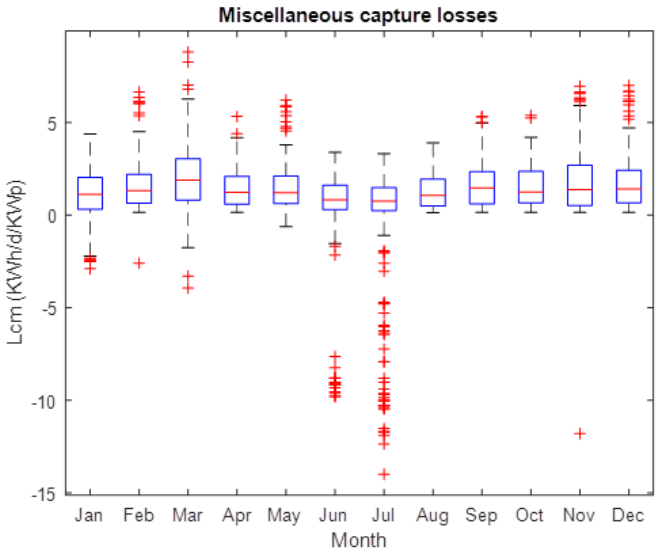

Figure 4.19: Monthly miscellaneous capture losses Lcm of field data (boxplot) for CDER plant over the year of 2017.

c) Capture and system reference losses

The Figure 4.20 shows the reference capture losses and reference system losses. From the Figure 4.20a we can observe that the median explains the effect of temperature

which can clearly be seen in summer. On the other hand, the dispersion of the first and third quartile, explain the effect of shading in winter. We can see that the reference system losses Lsr in Figure 4.20b is stable which explains the losses in the inverter and grid are small.

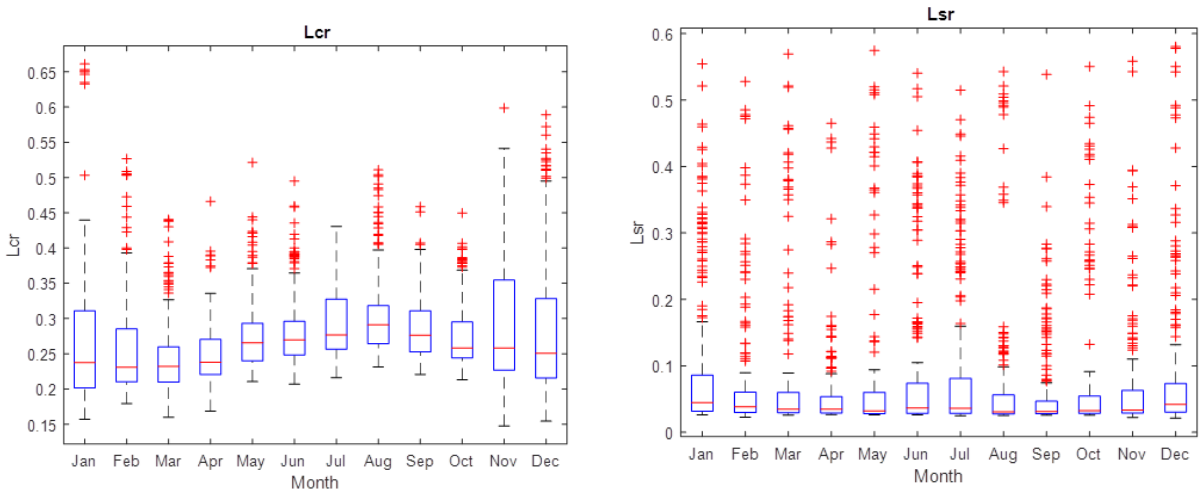

(a) (b)

Figure 4.20: ratio losses to the the reference yield .(a)array ratio (b) system ratio

4.4.3.2 Capacity Factor

The average monthly capacity factor (CF) values between 2016 and 2018, represented in Figure4.21, were calculated theoretically using the formula 2.16. The study results show that CF of the system varied from a month to another. The monthly average CF value was high for June, accounting for about 20%, and was the least for December, accounting for 7.14% while an annual average of 13.98%.

4.4.3.3 Performance Ratio

The measured annual performance ratio (PR) of the solar plant is found to be 69.87 %, 70.72% and 67.50% for the years 2016, 2017 and 2018 respectively (see Figure4.22). It is important to note that the performance ratio in August 2018 reached as low as 43.41% since the plant was undergoing the installation of new equipment, causing a lot

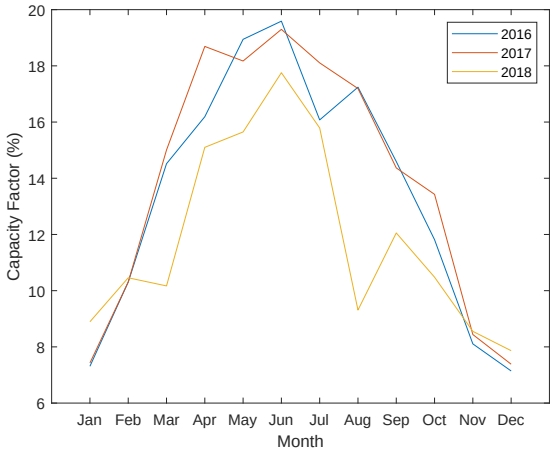

Figure 4.21: Capacity factor of the installed PV system over the three years of 2016, 2017 and 2018.

of disconnection for sub-system3 as mentioned in previous sections. Generally assessing

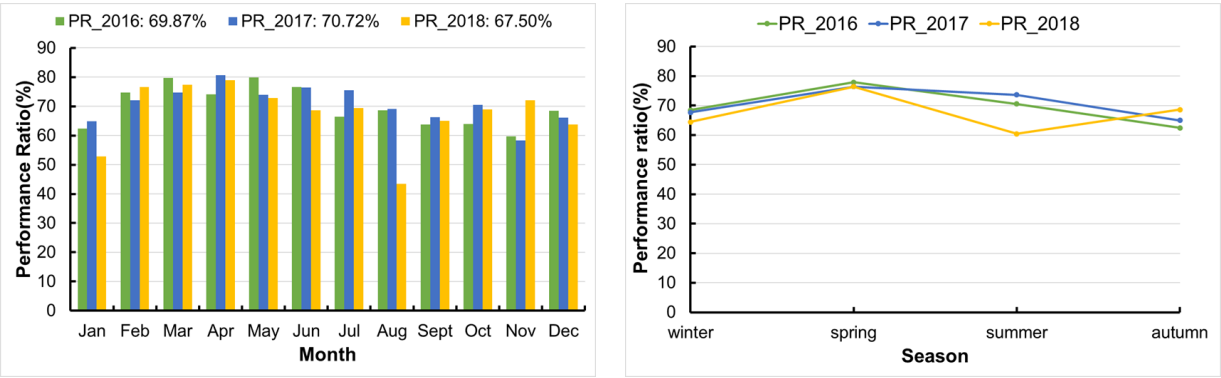

(a) (b)

Figure 4.22: (a)Performance ratio for three years 2016,2017 and 2018 (b) Seasonal performance ratio

the results, it is observed that best performance ratios don't necessarily occur with the best radiation (See Figure4.22b). Although summer months have the highest radiation values, performance decreases due to high temperatures and humidity affecting the functionality of the PV arrays. Likewise, winter and autumn have lower performances due to fewer hours of radiation and shading from near buildings. In our case study, spring (March, April, and May) proves to have the highest performance ratios throughout the years.

4.4.3.4 Weather corrected performance ratio

the Seasonal variation of the traditional PR is removed by calculating a temperature-corrected performance ratio. The Figure 4.23 shows both the PR and the weather corrected performance ratio (WCPR). The average monthly absolute differences between the measured and corrected performance ratios were 6.5% in winter season and 0.4% in summer. WCPR appears therefore to provide a more complete correction of ambient conditions of module performance than PR. This is to be expected, because the use of module temperature implicitly includes all factors affecting the thermal coupling of the PV modules to the environment, such as wind speed.

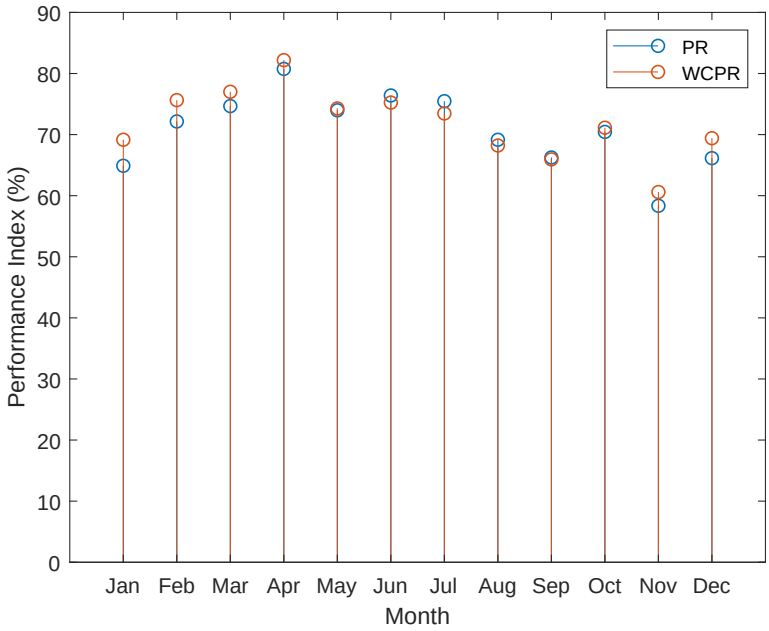

Figure 4.23: weather corrected WCPR and PR.

4.5 Comparison of three sub-systems

4.5.1 Capture losses and system losses

Comparing the losses from the three sub-systems, we observe that sub-system 3 has the highest losses in terms of capture losses and system losses with 1.28 and 0.13

kWh/kWp/day, which is about (28.88% and 2.95%) respectively.Conversely, sub-system 2 performs the best as it is associated with the lowest losses at 1.12 and 0.12 kWh/kWp/day which is about (24.07% and 2.71%) Figure4.24.

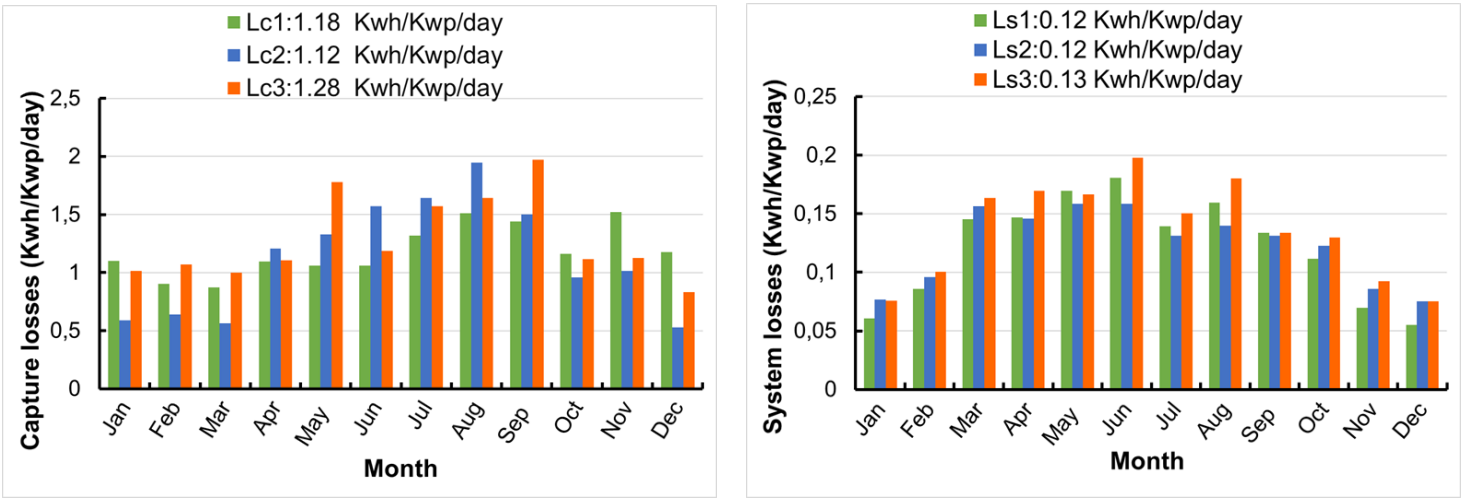

Figure 4.24: different losses of the array and system for the three sub-system .(a)capture loss (b)system loss

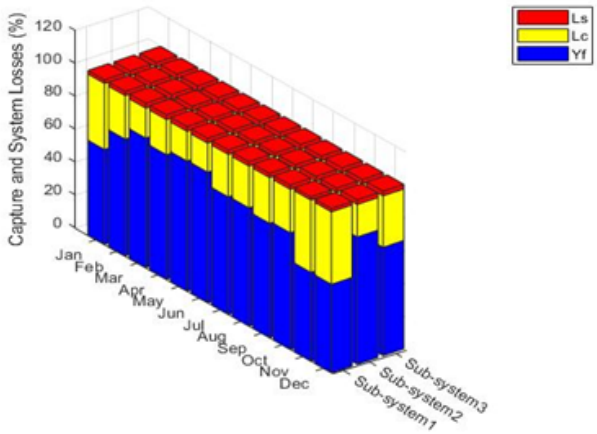

Figure 4.25: different losses for three sub-system

4.5.2 Efficiency of three sub-systems

Figure4.26 shows a comparison between the three sub-systems. The average array efficiency of subarrays 1, 2, and 3 is 8.40%, 8.84%, and 8.28% respectively, while the

efficiency of the subsystem1,2 and 3 is 8.10%, 8.53%, and 7.93% respectively.

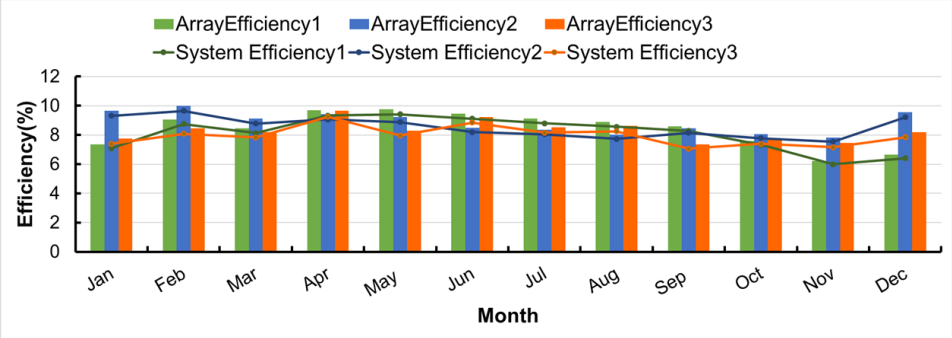

Figure 4.26: the array, system efficiency for three sub-system

4.5.2.1 Inverter Efficiency of three sub-systems

The average efficiency for the inverters of sub-systems 1, 2, 3, are 96.40%, 96.42%, and 95.83%, respectively see Figure4.27. It observed that the inverter of subsystem 3 has less than the standard inverter efficiency for the sunny-boy, which is 96%. For that, we measured the total harmonic distortion (THD) of the three inverters for one week (our equipment is limited to a period of one-week data capture) every month in the PCC. From Figure4.28, which presents the week of 13/04/2017 to 19/04/2017, we can see that inverter 3 has harmonic parameters (THD) between 10%-20% during the day compared to less than 10% for inverters 1 and 2. This explains the reduction in the efficiency of inverter 3. Measurement points with very high harmonic THD (more than 50%) happen in the PCC when the current is very weak which occur during the night when there isn't any radiation.

4.5.2.2 Performance Ratio

The performance ratio for sub-systems1,2 and 3 are 69.47%, 73.20% and 68.15% respectively. In Figure4.29, we can see that sub-system 3 performs the lowest in terms of capture losses and system losses as well as the efficiency which was confirmed by it corresponding performance ratio (less than 5% of sub-system 2).

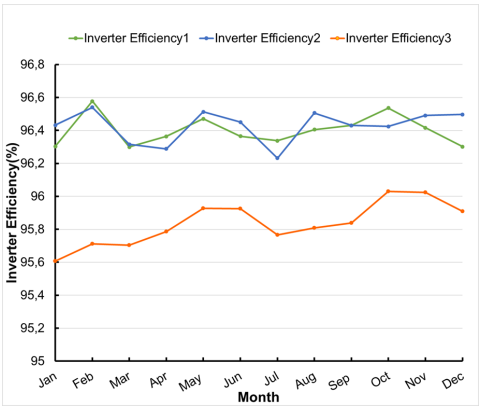

Figure 4.27: Inverter efficiency for sub-systems 1, 2 and 3 for the year 2017

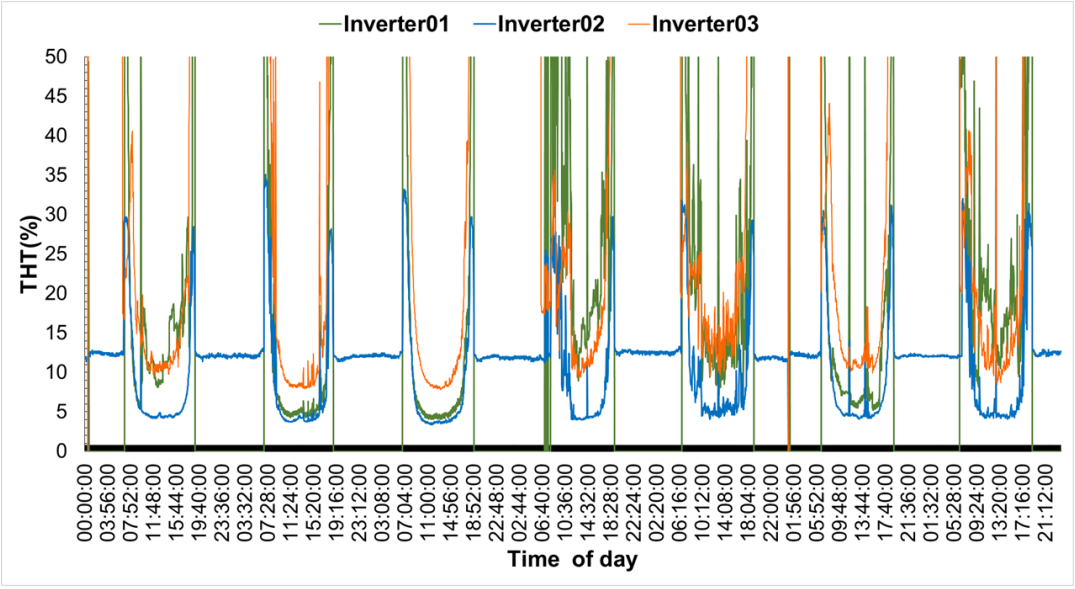

Figure 4.28: THD from 13/04/2017 to 19/04/2017

4.6 Simulated performance results

4.6.1 Diagram losses

When performing a simulation, PVsyst produces a six page report containing the system configuration and simulation results. PVsyst calculates the losses mentioned in subsection 3.4.5, and shows them in a loss diagram as illustrated in Figure 4.30. The upper part of the diagram are optical losses, the middle part are array losses, and lower part are system losses. For the optical loss where the IAM (Incidence Angle Modifier)

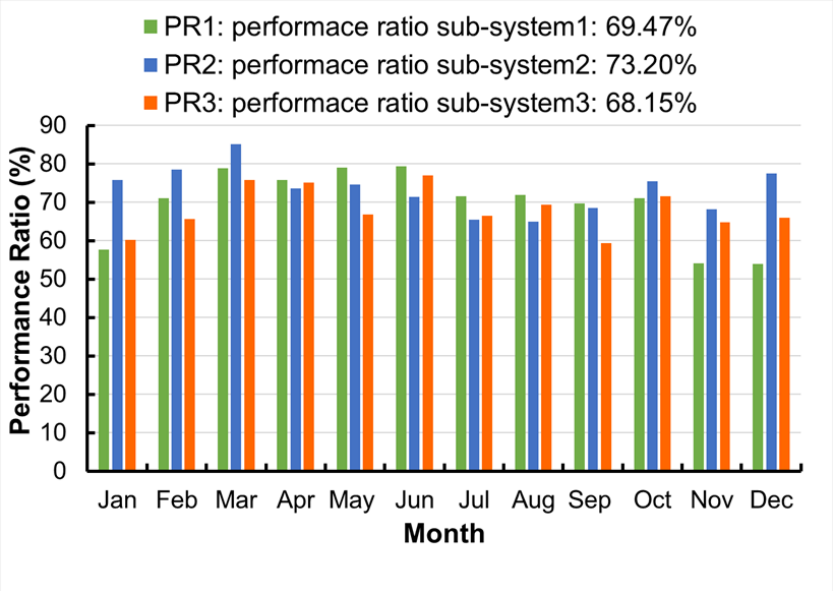

Figure 4.29: performance ratio for three sub-systems

factor on global corresponds to the decrease of irradiance really reaching the PV cells. It is due to the reflexions on the glass cover and is about 2.3%[141]. From 4.30 loss diagram for the year 2017, we can see that the most important losses in CDER plant system are: the loss due to the temperature with 5.7%, the near shading with irradiance loss with 5.4%, and after entering the results of previous work in [110]which is the derating factor for each module of our plant the module degradation loss is 5%. Figure4.31 presents the different losses for each month where we can see that shading loss is high in the winter varying between 10.2-11.4 % , because the sun is low, meanwhile the loss due to the temperature is high in summer values ranging between 7.1-8.1%.

4.6.2 Near shading

The impact of the shadow created by the new structure next to the building and the tall telecommunications tower have different impacts on the sub-arrays of our CDER plant. Next is showed a set of figures, for a specific time of the day of 09/14/2019, an example of the disposition of the shadow in the PV array as well as the corresponding I-V and P-V curves (Figures: 4.32) for the three sub-arrays of our CDER plant.

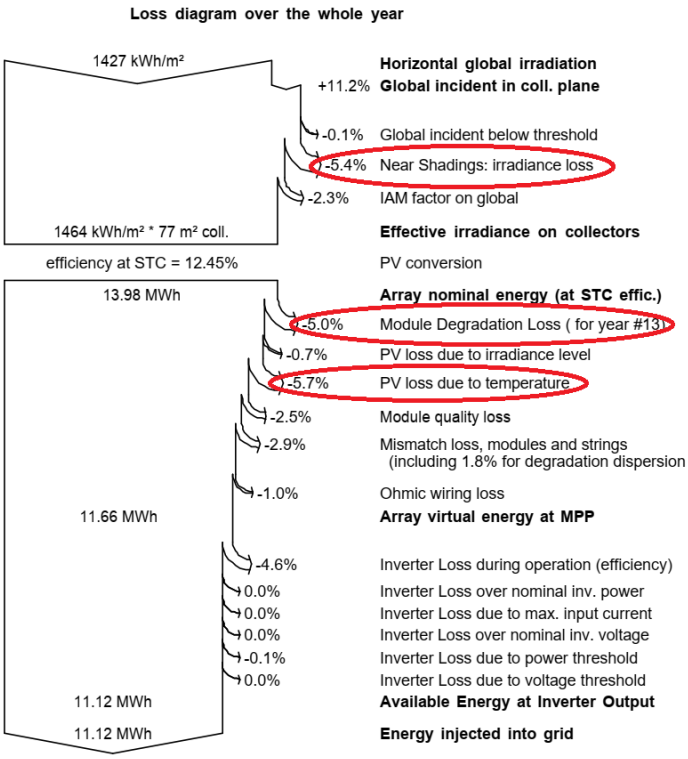

Figure 4.30: Diagram of the system loss

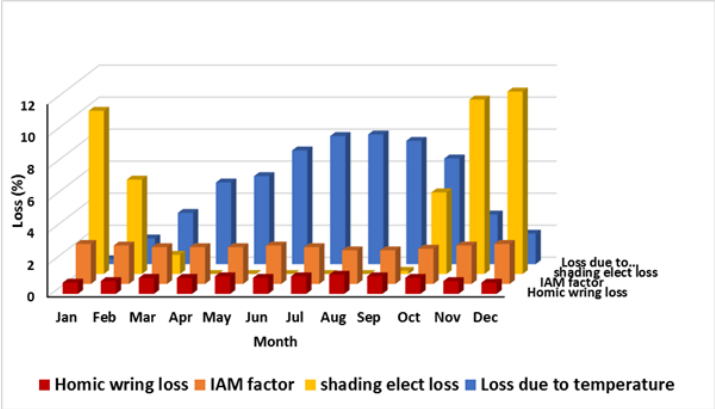

Figure 4.31: Different monthly loss

The shadow in the panels have a strong impact as can be seen in the I-V curve of the sub-array3(string $S\#1$,$S\#2$). Most of the module of string2(S#2) are shadowed which strongly reduces the current output from the system as can be seen in the Figure I_V. In the Figure, the blue line represents the I-V curve when the array is not effected by the shadow. Since the power is given by the multiplication of the current by voltage, the

respective P-V curve has multiple power peaks but only one is the real one. One of the inverters function discovers this power peak. The shading loss for sub-array3 is 27.8%, meanwhile less impact is seen for the sub-array2 with shading loss 9% .

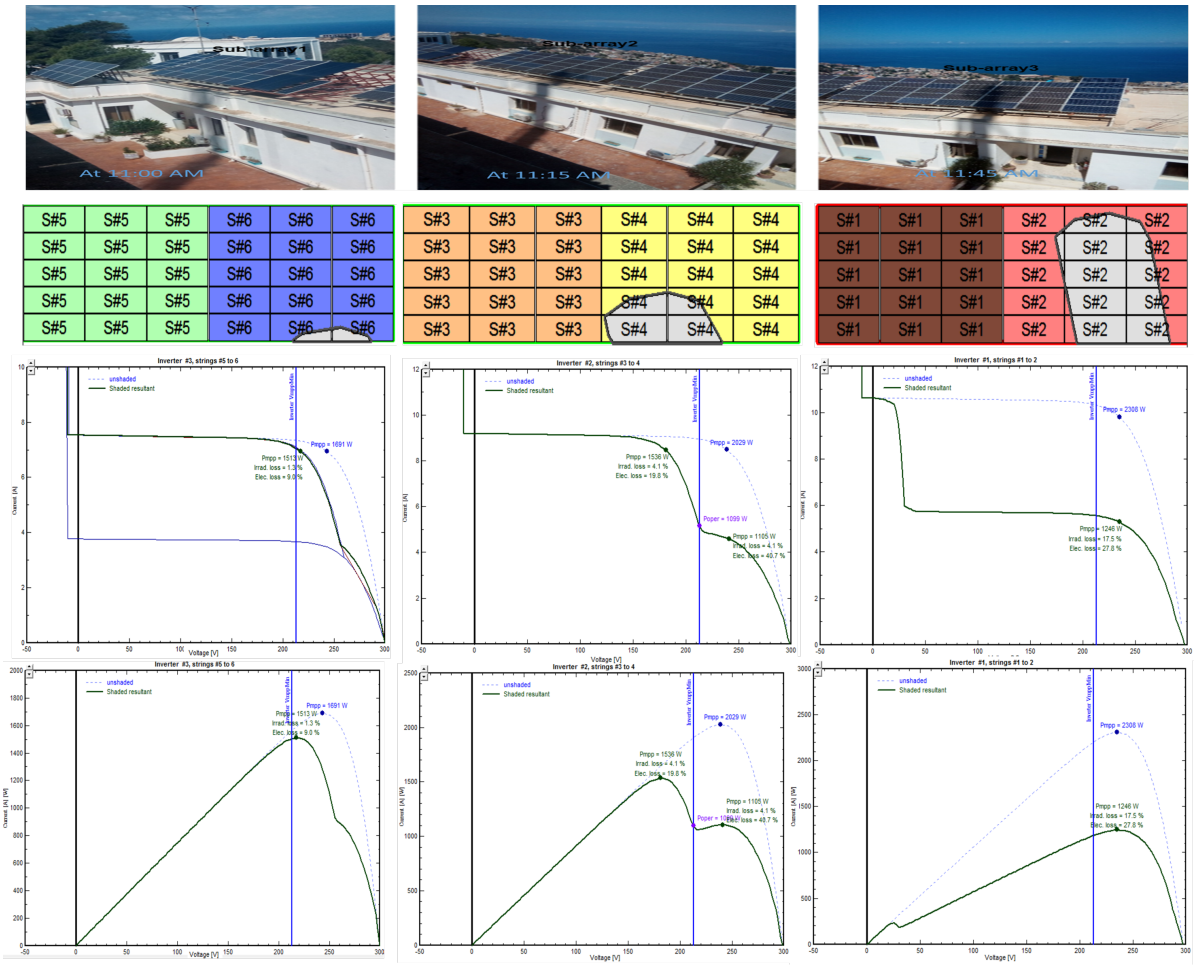

Figure 4.32: Position of the shadow in the three sub-array and I-V, P-V curve with respect to the shadow condition for 09/14/2019

4.7 Soiling

In general, the dust accumulation depends on the dust type, wind speed and direction,humidity, clearness index, last rainfall, the array texture and tilt angle [144].The dust reduces the proportion of the insolation that a system could receive due to the scattering of the solar radiation and due to the dust accumulation on the PV array

[145]. Our site is considered as a low dusty environment when compared to other sites in Algeria such as the South and the desert. To assess the soiling effect on our PV system. We applied a PV soiling experiment for one month by letting dust accumulate in sub-array1 while regularly cleaning sub-array2 and sub-array3. We have chosen the summer season to eliminate any shading effect.

The mechanical cleaning method is the most suit cleaning technique for small scale, which in our case. We chose the type that includes the water during cleaning using brush to wipe off the dirt from the modules and was carried out through manual labor. The first cleaning exercise was conducted on 10/08/2020 for sub-array2 and 3 while

Figure 4.33: Dirty sub-array1 and cleaned sub-array2,3

keeping sub-array1 as is, dirty with dust, see Figure4.33. Figure 4.34 shows the production of the three sub-arrays on 09/08/2019 before the cleaning took place. We can see that sub-array1 and 3 have the same production. We calculated the production ratio between sub-array1 and sub-array3 and found it was 100%. To confirm this, we calculated the difference ratio between those two arrays for each day between 01/08/2019 and 09/08/2019 and found all ratios ranged between 96%-100% throughout the nine days.The production of sub-array2 is little better than the other two sub-arrays. The planning of cleaning days is illustrated in Table4.5. After cleaning sub-array2 and 3

Table 4.5: cleaning planning

	09/08/2019	10/08/2019	17/08/2019	25/08/2019	01/09/2019
Sub-array1	x	x	x	x	✓
Sub-array2	x	✓	✓	✓	✓
Sub-array3	x	✓	✓	✓	✓

for the third time on 25/08/2019, we plot the production of the three sub-arrays 1, 2, 3 as

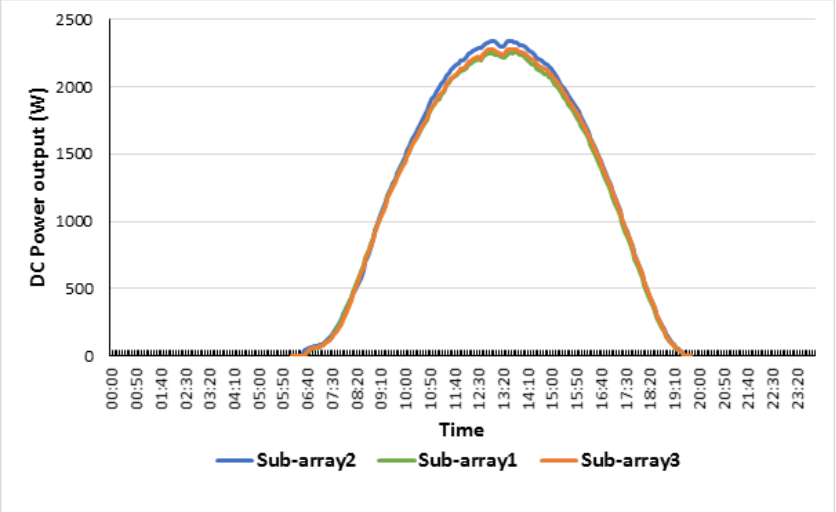

Figure 4.34: the DC power output for three sub-array of 09/08/2019 before cleaning

shown in Figure 4.35. We can see a clear difference in production between the sub-array 2, 3 and sub-array1.

We can even see a difference in production rates within the sub-arrays themselves (sub-array2, 3) before and after cleaning at 11:20.

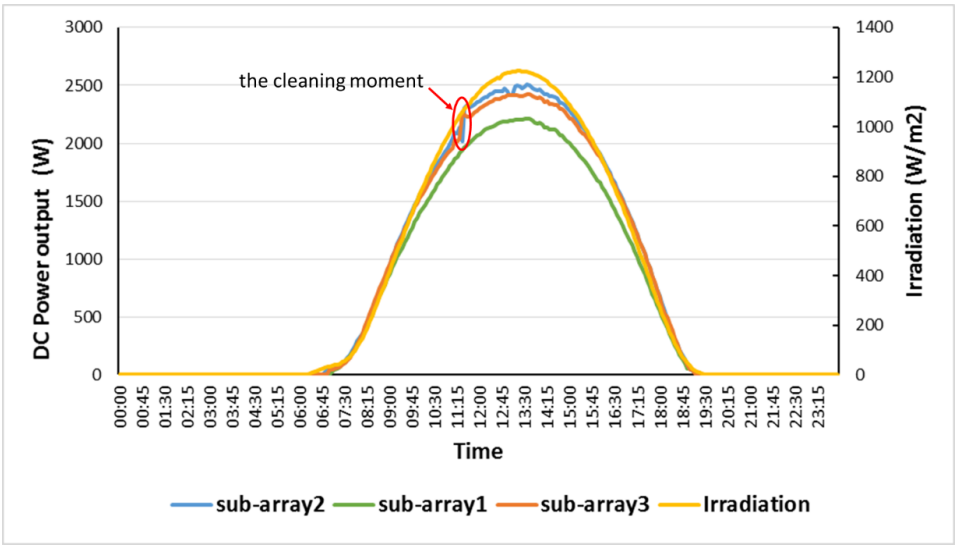

Figure 4.35: The DC power of three sub-array on the third time of cleaning for sub-array2,3

We plot the difference between the production of sub-array1 and 2 as shown in the Figure 4.36. We can see that the difference of production before cleaning was about 200

w because this is the third time that the array was cleaned. However, after cleaning, the difference in production reaches up to 341w. We calculated the ratio between the production of sub-array1 and sub-array3 to be 10%. Similarly, we get the same results for the days between 25/08/2020 to 01/09/2020 where three sub-array was cleaned. Therefore, it is very important, especially for dusty environments, to clean the PV arrays regularly and to take into account the reduction in output due to soiling loss.

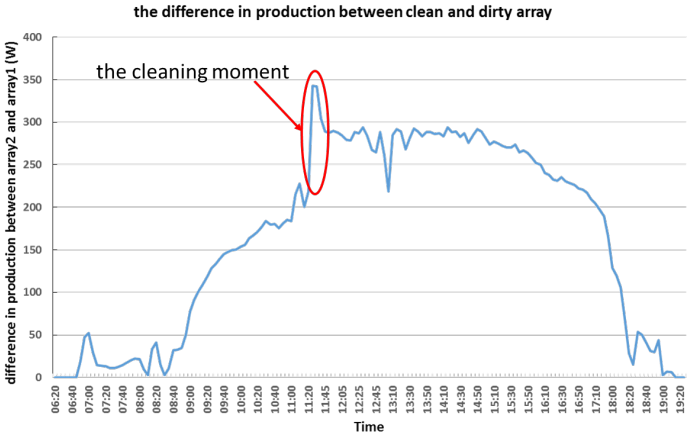

Figure 4.36: ratio production between the cleaned and dirty sub-array.

The impact of soiling on PV performance ratio means that panel cleaning is imperative. Many PV plants opt for periodic cleaning, with cleaning frequency based on historical data [146] .However, even for modestly sized PV plants, the costs of cleaning every panel can be significant, especially where desalinated water is in short supply.Some research is directed toward predictive models that are also unable to respond to long-term changes or isolated weather events that influence the soiling rates [147].

The only way to address soiling efficiently is to accurately monitor levels of soiling on site. the soiling monitoring system that offers accurate and continual monitoring of soiling in a PV plant that works by comparing signals from soiled cells to a clean reference cell.

4.8 Recommendations for Improved Performance

The performance of the photovoltaic system is not related to one factor but a variety of factors. Some of these factors are not in the field of human control, namely solar radiation, ambient temperature, wind speed, and direction, but some factors can be controlled. Where some of them can be controlled at the design and construction phase and others at the Operation and Maintenance (OM) phase. The choice of location of the system, the type of the module and their tilt and orientation, the size and type of inverter, and correct dimension of cable are the most control parameter in the design and construction phase. When looking at potential improvements in the Operation and Maintenance (OM) phase which are :

1. It is worthwhile to note that achieving optimal performance is next to impossible without monitoring the efficiency or Performance Ratio of the system. Only when monitoring exists, it is possible to ascertain that all systems are working as expected. When the PR drops, the operator must search for the reason for the drop, to allow for improved performance.

2. Appropriate measures for keeping monitoring sensors in optimal conditions

3. Quality of galvanic connections (DC and AC cabling), it alleviated by ensuring tight connections. currently, applied it to our plant by changing all cables.

4. Making available simple access to the inverters setting parameters from applications. Some inverter manufacturers allow easy access to the Parameters setting, some seem to practically forbid access, allowing only a limited number of parameters to be manually set, which is our case.

5. Shading can be noticed in the monitoring system, particularly when strings are monitored. Occasional drops in string current with no drop in solar irradiance can point to shading[]. Meanwhile, the simulation can be used to modify the PV module arrangement and reconfiguration to find an optimal interconnection to decrease the shading and eventually apply it to our plant

6. the severe protection features of the installed inverter (transformer-less inverter), although proven to have high efficiency, lead to the frequent disconnection of the sub-system for leakage current problem, resulting in the reduction of the total production. The replacement of surge the sensitivities of the differential at the output of the inverter

7. The PR will drop over time once the dust settles onto the modules and a soiling film evolves on the module cover. When cleaned, the PR rises.

4.9 Comparison between measured and simulated performance

The results of estimation of energy yield using PVsyst software are in close agreement with the actual measured results with uncertainty of 3% when measured solar radiation data of the site is used as input to the simulation software as shown in Figure 4.37. The

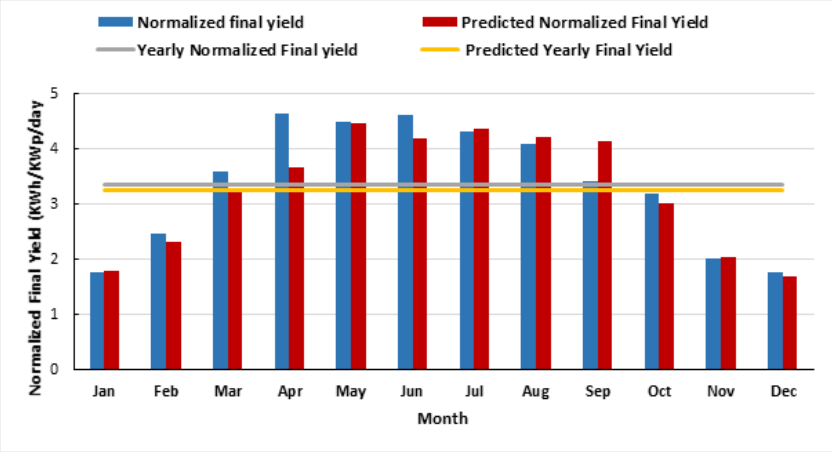

Figure 4.37: measured and predicted normalized final yields.

measured annual PR of the solar plant is found to be 70% which is very close to the PVsyst predicted PR of 69% as shown in Figure4.38.

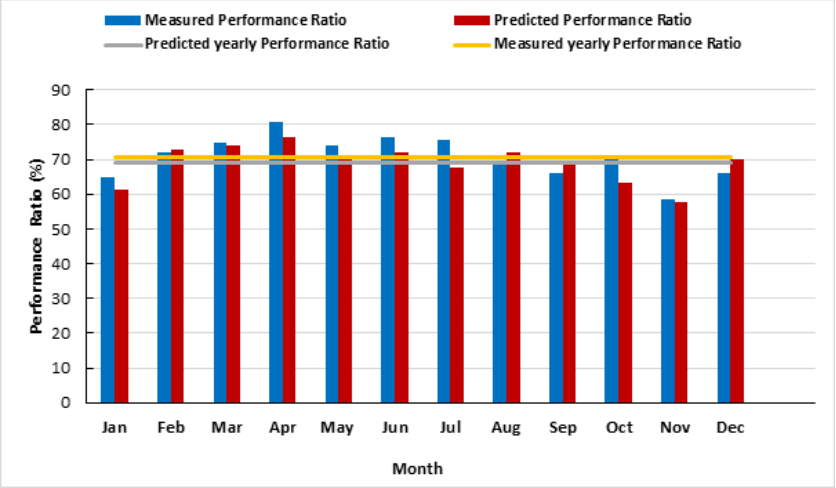

Figure 4.38: measured and predicted performance ratio PR.

4.10 Power Quality Experimental Analysis according to 50160

PV systems may in some cases affect voltage quality in public distribution networks[148], which is why analysis of the voltage quality at the common connection point (PCC) of our CDER system was required by using the European standard EN 50160 standards. Our team had many experimental measurements analysis in term of the frequency, voltage, power factor and total harmonic distortion (current and voltage) were performed at Point of Common Coupling (PCC). The measurements were carried out by a network analyzer as descripted in 3.2.6 over two weeks (15 days) during the months of July. The measured electrical parameters are recorded for each phase,which are: the true rms values (TRMS) of the three-phase voltages, the true rms values (TRMS) of the three-phase currents, the harmonic distortion rate (THD) of the voltages and currents.

4.10.1 Frequency

The EN 50160 standard requires that the average value of the fundamental frequency measured per period of 10 seconds must be within the interval ±1% of 50 Hz for 99.5% of a week and between −6% and +4% of 50 Hz for 100% of the time [149]. Table 4.6 shows

a comparison between the requirements of EN 50160 and the measured values of the voltage frequency. The results show that the frequency varies in an interval between -0.4% and + 0.2% of 50 Hz for 100% during the monitored period.

Table 4.6: Frequency characteristic

	Measured(CA 8335)	**EN 50160**
Frequency	49.8Hz-50.2Hz	49.5 Hz - 50.5 Hz (99.5 %)
		47 Hz - 52 Hz - (100%)

4.10.2 Effective voltage

The EN 50160 standard requires that the rms values, averaged over a period of 10 minutes, must be within the range ±10% of 230 V for 95% of a week [149]. Table 4.7 shows a comparison between the requirements of EN 50160 and the measured RMS voltage values at the PCC. Over the measurement period (three weeks), we observe that the rms voltage varies in the range between −9.65% and +3.43% of 230 V; which complies with the requirements of EN50160.

Table 4.7: voltage variation characteristic

	Effective voltage variation values(V)	**EN 50160**
Phase1	207.8-235.9	230V - 253 V (95%) for one week
Phase2	227.8-235.2	
Phase3	227.7-234.1	

4.10.3 Harmonic voltages

Table 4.10.3 shows the individual odd harmonic voltages according to EN 50160 and measured at the PCC. This individual assessment shows that the voltage at the PCC complies with the maximum limits required by this standard with the exception of the order 15 harmonic voltage [113].this result was for three week for different month July, August and September.

Table 4.8: Comparison of harmonic voltage requirements according to EN 50160 and the values measured at the PCC [113]

Non-multiple of 3.			Multiple of 3.		
Order	Relative voltage in% (EN 50160).	Relative voltage in% (measured).	Order	Relative voltage in% (EN 50160).	Relative voltage in% (measured).
5	6	0.6-5	3	5	0.1-2.9
7	5	0 - 1.9	9	1.5	0.1-1.3
11	3.5	0 - 0.5	15	0.5	0-1
13	3	0 - 0.9	21	0.5	0-0.4
17	2	0 - 0.6			
19	1.5	0 - 0.5			
23	1.5	0 - 0.2			
25	1.5	0 - 0.4			

4.11 Fulfillment of CDER system to the requirements of Technical Connection Rules

The normal operation requirements can be divided into frequency deviation, voltage deviation, active power control, and reactive power control.

4.11.1 Frequency deviation

Figure 4.39 shows the frequency on PCC for the sub-system2 for the month of July 2020. We can see that the measured frequency is operating properly within a frequency range of 49.8Hz-50.2Hz.

4.11.2 Voltage deviation and reactive power

In our study we extracted the measurements at PCC for three phases: 1)sub-system2 2)load and 3)grid using the power quality analyzer CA8335. The new TCR of connecting PV power plants to the LV network is analyzed. After analyzing the P-Q curves and V-Q for different values of injected active power it can be stated that, the voltage and reactive power is within the required curve (see Figure 4.40).

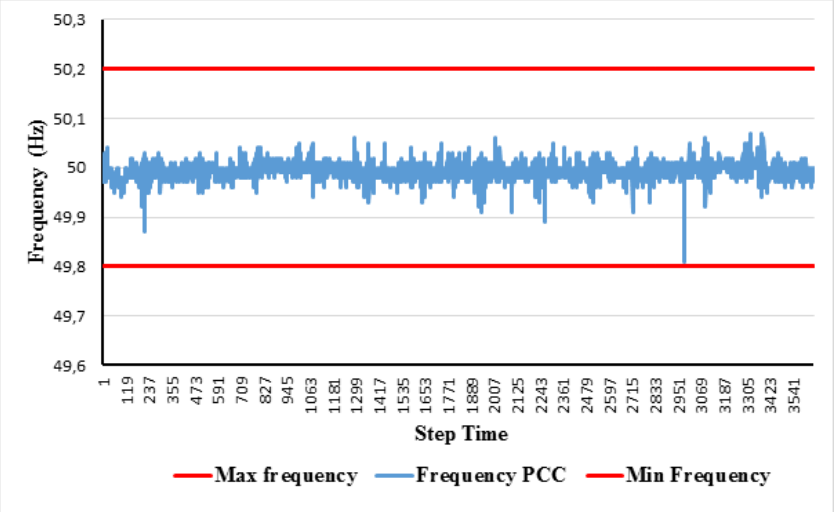

Figure 4.39: frequency deviation.

4.11.3 Voltage during fault and Voltage control

Our PV plants connected to the LV power grid have to be able to supply reactive power to the grid at any point of operation to support grid voltage stability under normal operation and have to ride-through the grid fault without disconnection from the Grid. This two-option is an intelligent function found in Smart Inverters. Unfortunately our inverters don't have this two function [150] of FRT(fault ride through capability) as explained in 2.9.4 and curve Figure 2.15. On the other hand, voltage controlling can be managed through Q(v) or Q(p), however the the curve to be followed or its specific setting were not provided.

4.11.4 Discussion of the new Technical Connection Rules (TCR) requirement on the CDER plant

After checking all requirements of Algeria's New TCR for integration of the PV plant to the Low Voltage network, we can see that our plant satisfied the technical equipment at the Grid Connection Point, such as the data Measuring, Monitoring and energy metering equipment. On the other hand, only the Anti Islanding Protection is activated for the controlling function in our inverters, meanwhile the reactive control and ride-through

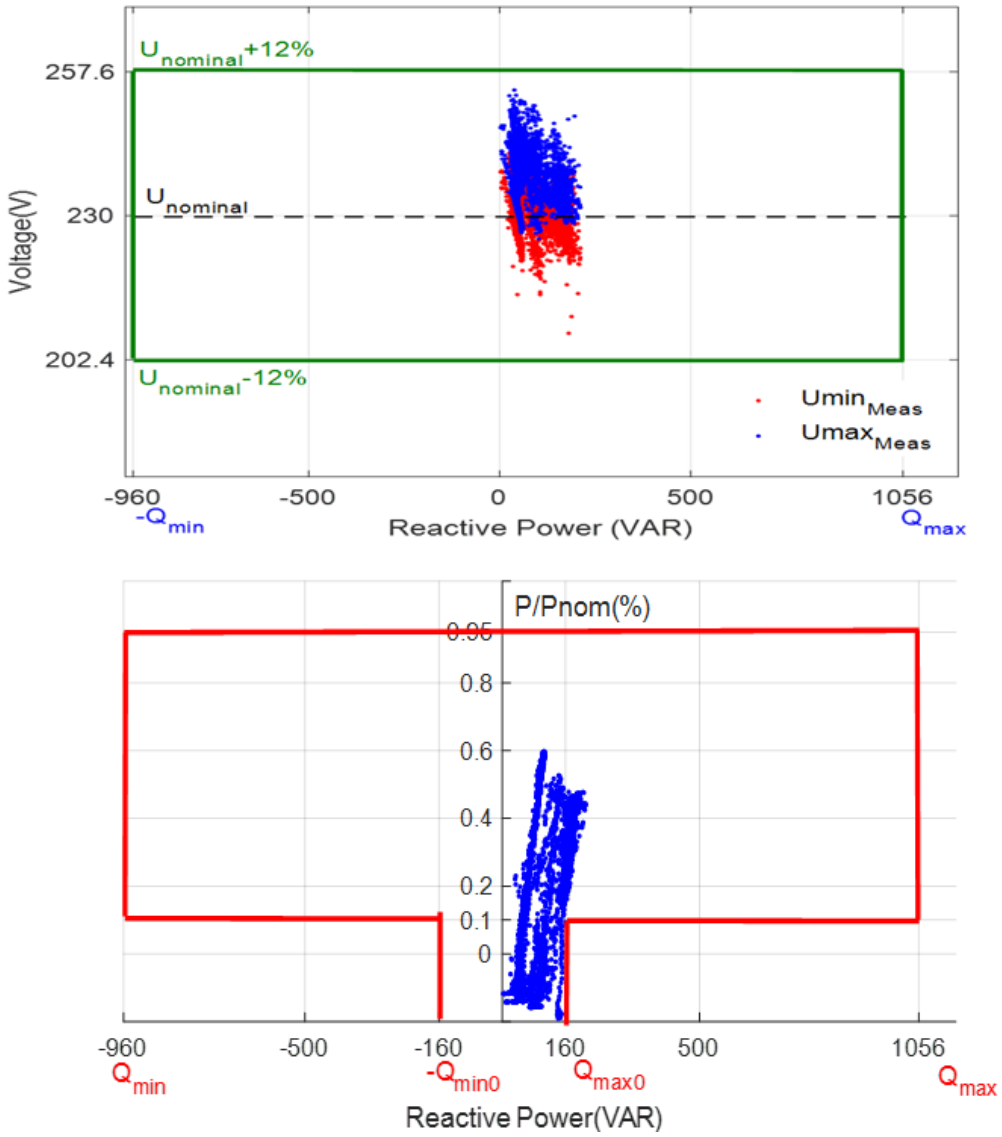

Figure 4.40: Capability curve of CDER plant for month July.

the grid fault was deactivated in our SMA Sunny Boy 3000TLST-21 inverter by the manufacturer, which can only be activated by authorized/specialized centers. Analyzed the P-Q curves and V-Q curve for different values of injected active power was in the required curves and the frequency measurement within the acceptable range, however we can't see any controlling of voltage or frequency or FRT in our inverters since the inverters disconnect automatically.

4.12 Conclusion

The short-term investigation between the measured and the simulated data shows that the differences in the PR and/or energy output values were mostly due to the difference in the irradiation values. This leads to two results: first, that the simulation package used for this research could give results close to the actual values if the on-site measured irradiation values are used as an input and second, PVsyst is found to be a good tool to simulate a PV system with projected yield, most likely with results being more conservative.The software is only good as long as the person using it is an expert within the solar energy. Despite the fact that the results from PVsyst already take into account an annual soiling loss factor. However, especially for the examined site and after conducting a further investigation, it is found that the importance of the regular cleaning of the PV modules in such sites is important. Regarding the short-term performance, the effect of temperature on the performance ratio is observed for the plant at high irradiation levels, and inverter threshold and shading issues have been revealed for the three sub-arrays.

General conclusion and future works

The main objective of this thesis is to study the first photovoltaic power plant connected to the electricity distribution network in Algeria. The conclusions made are aimed at providing more information regarding the performance of the pv grid connected and power quality and the Technical Connection Rules (TCR) requirement to integrate the PV plant to the distribution network. The studied field plant was a 9.5kWp PV plant divided into three sub-systems installed on the roof of the renewable center in Bouzareah, Algeria. A selection of three-year analysis was evaluated in an hourly, daily, monthly and yearly basis. The data analyzed include the measured output power of the PV array, DC/AC inverter output powers, cell temperature, and solar irradiation which were monitored between 2016 and 2018. The evaluation parameters used in this study are based on those outlined in the International Electro-Technical Commission (IEC) Standard 61724. The results show that based on the average solar energy potential (radiation) between 84.8 and 184.2 kWh/m2 on 29 tilt, the system was able to inject to the grid about 525kWh/m2 in January and 1243 kWh/m2 in June for the year 2017, while the annual total energy generated was 11,161 MWh. The monthly average daily reference, array, and final yields are 4.673.50 and 3.37 h/day respectively. The average capture losses and system losses are 1.16 and 0.13 kWh/kWp/day which represent 25.91% and 2.79% respectively. System losses remain more or less constant throughout the year, whereas capture losses are found to increase with increasing of effect of temperature and shading effect. In addition, the annual average efficiency of the PV module and system plant is 8.62% and 8.29% respectively, whereas the average inverter efficiency is 96.22%. The critical performance indicator, the performance ratio

(PR) is found to average at 70% across all the study Period. However, the corrected performance ratio appears to provide a more complete correction of ambient conditions of module performance than PR.

The comparison of the predictive performance parameters simulated through PVsyst show that they are in close agreement with the actual measured results with an uncertainty of 4% when the measured solar radiation data of the site is used as input to the simulation software. This concludes that the PVsyst is a powerful tool for predictive performance of PV grid connected system photovoltaic systems. The software is only good as long as the person using it is an expert within the solar energy to consider all the varrying possibilities and complications of modelling.

Further investigation was also done to understand and quantify system losses. One of the major parameter influencing our system's electric performance is: near shadowing effects which can be able to reduce the production to 50% in some cases. In order to reduce the influence of shading effect, the simulation can be used to modify the PV module arrangement and reconfiguration to find an optimal interconnection to decrease the shading and eventually apply it on our plant. Additionally, due to the severe protection features of the installed inverter (transformer-less inverter), although proven to have high efficiency, lead to the frequent disconnection of the sub-system for leakage current problem, resulting in the reduction of the total production.

Thus, understanding and tackling these external factors is essential for improving our PV grid connected system performance. Maximizing the utilization of the system by eliminating or mitigating energy losses will improve the reliability of the PV system.

The analysis of the measured power quality parameters at the inverter output side which are apparent, active and reactive powers, current, voltage and power factor, total harmonic distortion (THD) (measured over a period of one week for each month) reveals a good relation between power quality injected into the network and solar irradianc e.

In order to connect our PV power plants to the low-voltage grid according to the new Technical Connection Rules (TCR), we have to make sure that all requirements are fulfilled. First the technical equipment requirement were found to be compliant. Although

anti-islanding is activated, we found that the control function for under-voltage and over-voltage, under-frequency and over-frequency, and fault ride through are deactivated in our inverters plant. In order to activate the control function in our inverters, the constructor of our inverter SMA 3000sunny boy should be contacted to activate these functions to be able to set the curve that responds to our grid.

After analyzing the P-Q curves and V-Q and frequency for different values of injected active power it can be stated that, the voltage and reactive power is within the required curve.

Connecting a PV plant to the low voltage of Algeria utility grid is facing a lot of challenges : one, due the requirement of control functions, which are in reality function of smart inverters and most inverter manufacturers don't activate the intelligent function because the TCR changes from country to country. Accordingly, the inverter manufacturers don't give authorisation except for qualified entities to do the setting. Therefore, the challenge for the case of Algeria in the future case is identifying the responsible entity for setting the intelligent functions. Second, according to Algeria's TCR, the voltage control set point can be one of the following operational modes: 1) a variable active power depending on the voltage and 2) a variable reactive power depending on the voltage Q(V). The first mode doesn't fit the investor's interest because it reduces their return. The second mode Q(v), which is required in most countries' TCR, Algeria's Technical Connection Rules (TCR) lacks any clear guidance and doesn't illustrate any curve to follow. As a future work is to set the curve of smart inverter to correspond with the our grid.

The outcomes of this study are twofold. Since most installed PV grid connected plants integrated into the distribution network are affiliated with research centers this facilitates the corresponding entities to conduct studies and analysis of the connection to the distribution network. Since the introduction of the new TCR in Algeria, such studies provide a rich resource for identifying the requirements and updating the current TCR based on these analyses.

The selection of phase one PV plant location have proven to be successful. However,

this performance case study provides a thorough explanation on how the system is working and what are the different sources of losses. Based on this analysis, such studies prove to be essential for locating the future sites in phase two of Algeria's Renewable Energy National Program. This is the case due to the vast difference in Algeria's climate conditions.

BIBLIOGRAPHY

[1] H.-W. Schiffer, T. Kober, and E. Panos, "World Energy Council Global Energy Scenarios to 2060," *Zeitschrift für Energiewirtschaft*, vol. 42, no. 2, pp. 91–102, 2018.

[2] H. Hafeznia, H. Yousefi, and F. Razi Astaraei, "A novel framework for the potential assessment of utility-scale photovoltaic solar energy, application to eastern Iran," *Energy Conversion and Management*, vol. 151, no. August, pp. 240–258, 2017.

[3] Y. K. Ramgolam and K. M. S. Soyjaudah, "Holistic performance appraisal of a photovoltaic system," *Renewable Energy*, vol. 109, pp. 440–448, 2017. [Online]. Available: http://dx.doi.org/10.1016/j.renene.2017.03.038

[4] A. Ghezloun, A. Saidane, N. Oucher, and H. Merabet, "Actual Case of Energy Strategy in Algeria and Tunisia," *Energy Procedia*, vol. 74, pp. 1561–1570, 2015. [Online]. Available: http://dx.doi.org/10.1016/j.egypro.2015.07.720

[5] A. Razagui, N. I. Bachari, K. Bouchouicha, and A. Hadj Arab, "Modeling the Global Solar Radiation Under Cloudy Sky Using Meteosat Second Generation High Resolution Visible Raw Data," *Journal of the Indian Society of Remote Sensing*, vol. 45, no. 4, pp. 725–732, 2017.

[6] K. Abdeladim, S. Bouchakour, A. H. Arab, S. Ould, C. Farida, and B. Taghezouit, "Renewable Energies in Algeria : Current," in *29th European Photovoltaic Solar Energy Conference and Exhibition*, no. August 2014, 2014.

[7] A. Pegels, “Feed-in tariffs for renewable energy : which determination option works for whom ?” German Development Institute, Tech. Rep. January, 2016.

[8] M. Díez-Mediavilla, C. Alonso-Tristán, M. C. Rodríguez-Amigo, T. García-Calderón, and M. I. Dieste-Velasco, “Performance analysis of PV plants: Optimization for improving profitability,” *Energy Conversion and Management*, vol. 54, no. 1, pp. 17–23, 2012. [Online]. Available: http://dx.doi.org/10.1016/j.enconman.2011.09.013

[9] U. Jahn and W. Nasse, “Operational performance of grid-connected PV systems on buildings in Germany,” *Progress in Photovoltaics: Research and Applications*, vol. 12, no. 6, pp. 441–448, 2004.

[10] N. Tong, R. Salazar, T. Brasil, B. Blackburn, and D. Johnson, “Emerging Renewables Program Systems Verification Report California Energy Commission,” no. December, 2005. [Online]. Available: https://www.energy.ca.gov/2005publications/CEC-300-2005-019/CEC-300-2005-019.PDF

[11] A. M. Khalid, I. Mitra, W. Warmuth, and V. Schacht, “Performance ratio ‚Äì Crucial parameter for grid connected PV plants,” *Renewable and Sustainable Energy Reviews*, vol. 65, pp. 1139–1158, 2016. [Online]. Available: http://dx.doi.org/10.1016/j.rser.2016.07.066

[12] IRENA, “Renewable capacity statistics 2021,” Abu Dhabi, Tech. Rep., 2021. [Online]. Available: www.irena.org/Publications

[13] E. A. IEA, International, “Country Analysis Brief : Algeria,” U.S. Energy Information Administration, Tech. Rep. July, 2014.

[14] M. Bouznit, M. P. Pablo-Romero, and A. Sánchez-Braza, “Residential electricity consumption and economic growth in algeria,” *Energies*, vol. 11, no. 7, pp. 1–18, 2018.

[15] S. Michaut, "Market Analysis for Gas Engine Technology in Algeria," Ph.D. dissertation, School of Industrial Engineering and Management, 2013.

[16] N. Bailek and K. Bouchouicha, "Updated status of Renewable and Sustainable Energy Projects in Algeria," *Economics of Variable Renewable Sources for Electric Power Production*, no. November, pp. 519–528, 2017.

[17] D. Direction Analyse & Prévisions, "Bulletin Statistiques des societes energetiques du Group Sonalgaz 2019," Société Nationale de l'Electricité et du Gaz, Algeria, Tech. Rep., 2019.

[18] M. Bouznit, M. del P. Pablo-Romero, and A. Sánchez-Braza, "Measures to promote renewable energy for electricity generation in Algeria," *Sustainability (Switzerland)*, vol. 12, no. 4, pp. 1–17, 2020.

[19] République Algérienne Démocratique et Populaire, "Journal Officiel de la République Algérienne N. 23," *23 April 2014*, 2014. [Online]. Available: http://www.cder.dz/IMG/pdf/arrete_tarifs_achat_garantis_photovoltaique_eolien.pdf

[20] H. Z. Al Garni, "Optimal Design and Analysis of Grid-Connected Solar Photovoltaic Systems," Ph.D. dissertation, Concordia University, 2018.

[21] J. M. Xavier, "Performance Analysis of a PV Grid-connected System at the Universidade Nacional Timor Lorosa," Ph.D. dissertation, University of Porto, 2019.

[22] A. Ruiz, "System aspects of large scale implementation of a photovoltaic power plant," Ph.D. dissertation, Stockholm, 2011.

[23] I.-T. K. Theologitis, "Comparison of existing PV models and possible integrtion under EU grid specifications," Ph.D. dissertation, Electrical Engineering of STOCKHOLM, 2011. [Online]. Available: http://kth.diva-portal.org/smash/get/diva2:470828/FULLTEXT01.pdf

[24] P. Breza, "Modelling and simulation of a PV generator for applications on distributed generation systems," Ph.D. dissertation, Delft University of Technology, 2013.

[25] J. Meyer, "Solar Electricity Utilization in Finland," Ph.D. dissertation, Helsinki Metropolia University of, 2015.

[26] K. Alzaareer, C. Z. El-Bayeh, and Q. Salem, "Grid-connected PV systems: Impact evaluation & optimal allocation and sizing for losses minimization and voltage improvement (Jordanian case study)," *Journal of Electrical and Electronics Engineering*, vol. 12, no. 2, pp. 17–22, 2019.

[27] W. Omran, "Performance Analysis of Grid-Connected Photovoltaic Systems, University of Waterloo," Ph.D. dissertation, University of Waterloo,Ontario, Canada,, 2010.

[28] F. F. Rakotomananandro, "Study of Photovoltaic System," Ph.D. dissertation, The Ohio State University, 2011.

[29] L. Maturi and J. Adami, *Building Integrated Photovoltaic (BIPV) in Trentino Alto Adige*. Springer International Publishing AG, 2018. [Online]. Available: http://link.springer.com/10.1007/978-3-319-74116-1

[30] M. S. Montaser Abd El-Sattar, "Study , Design and Performance Analysis of Grid- Connected Photovoltaic Power Systems Study , Design and Performance Analysis of," Ph.D. dissertation, Minia University, 2015.

[31] G. Notton, V. Lazarov, and L. Stoyanov, "Optimal sizing of a grid-connected PV system for various PV module technologies and inclinations, inverter efficiency characteristics and locations," *Renewable Energy*, vol. 35, no. 2, pp. 541–554, 2010. [Online]. Available: http://dx.doi.org/10.1016/j.renene.2009.07.013

[32] G. M. G. David L. King, Sigifredo Gonzalez and W. E. Boyson, "Performance Model for Grid-Connected Photovoltaic Inverters," Sandia National Laboratories SAND2007-5036, Tech. Rep., 2007.

[33] M. Pierro, F. Bucci, and C. Cornaro, "Full characterization of photovoltaic modules in real operating conditions: theoretical model, measurement method and results," *Ieee Trans Fuzzy Syst*, vol. 20, no. 6, pp. 1114–1129, 2014.

[34] International Electrotechnical Commission, "Photovoltaic system performance monitoring Guidelines for measurement , data exchange and analysis," Tech. Rep., 1998.

[35] A. Hadj Arab, B. Taghezouit, K. Abdeladim, S. Semaoui, A. Razagui, A. Gherbi, S. Boulahchiche, and I. Hadj Mahammed, "Maximum power output performance modeling of solar photovoltaic modules," *Energy Reports*, vol. 6, pp. 680–686, 2020. [Online]. Available: https://doi.org/10.1016/j.egyr.2019.09.049

[36] A. Arab, B. Taghezouit, K. Abdeladim, S. Semaoui, S. Boulahchiche, A. Razagui, A. Gherbi, Bouacha, M. S., N. S., S., and A. Djoudi, "Modélisation de l'onduleur photovoltaïque connecté au réseau électrique," *Journal of Renewable Energies*, vol. 23, pp. 217–235, 2020.

[37] H. Rodriguez-Murcia, "Analysis of the generation of a photovoltaic system connected to an internal grid," *Journal of Physics: Conference Series*, vol. 1173, no. 1, 2019.

[38] The International Electrotechnical Commission, "IEC 61724-1," Tech. Rep., 2017.

[39] Hukseflux, "IEC 61724-1:2017 What is new in the 2017 version," pp. 1–4, 2017. [Online]. Available: info@hukseflux.com

[40] W. C. Lee, T. Sales, and S. Manager, "Explaining PV plant monitoring to IEC 61724-1," Tech. Rep., 2017.

[41] International Electrotechnical Commission (IEC), "Photovoltaic system performance - IEC TS 61724-2: Capacity evaluation method," Tech. Rep., 2016.

[42] International Electrotechnical Commission(IEC), "Photovoltaic system performance -IEC TS 61724-3: Energy evaluation method," Tech. Rep., 2016.

[43] S. Fraser and G. Fraser, "Solar PV Capacity Factor," The Ravina Project, Toronto, Ontario, Canada M4J3L9, Tech. Rep., 2014. [Online]. Available: www.theravinaproject.org

[44] T. Dierauf, A. Growitz, S. Kurtz, and C. Hansen, "Weather-Corrected Performance Ratio Technical Report NREL/TP-5200-57991," National Renewable Energy Lab.(NREL), Golden, CO (United States), Tech. Rep., 2013.

[45] G. Aaditya, R. Pillai, and M. Mani, "An insight into real-time performance assessment of a building integrated photovoltaic (BIPV) installation in Bangalore (India)," *Energy for Sustainable Development*, vol. 17, no. 5, pp. 431–437, 2013. [Online]. Available: http://dx.doi.org/10.1016/j.esd.2013.04.007

[46] V. Sharma and S. S. Chandel, "Performance and degradation analysis for long term reliability of solar photovoltaic systems: A review," *Renewable and Sustainable Energy Reviews*, vol. 27, pp. 753–767, 2013. [Online]. Available: http://dx.doi.org/10.1016/j.rser.2013.07.046

[47] L. M. Ayompe, A. Duffy, S. J. McCormack, and M. Conlon, "Measured performance of a 1.72 kW rooftop grid connected photovoltaic system in Ireland," *Energy Conversion and Management*, vol. 52, no. 2, pp. 816–825, 2011. [Online]. Available: http://dx.doi.org/10.1016/j.enconman.2010.08.007

[48] S. Sundaram and J. S. C. Babu, "Performance evaluation and validation of 5MW grid connected solar photovoltaic plant in South India," *Energy Conversion and Management*, vol. 100, no. 2015, pp. 429–439, 2015. [Online]. Available: http://dx.doi.org/10.1016/j.enconman.2015.04.069

[49] M. A. Eltawil and Z. Zhao, "Grid-connected photovoltaic power systems: Technical and potential problems-A review," *Renewable and Sustainable Energy Reviews*, vol. 14, no. 1, pp. 112–129, 2010.

[50] D. Okello, E. E. Van Dyk, and F. J. Vorster, "Analysis of measured and simulated performance data of a 3.2 kWp grid-connected PV system in Port Elizabeth, South Africa," *Energy Conversion and Management*, vol. 100, pp. 10–15, 2015. [Online]. Available: http://dx.doi.org/10.1016/j.enconman.2015.04.064

[51] A. R. Malekpour and A. Pahwa, "A Dynamic Operational Scheme for Residential PV Smart Inverters," *IEEE Transactions on Smart Grid*, pp. 1–10, 2016.

[52] M. Al Ali and M. Emziane, "Performance analysis of rooftop PV systems in Abu Dhabi," *Energy Procedia*, vol. 42, pp. 689–697, 2013. [Online]. Available: http://dx.doi.org/10.1016/j.egypro.2013.11.071

[53] N. Ketjoy, C. Sirisamphanwong, and N. Khaosaad, "Performance evaluation of 10 kWp photovoltaic power generator under hot climatic condition," *Energy Procedia*, vol. 34, pp. 291–297, 2013. [Online]. Available: http://dx.doi.org/10.1016/j.egypro.2013.06.757

[54] D. Micheli, S. Alessandrini, R. Radu, and I. Casula, "Analysis of the outdoor performance and efficiency of two grid connected photovoltaic systems in northern Italy," *Energy Conversion and Management*, vol. 80, pp. 436–445, 2014. [Online]. Available: http://dx.doi.org/10.1016/j.enconman.2014.01.053

[55] M. E. Başo álu, A. Kazdalo álu, T. Erfidan, M. Z. Bilgin, and B. Cąkir, "Performance analyzes of different photovoltaic module technologies under ÃÑzmit, Kocaeli climatic conditions," *Renewable and Sustainable Energy Reviews*, vol. 52, pp. 357–365, 2015.

[56] S. Edalati, M. Ameri, and M. Iranmanesh, "Comparative performance investigation of mono- and poly-crystalline silicon photovoltaic modules for

use in grid-connected photovoltaic systems in dry climates," *Applied Energy*, vol. 160, pp. 255–265, 2015. [Online]. Available: http://dx.doi.org/10.1016/j.apenergy.2015.09.064

[57] E. Elibol, O. T. Ozmen, and N. Tutkun, "Outdoor performance analysis of different PV panel types," *Renewable and Sustainable Energy Reviews*, vol. 67, pp. 651–661, 2017.

[58] D. A. Quansah, M. S. Adaramola, G. K. Appiah, and I. A. Edwin, "Performance analysis of different grid-connected solar photovoltaic (PV) system technologies with combined capacity of 20kW located in humid tropical climate," *International Journal of Hydrogen Energy*, vol. 42, no. 7, pp. 4626–4635, 2017. [Online]. Available: http://dx.doi.org/10.1016/j.ijhydene.2016.10.119

[59] K. M. K. Armijo, "Performance Impact of Solar Gain on Photovoltaic Inverters and Utility-Scale Energy Generation Systems." *2013 IEEE 39th Photovoltaic Specialists Conference (PVSC)*, pp. 0740–0745, 2013. [Online]. Available: http://ieeexplore.ieee.org/lpdocs/epic03/wrapper.htm?arnumber=6744256%5Cnhttp://energy.sandia.gov/wp/wp-content/gallery/uploads/Armijo_SAND2013-4859C_PVSC391.pdf

[60] T. Khatib, K. Sopian, and H. A. Kazem, "Actual performance and characteristic of a grid connected photovoltaic power system in the tropics: A short term evaluation," *Energy Conversion and Management*, vol. 71, pp. 115–119, 2013. [Online]. Available: http://dx.doi.org/10.1016/j.enconman.2013.03.030

[61] F. Spertino and F. Corona, "Monitoring and checking of performance in photovoltaic plants: A tool for design, installation and maintenance of grid-connected systems," *Renewable Energy*, vol. 60, pp. 722–732, 2013. [Online]. Available: http://dx.doi.org/10.1016/j.renene.2013.06.011

[62] S. Messina, I. P. H. Rosales, C. E. Durán, J. J. Quiñones, and P. K. Nair, "Comparative study of system performance of two 2.4 kW grid-

connected PV installations in Tepic-Nayarit and Temixco-Morelos in México," *Energy Procedia*, vol. 57, pp. 161–167, 2014. [Online]. Available: http://dx.doi.org/10.1016/j.egypro.2014.10.020

[63] H. A. Kazem, T. Khatib, K. Sopian, and W. Elmenreich, "Performance and feasibility assessment of a 1.4 kW roof top grid-connected photovoltaic power system under desertic weather conditions," *Energy and Buildings*, vol. 82, pp. 123–129, 2014. [Online]. Available: http://dx.doi.org/10.1016/j.enbuild.2014.06.048

[64] M. S. Adaramola, "Techno-economic analysis of a 2.1 kW rooftop photovoltaic-grid-tied system based on actual performance," *Energy Conversion and Management*, vol. 101, pp. 85–93, 2015. [Online]. Available: http://dx.doi.org/10.1016/j.enconman.2015.05.038

[65] A. Elkholy, F. Fahmy, A. Abou El-Ela, A. E.-S. A. Nafeh, and S. Spea, "Experimental evaluation of 8kW grid-connected photovoltaic system in Egypt," *Journal of Electrical Systems and Information Technology*, vol. 3, no. 2, pp. 217–229, 2016. [Online]. Available: http://linkinghub.elsevier.com/retrieve/pii/S2314717216300356

[66] L. C. de Lima, L. de Araújo Ferreira, and F. H. B. de Lima Morais, "Performance analysis of a grid connected photovoltaic system in northeastern Brazil," *Energy for Sustainable Development*, vol. 37, pp. 79–85, 2017. [Online]. Available: http://dx.doi.org/10.1016/j.esd.2017.01.004

[67] M. E. Ya'Acob, H. Hizam, T. Khatib, and M. A. M. Radzi, "A comparative study of three types of grid connected photovoltaic systems based on actual performance," *Energy Conversion and Management*, vol. 78, pp. 8–13, 2014.

[68] D. Martinez-Plaza, A. Abdallah, B. W. Figgis, and T. Mirza, "Performance Improvement Techniques for Photovoltaic Systems in Qatar: Results of First year of Outdoor Exposure," *Energy Procedia*, vol. 77, pp. 386–396, 2015. [Online]. Available: http://dx.doi.org/10.1016/j.egypro.2015.07.054

[69] T. Somsak, S. Jumpaim, J. Thongporn, and D. Chenvidhya, "Techno evaluation on a grid connected 9.8 kWp PV rooftop at various orientation in Thailand," in *13th International Conference on Electrical Engineering/Electronics, Computer, Telecommunications and Information Technology, (ECTI-CON)*. IEEE, 2016, pp. 1–4.

[70] R. R. Rao, H. R. Swetha, J. Srinivasan, and S. K. Ramasesha, "Comparison of performance of solar photovoltaics on dual axis tracker with fixed axis at 13°N latitude," *Current Science*, vol. 108, no. 11, pp. 2087–2094, 2015.

[71] R. Dabou, F. Bouchafaa, A. H. Arab, A. Bouraiou, M. D. Draou, A. Neçaibia, and M. Mostefaoui, "Monitoring and performance analysis of grid connected photovoltaic under different climatic conditions in south Algeria," *Energy Conversion and Management*, vol. 130, pp. 200–206, 2016. [Online]. Available: http://dx.doi.org/10.1016/j.enconman.2016.10.058

[72] D. H. Daher, L. Gaillard, M. Amara, and C. Ménézo, "Impact of tropical desert maritime climate on the performance of a PV grid-connected power plant," *Renewable Energy*, vol. 125, pp. 729–737, 2018.

[73] H. A. Kazem and T. Khatib, "Techno-economical assessment of grid connected photovoltaic power systems productivity in Sohar, Oman," *Sustainable Energy Technologies and Assessments*, vol. 3, pp. 61–65, 2013. [Online]. Available: http://dx.doi.org/10.1016/j.seta.2013.06.002

[74] P. K. Mochi, "Simulation and Performance Analysis of 100kWp Solar Rooftop using Solar Pro software," *National Workshop on Research challenges in Power Electronics & Power System.NIT Calicut*, pp. 1–5, 2017.

[75] B. K. Gautam, F. A. Khan, A. Singh, P. G. S. Cse, U. Pradesh, and U. Pradesh, "5 MWp grid-connected solar pv power plant using iec 61724," *International Research Journal of Engineering and Technology(IRJET)*, vol. 4, no. 7,

pp. 2801–2805, 2017. [Online]. Available: https://irjet.net/archives/V4/i7/IRJET-V4I7566.pdf

[76] M. Emmanuel, D. Akinyele, and R. Rayudu, "Techno-economic analysis of a 10 kWp utility interactive photovoltaic system at Maungaraki school, Wellington, New Zealand," *Energy*, vol. 120, pp. 573–583, 2017. [Online]. Available: http://dx.doi.org/10.1016/j.energy.2016.11.107

[77] N. M. Kumar, M. R. Kumar, P. R. Rejoice, and M. Mathew, "Performance analysis of 100 kWp grid connected Si-poly photovoltaic system using PVsyst simulation tool," *Energy Procedia*, vol. 117, pp. 180–189, 2017. [Online]. Available: http://dx.doi.org/10.1016/j.egypro.2017.05.121

[78] G. A. Dávi, E. Caamaño-Martín, R. Rüther, and J. Solano, "Energy performance evaluation of a net plus-energy residential building with grid-connected photovoltaic system in Brazil," *Energy and Buildings*, vol. 120, pp. 19–29, 2016.

[79] E. A. Essah, A. R. Arguelles, and N. Glover, "Assessing the performance of a building integrated BP c-Si PV system," *Renewable Energy*, vol. 73, pp. 36–45, 2015. [Online]. Available: http://dx.doi.org/10.1016/j.renene.2014.04.002

[80] X. Wu, Y. Liu, J. Xu, W. Lei, X. Si, W. Du, C. Zhao, Y. Zhong, L. Peng, and J. Lin, "Monitoring the performance of the building attached photovoltaic (BAPV) system in Shanghai," *Energy and Buildings*, vol. 88, pp. 174–182, 2015. [Online]. Available: http://dx.doi.org/10.1016/j.enbuild.2014.11.073

[81] E. M. Saber, S. E. Lee, S. Manthapuri, W. Yi, and C. Deb, "PV (photovoltaics) performance evaluation and simulation-based energy yield prediction for tropical buildings," *Energy*, vol. 71, pp. 588–595, 2014. [Online]. Available: http://dx.doi.org/10.1016/j.energy.2014.04.115

[82] T. Bano and K. V. S. Rao, "Performance analysis of 1MW grid connected photovoltaic power plant in Jaipur , India," in *International Conference on*

Energy Efficient Technologies for Sustainability (ICEETS). IEEE, 2016, pp. 165–170.

[83] L. Boughamrane, M. Boulaid, A. Tihane, A. Sdaq, K. Bouabid, and A. Ihlal, "Comparative analysis of measured and simulated performance of the Moroccan first MV grid connected photovoltaic power plant ofassa, southern Morocco," *Journal of Materials and Environmental Science*, vol. 7, no. 12, pp. 4682–4691, 2016.

[84] A. Chouder, S. Silvestre, B. Taghezouit, and E. Karatepe, "Monitoring, modelling and simulation of PV systems using LabVIEW," *Solar Energy*, vol. 91, pp. 337–349, 2013. [Online]. Available: http://dx.doi.org/10.1016/j.solener.2012.09.016

[85] L. Danny, K. L. Cheung, T. N. Lam, and W. W. Chan, "A study of grid-connected photovoltaic (PV) system in Hong Kong," *Applied Energy*, vol. 90, no. 1, pp. 122–127, 2012. [Online]. Available: http://dx.doi.org/10.1016/j.apenergy.2011.01.054

[86] W. Chine, A. Mellit, A. M. Pavan, and S. A. Kalogirou, "Fault detection method for grid-connected photovoltaic plants," *Renewable Energy*, vol. 66, pp. 99–110, 2014. [Online]. Available: http://dx.doi.org/10.1016/j.renene.2013.11.073

[87] J. A. Urbano, Y. Matsumoto, O. I. Gómez, R. Asomoza, E. Galván, R. Dorantes, T. Itoh, S. Nonomura, C. López, G. López, and R. Peña, "One-year 60 kWp photovoltaic system energy performance at CINVESTAV, Mexico City," *Energy Procedia*, vol. 57, pp. 217–225, 2014. [Online]. Available: http://dx.doi.org/10.1016/j.egypro.2014.10.026

[88] A. El Fathi, L. Nkhaili, A. Bennouna, and A. Outzourhit, "Performance parameters of a standalone PV plant," *Energy Conversion and Management*, vol. 86, pp. 490–495, 2014. [Online]. Available: http://dx.doi.org/10.1016/j.enconman.2014.05.045

[89] D. D. Milosavljević, T. M. Pavlović, and D. S. Piršl, "Performance analysis of A grid-connected solar PV plant in Niš, republic of Serbia," *Renewable and Sustainable Energy Reviews*, vol. 44, pp. 423–435, 2015.

[90] C. E. B. Elhadj Sidi, M. L. Ndiaye, M. El Bah, A. Mbodji, A. Ndiaye, and P. A. Ndiaye, "Performance analysis of the first large-scale (15 MWp) grid-connected photovoltaic plant in Mauritania," *Energy Conversion and Management*, vol. 119, pp. 411–421, 2016. [Online]. Available: http://dx.doi.org/10.1016/j.enconman.2016.04.070

[91] K. Attari, A. Elyaakoubi, and A. Asselman, "Performance analysis and investigation of a grid-connected photovoltaic installation in Morocco," *Energy Reports*, vol. 2, no. December 2015, pp. 261–266, 2016. [Online]. Available: http://dx.doi.org/10.1016/j.egyr.2016.10.004

[92] K. Otani, K. Kato, T. Takashima, T. Yamaguchi, and K. Sakuta, "Field experience with large-scale implementation of domestic PV systems and with large PV systems on buildings in Japan," *Progress in Photovoltaics: Research and Applications*, vol. 12, no. 6, pp. 449–459, 2004.

[93] K. Kerkouche, F. Cherfa, A. Hadj, A. S. Bouchakour, K. Abdeladim, and K. Bergheul, "Evaluation de l'irradiation solaire globale sur une surface inclinée selon différents modèles pour le site de Bouzaréah," *Revue des Energies Renouvelables*, vol. 16, no. May 2014, pp. 269–284, 2013.

[94] I. Drouiche, S. Harrouni, and A. H. Arab, "A new approach for modelling the aging PV module upon experimental I-V curves by combining translation method and five-parameters model," *Electric Power Systems Research*, vol. 163, no. February, pp. 231–241, 2018. [Online]. Available: https://doi.org/10.1016/j.epsr.2018.06.014

[95] S. Bouchakour, A. H. Arab, K. Abdeladim, S. Boulahchiche, S. O. Amrouche, and A. Razagui, "Evaluation of the PV energy production after 12-years of operating," *AIP Conference Proceedings*, vol. 1968, 2018.

[96] A. Chouder, S. Silvestre, N. Sadaoui, and L. Rahmani, "Modeling and simulation of a grid connected PV system based on the evaluation of main PV module parameters," *Simulation Modelling Practice and Theory*, vol. 20, no. 1, pp. 46–58, 2012. [Online]. Available: http://dx.doi.org/10.1016/j.simpat.2011.08.011

[97] F. Slama, C. Aissa, and H. Radjeai, "Simulation of Photovoltaic generator Connected To a Grid," *Mediterranean Journal of Modeling and Simulation*, vol. 01, no. January, pp. 25–33, 2014.

[98] F. Cherfa, A. Chouder, and a. H. Arab, "Modélisation et simulation des composants de la mini-centrale photovoltaïque connectée au réseau du CDER," *Revue des Energies rnouvelables ICRESD-07 Tlemcen*, no. January, pp. 29–34, 2007.

[99] S. Bouchakour, A. Tahour, K. Abdeladim, H. Sayah, and A. Arab, "Estimation and monitoring of grid connected PV system generation," *Journal of Renewable Energies*, vol. 19, no. January 2017, pp. 277–290, 2016.

[100] B. Taghezouit, A. H. Arab, C. Larbes, S. Bouchakour, and M.-c. Si, "Dynamic Modelling and Performance Analysis for a Grid-Connected PV System under LabVIEW," in *The 5th International Seminar on New and Renewable Energies*, 2018, pp. 1–6.

[101] B. Taghezouit, A. H. Arab, C. Larbes, S. Smail, and A. Kamel, "Design of an accurate monitoring system for a grid-connected PV system based on LabVIEW," in *International Symposium on Mechatronics and Renewable Energies*, 2018, p. 6.

[102] A. H. Arab, S. O. Amrouche, K. Abdeladim, S. Bouchakour, F. Cherfa, and B. Taghezouit, "Power Quality Monitoring of the grid-connected PV System at

CDER , Algeria Power Quality Monitoring of the grid-connected PV System at CDER , Algeria," in *International Conference on Nuclear and Renewable Energy Resources, NuRER*, no. November, 2014, p. 6.

[103] A. H. Arab, B. Taghezouit, A. H. Arab, C. Larbes, and S. Smail, "Real-time Monitoring for a Grid-Connected PV System based on Virtual Instrumentation," in *InSecond Int. Conf. Electr. Eng. ICEEB*, no. December, 2018, p. 6. [Online]. Available: https://www.researchgate.net/publication/329444186

[104] Y. Chaibi, M. Malvoni, A. Chouder, M. Boussetta, and M. Salhi, "Simple and efficient approach to detect and diagnose electrical faults and partial shading in photovoltaic systems," *Energy Conversion and Management*, vol. 196, no. February, pp. 330–343, 2019. [Online]. Available: https://doi.org/10.1016/j.enconman.2019.05.086

[105] E. Garoudja, F. Harrou, Y. Sun, K. Kara, A. Chouder, and S. Silvestre, "Statistical fault detection in photovoltaic systems," *Solar Energy*, vol. 150, pp. 485–499, 2017. [Online]. Available: http://dx.doi.org/10.1016/j.solener.2017.04.043

[106] S. Silvestre, A. Chouder, and E. Karatepe, "Automatic fault detection in grid connected PV systems," *Solar Energy*, vol. 94, pp. 119–127, 2013. [Online]. Available: http://dx.doi.org/10.1016/j.solener.2013.05.001

[107] S. Silvestre, M. A. D. Silva, A. Chouder, D. Guasch, and E. Karatepe, "New procedure for fault detection in grid connected PV systems based on the evaluation of current and voltage indicators," *Energy Conversion and Management*, vol. 86, pp. 241–249, 2014. [Online]. Available: http://dx.doi.org/10.1016/j.enconman.2014.05.008

[108] S. Semaoui, A. Hadj Arab, H. Zeraia, E. K. Boudjeltia, and S. Bacha, "Soiling effect on the incidence of solar inrradiance on photovoltaic array plane," *2014 International Conference on Electrical Sciences and Technologies in Maghreb, CISTEM 2014*, no. November, 2014.

[109] S. Semaoui, K. Abdeladim, B. Taghezouit, A. Hadj Arab, A. Razagui, S. Bacha, S. Boulahchiche, S. Bouacha, and A. Gherbi, "Experimental investigation of soiling impact on grid connected PV power," *Energy Reports*, vol. 6, pp. 302–308, 2020. [Online]. Available: https://doi.org/10.1016/j.egyr.2019.08.060

[110] A. H. Arab, I. H. Mahammed, S. O. Amrouche, B. Taghezouit, and N. Yassaa, "Performance degradation of photovoltaic modules at different sites," *IOP Conference Series: Earth and Environmental Science*, vol. 154, no. 1, 2018.

[111] A. Chouder and S. Silvestre, "Analysis model of mismatch power losses in pv systems," *Journal of Solar Energy Engineering, Transactions of the ASME*, vol. 131, no. 2, pp. 0 245 041–0 245 045, 2009.

[112] A.Chouder and S.Silvestre, "Analysis of Power Losses in Pv Systems," *Journal of Chemical Information and Modeling*, vol. 53, no. 9, pp. 1689–1699, 2013.

[113] A. H. Arab, S. Bouchakour, S. O. Amrouche, K. Abdeladim, and S. Semaoui, "Qualité de la tension au point d'injection du système photovoltaïque du CDER," *Journal of Renewable Energies*, vol. 20, no. March, pp. 1–9, 2017.

[114] S. Bouchakour, A. H. Arab, K. Abdeladim, S. O. Amrouche, S. Semaoui, B. Taghezouit, S. Boulahchiche, and A. Razagui, "Investigation of the voltage quality at PCC of grid connected PV system," *Energy Procedia*, vol. 141, pp. 66–70, 2017. [Online]. Available: https://doi.org/10.1016/j.egypro.2017.11.013

[115] A. H. Arab, S. Bouchakour, K. Abdeladim, S. O. Amrouche, S. Semaoui, B. Taghezouit, and N. Yassaa, "Connection of the CDER-Algiers photovoltaic system to low-voltage distribution grid," *Energy Procedia*, vol. 136, no. November, pp. 145–150, 2017. [Online]. Available: https://doi.org/10.1016/j.egypro.2017.10.311

[116] S. Bouchakour, K. Abdeladim, F. Cherfa, and A. H. Arab, "Pv systems and power quality in algerian distribution grid," in *29th European Photovoltaic Solar Energy Conference and Exhibition*, no. November, 2014, pp. 1–5.

[117] S. Boulahchiche, S. Makhloufi, S. Semaoui, A. H. Arab, and K. Abdeladim, "Experimental Analysis of Grid Connected to PV System According to DIN VDE 0126-1-1," in *The 5th International Seminar on New and Renewable Energies*, 2018, pp. 1–6.

[118] S. O. Amrouche, S. Bouchakour, A. H. Arab, K. Abdeladim, F. Cherfa, K. Kerkouche, C. D. Développement, and R. De, "Reactive power issues in grid connected photovoltaic systems," *International Conference on Nuclear and Renewable Energy Resources (NURER)*, no. October, pp. 1–6, 2014.

[119] F. Cherfa, A. Hadj Arab, R. Oussaid, K. Abdeladim, and S. Bouchakour, "Performance analysis of the mini-grid connected photovoltaic system at Algiers," *Energy Procedia*, vol. 83, pp. 226–236, 2015. [Online]. Available: http://dx.doi.org/10.1016/j.egypro.2015.12.177

[120] B. Shiva Kumar and K. Sudhakar, "Performance evaluation of 10 MW grid connected solar photovoltaic power plant in India," *Energy Reports*, vol. 1, pp. 184–192, 2015. [Online]. Available: http://dx.doi.org/10.1016/j.egyr.2015.10.001

[121] A. McEvoy, T. Markvart, and L. Castaner, *Practical Handbook of Photovoltaics - Fundamentals and Applications*. Elsevier, 2012.

[122] B. R. Paudyal, A. G. Imenes, and T. O. Saetre, "Review of guidelines for PV systems performance and degradations monitoring," in *35th European Photovoltaic Solar Energy Conference and Exhibition*, 2015, pp. 123–128.

[123] J.-h. Shin and J.-o. Kim, "On-Line Diagnosis and Fault State Classification," *Energies*, vol. 13, no. 17, p. 4584, 2020.

[124] R. A. Shalwala, "Pv Integration Into Distribution Networks in SAUDI ARABIA," Ph.D. dissertation, University of Leicester, 2012.

[125] A. Q. Al-Shetwi, M. A. Hannan, K. P. Jern, A. A. Alkahtani, and A. E. Abas, "Power quality assessment of grid-connected PV system in compliance with the recent integration requirements," *Electronics*, vol. 9, no. 2, pp. 1–22, 2020.

[126] Standing Committee for monitoring and updating Technical Rules, *règles techniques de raccordement et règles de conduite du système électrique*, 2019th ed. Ministry of Energy and Mining, 2019.

[127] S. Bouchakour, "Contribution à l'étude et commande d'un couplage des systèmes hybrides (réseau et photovoltaïque) pour la production d'énergie électrique," Ph.D. dissertation, Universite Djillali Liabes de Sidi-Bel-Abbes, 2015.

[128] M. Mpholo, T. Nchaba, and M. Monese, "Yield and performance analysis of the first grid-connected solar farm at Moshoeshoe I International Airport, Lesotho," *Renewable Energy*, vol. 81, pp. 845–852, 2015. [Online]. Available: http://dx.doi.org/10.1016/j.renene.2015.04.001

[129] L. Danny HW and T. N. T. Lam, "Determining the Optimum Tilt Angle and Orientation for Solar Energy Collection Based on Measured Solar Radiance Data," *International Journal of Photoenergy*, vol. 2007, pp. 1–9, 2007.

[130] A. Hadj Arab, F. Cherfa, A. Chouder, and F. Chenlo, "Grid-Connected Photovoltaic System at CDER-Algeria," *20th European Photovoltaic Solar Energy Conference and Exhibition*, no. May 2014, p. 2724, 2005. [Online]. Available: c:/pdflib/00018529.pdf

[131] A. Korde, "Assessment of a Solar PV Re-Powering Project in Sweden Using Measured and Simulated," Ph.D. dissertation, Dalarna University, 2017.

[132] S. Elfberg, S. Elfberg, and F. Kristofersson, "Maximizing Solar Energy Production for Västra Stenhagenskolan Designing an Optimal PV System," Ph.D. dissertation, UPPSALA University, 2019.

[133] Chauvin Arnoux, "Analyser Qualistar Plus," Tech. Rep., 2015.

[134] L. A. El-Leathey, A. Nedelcu, and M. Dorian, "Power quality monitoring and analysis of a grid-connected PV power plant," *EEA - Electrotehnica, Electronica, Automatica*, vol. 65, no. 3, pp. 26–33, 2017.

[135] S. Kurtz, J. Newmiller, A. Kimber, R. Flottemesch, E. Riley, T. Dierauf, J. McKee, and P. Krishnani, "Analysis of Photovoltaic System Energy Performance Evaluation Method," Tech. Rep. November 2013, 2013.

[136] R. A. Messenger and A. Abtahi, *Photovoltaic Systems Engineering*, 4th ed. CRC press Taylor & Francis Group, 2017.

[137] J. Freeman, J. Whitmore, N. Blair, and A. P. Dobos, "Validation of multiple tools for flat plate photovoltaic modeling against measured data," in *2014 IEEE 40th Photovoltaic Specialist Conference, PVSC 2014*. IEEE, 2014, pp. 1932–1937.

[138] R. V. F. Batista, "The impact of shadowing in photovoltaic systems and how to minimizing it," Ph.D. dissertation, University of Gavle, 2018. [Online]. Available: UniveristyofG\protect{\mathchar"1270}\protect\T1\textsectionvle

[139] D. Cormode, "Large and small photovoltaic power plants," Ph.D. dissertation, The University of Arizona, 2015.

[140] S. S. Koram, "How to use the theodolite for vertical and horizontal measurements in surveying," *Journal of Solid Mechanics*, no. November, pp. 17–19, 2019.

[141] M. H. Tapia and R. H., "Evaluation of Performance Models against Actual Performance of Grid Connected PV Systems," Ph.D. dissertation, Diss. Carl von Ossietzky Universität, 2014. [Online]. Available: http://oops.uni-oldenburg.de/2433/7/Thesis_TapiaM.pdf%0Ahttps://d-nb.info/1077657072/34

[142] B. B. Ekici, "Variation of photovoltaic system performance due to climatic and geographical conditions in Turkey," *Turkish Journal of Electrical Engineering and Computer Sciences*, vol. 24, no. 6, pp. 4693–4706, 2016.

[143] V. Sonti, S. Jain, and S. Bhattacharya, "Analysis of the modulation strategy for the minimization of the leakage current in the PV grid-connected cascaded multilevel inverter," *IEEE Transactions on Power Electronics*, vol. 32, no. 2, pp. 1156–1169, 2017.

[144] S. S. Kumar and C. Nagarajan, "Performance-Economic and Energy Loss Analysis of 80 KWp Grid Connected Roof Top Transformer Less Photovoltaic Power Plant," *Circuits and Systems*, vol. 07, no. 06, pp. 662–679, 2016.

[145] M. Theristis, V. Venizelou, G. Makrides, and G. E. Georghiou, "Energy yield in photovoltaic systems," in *McEvoy's Handbook of Photovoltaics: Fundamentals and Applications*. Elsevier, 2018, no. January, pp. 671–713.

[146] A. H. Shah, A. Hassan, M. S. Laghari, and A. Alraeesi, "The Influence of Cleaning Frequency of Photovoltaic Modules on Power Losses in the Desert Climate," *Sustainability*, vol. 12, no. 22, p. 9750, 2020. [Online]. Available: www.mdpi.com/journal/sustainability

[147] Y. Charabi and A. Gastli, "Spatio-temporal assessment of dust risk maps for solar energy systems using proxy data," *Renewable Energy*, vol. 44, pp. 23–31, 2012. [Online]. Available: http://dx.doi.org/10.1016/j.renene.2011.12.005

[148] I. Ibrik, "Power quality and performance of grid-connected solar PV system in Palestine," *International Journal of Engineering Research and Technology*, vol. 12, no. 9, pp. 1570–1577, 2019.

[149] H. Markiewicz and A. Klajn, "Guide Power Quality Section 5 : Perturbations de tension publics de distribution Norme EN 50160," Université de technologie de Vroclaw, Tech. Rep., 2007.

[150] SMA Solar Technology AG, "Grid Support Utility Interactive Inverters," SMA, Tech. Rep., 2015.